Estimation of the Optimum Wind Turbine Size for Two Different Offshore Sites and Wind Farm Rated Powers

Shajid Kairuz Fonseca

Master of Science Thesis

TU Delft Delft University of Technology

Estimation of the Optimum Wind Turbine Size for Two Different Offshore Sites and Wind Farm Rated Powers

Master of Science Thesis

For the degree of Master of Science in Sustainable Energy Technology
at Delft University of Technology

Shajid Kairuz Fonseca

August 17, 2017

Faculty of Aerospace Engineering (AE) and Electrical Engineering,
Mathematics, and Computer Science (EEMCS)

Delft University of Technology
Department of
Wind Energy, Aerospace Engineering (TU Delft)

The following academic staff certifies that it has read and recommends to the Faculty of Aerospace Engineering (AE) and Electrical Engineering, Mathematics, and Computer Science (EEMCS) for acceptance a thesis entitled

Estimation of the Optimum Wind Turbine Size for two Different Offshore Sites and Wind Farm Rated Powers

by

Shajid Kairuz Fonseca

in partial fulfillment of the requirements for the degree of

Master of Science Sustainable Energy Technology

Dated: August 17, 2017

Supervisor: Dr. ir. M.B. Zaaijer

Thesis committee:

Prof. dr. G.J.W. van Bussel

Dr. ir. M.B. Zaaijer

Dr. J.J.E. Teuwen

Abstract

Large turbines are a synonym of more energy harvested from the wind, but also of increment in the costs. This dilemma has led many researchers on the field of wind energy to wonder about the optimum size for wind turbines concerning the lowest cost of energy. This project studies the optimum turbine size for offshore applications through the modeling of the costs of the components that have the largest contribution to the Levelized Production Cost (LPC). Since at different power ratings different power densities are optimal, the turbine size is considered in terms of the rotor diameter and the turbine rated power. Therefore, the cost models developed in this work are a function of these two parameters. To develop the cost models, classical scaling approaches are used along with an offshore wind farm design emulator tool. Regarding that the optimum turbine size is not the same for all situations, two case studies of offshore wind farms are established. These case studies contrast some of the relevant characteristics of an offshore wind farm as the power installed capacity, the distance from shore, the water depth, and the wind and wave environment. The optimal size for large, far offshore wind farms was found to be in the range of 10-13 MW, while it was around 5-7 MW for small near shore farms. The optimum turbine size depends mostly on the reduction in the cost of the O&M and the increment in the costs of the turbines and support structure as the turbine scale employed in the wind farm becomes larger. Finally, the blades cost appears to be a limiting factor for the increment in the rotor diameter for the large turbines scales.

Acknowledgements

I want to express my gratitude to my supervisor Michiel Zaaijer for sharing his knowledge in the field of wind energy with me. Moreover, his guidance and feedback were of great importance to develop this project.

This work is dedicated to my father for the support and love he has given me all these years. Also, I want to make an especial dedication to my son Benjamín for making my life happy each day. Thanks to the rest of my family for their encouragement and assistance, especially my siblings Pablo, María Paula, and Aleshka.

I am very grateful for the chance of being able to do a master degree abroad since it helped me to grow up as a person apart from meeting a bunch of nice people in the way. Thanks to all the friends whom I had the fortune to make in the Netherlands for these great two years. Finally, I want to thank my friends in Colombia who made me feel closer from home.

Table of Contents

List of Figures

List of Tables

List of symbols

Latin Symbols

A	annuity factor
A_{farm}	farm area usage
a	weibull scale factor
b	consumables repairs cost exponent
$C_{decommissioning}$	decommissioning cost
C_I	insurance cost
$C_{investment}$	capital investment cost
$C_{O\&M}$	operation and maintenance cost
C_{PM}	preventive maintenance cost
C_p	power coefficient
C_R	consumables repairs cost
C_{RNA}	RNA cost
C_t	thrust coefficient
c_i	insurance cost coefficient
c_{pm}	preventive maintenance cost coefficient
c_r	consumables repairs cost coefficient
c_{r*}	consumables repairs cost per turbine of the reference turbine
D	turbine rotor diameter
D_{new}	rotor diameter of the scaled turbine
D_{ref}	rotor diameter of the reference turbine
d_{water}	water depth
E	axial modulus
E_c	axial modulus carbon fiber
E_g	axial modulus glass fiber
E_y	energy yield
$f_{warranty}$	one-off warranty premium percentage
h	height
h_{hub}	turbine hub height
h_{ref}	reference height
i	interest rate
k	weibull shape factor
L	RNA onshore transport distance
l	cable length
m_{jacket}	offshore platform jacket mass
m_{RNA}	RNA mass
$N_{turbines}$	number of turbines in the wind farm
P	turbine rated power
P_{farm}	farm rated power

P_{new}	rated power of the scaled turbine
P_{ref}	rated power of the reference turbine
r	real interest rate
r_{lc}	labor cost ratio
r_{mc}	material cost ratio
$r_{p\&o}$	profit & overhead cost ratio
r_{tc}	total cost ratio
r_w	weight ratio
S	specific gravity
S_c	specific gravity carbon fiber
S_g	specific gravity glass fiber
T	project lifetime
T_{hr}	number of hours in a year
Th	thrust force
Th_{new}	thrust force at rated power for the scaled turbine
Th_{ref}	thrust force at rated power for the reference turbine
t	index of year
U	wind speed
V	wind speed
V_{in}	cut-in wind speed
V_{new}	rated wind speed for the scaled turbine
V_{out}	cut-out wind speed
V_{ref}	rated wind speed for the reference turbine
$Vol_{c/g}$	carbon/glass volume ratio
v	inflation rate
z_0	surface roughness length

Greek Symbols

α	wind shear exponent
ρ	air density

Other Symbols

$\$_c$	carbon fiber cost per kg
$\$_g$	glass fiber cost per kg

1. Introduction

1.1. Background and Motivation

The power of the wind has been known to humanity for hundreds of years. In the Ancient World, sailing boats were the most important means of transport, permitting the trade of knowledge, culture, technology, and products; allowing the development of the World as it is today. Moreover, it is recorded that the inventor of the first wind-driven wheel that was used to drive a machine was Heron of Alexandria in the 1st century AD. By 1000AD windmills were already used in China and Sicily to pump seawater to produce salt. However, the first time that wind was exploited for power generation was around 1887-1888 when the inventor Charles Brush built a wind turbine with the aim of providing electricity for his mansion in Ohio (Shahan, 2014).

In 1973 during the Arab-Israeli War, Arab members of the Organization of Petroleum Exporting Countries (OPEC) introduced an oil embargo to the United States and several western European countries for supporting Israel. This event caused wind energy to start being considered as a solution for the energy supply, especially in countries that were directly affected by the embargo as The Netherlands, Denmark, and Germany. In Denmark, some manufacturing firms with a background in the agricultural sector started to build wind turbines in the 10-25kW class. Later on, other firms from countries like the United States, Germany, and The Netherlands entered the scene. Initially, the wind turbines were scaled up in small steps of 20-50kW, however, in the years afterward 50-150kW steps were made. By 1994 many wind turbine suppliers had turbines from 450-600kW in their portfolio. Nevertheless, it was in 1995-1996 that a big jump in wind turbines rated power took place. Four manufacturers introduced a 1.5MW class concept. These manufacturers were Nordtank (now Vestas), Vestas, Tacke (now GE Energy), and Enercon (de Vries, 2005).

Since the beginning of the wind industry, many critics foretold the maximum size and power capacity of wind turbines, saying that upscaling would limit the number of suitable potential locations. But the reasons they gave were more related to aesthetics, landscape integration, and logistics. However, the truth is that since the beginning of the wind energy industry, turbines have bigger rotors, higher hub heights, longer blades and larger rated power capacity. At this moment, Denmark is constructing the wind farm Horn Rev 3, which operates with forty-nine V164-8MW turbines, for a total rated power of 392MW. Certainly, something extraordinary to imagine 30 years ago.

At the end of 2015, wind energy installed capacity in the world was approximately 433GW. More than half of the world's installed capacity has been added in the past five years. Regarding offshore wind, in that same year, the total installed capacity exceeded 12GW from which 11GW was in Europe and the other 1GW in China. Moreover, turbine size is growing as well. In Europe the average turbine rated power for offshore was 4.2MW, and there were several orders for 7-8MW wind turbines by late 2015. Besides, research projects are looking for 10-20MW offshore wind turbines (REN21, 2016). Figure 1 depicts the size evolution that wind turbines have gone through in the last 30 years.

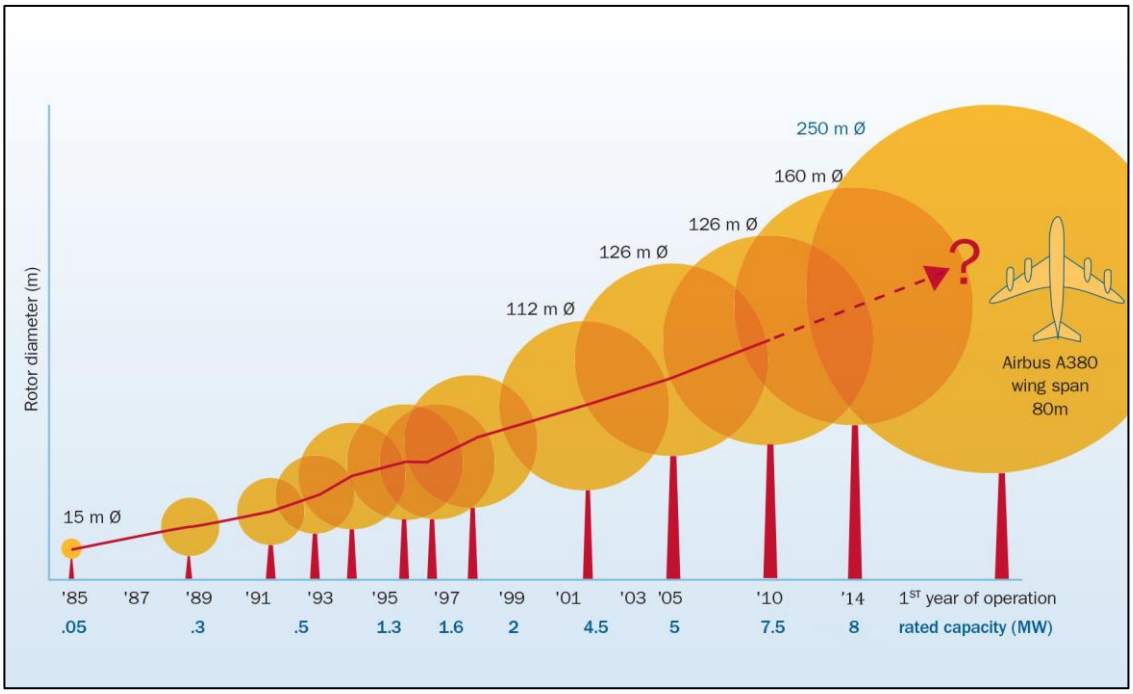

Figure 1. Wind turbine size evolution (GEAI, 2014)

1.2. Problem Analysis

Large turbines are a synonym of more energy harvested from the wind, but also of increment in the costs. This dilemma has led many researchers on the field of wind energy to wonder about the optimum size for wind turbines concerning the lowest cost of energy. However, there are some difficulties in determining this optimum size. One is that the industry may not have reached to this optimum scale yet since wind turbines are still becoming larger. Another difficulty is the lack of data regarding turbine components dimensions and costs because the wind turbine manufacturers prefer not to share this information. In addition, the optimum wind turbine size is not the same for all situations.

Therefore, to deal with these difficulties, researchers often make use of optimization tools and cost models to get a better understanding in the scaling of wind turbines and the estimation of an optimum wind turbine size.

1.3. Objectives

1.3.1. Main Objective

The principal objective of this project is to gain insight into the optimum size of wind turbines for offshore applications. The final production of the project is a computational model that calculates the optimum wind turbine scale considering different aspects of offshore wind farms.

1.3.2. Specific Objectives

With the purpose of achieving the main objective, a series of secondary goals or activities are accomplished, which are the following:

1. Determine the scaling approach for the main components that constitute the cost of energy in an offshore wind farm.

2. Determine how the cost of the components changes when scaling a wind turbine for different cases.

3. Establish a total cost of energy function and identify the wind turbine size that results in the optimum value of it in each case.

4. Determine which components have the largest impact on the cost of energy and the optimum wind turbine scale by performing a sensitivity analysis.

1.4. Approach

As said before in section 1.2, researchers employ optimization tools and cost models to estimate the optimum wind turbine size. Likewise, in the present project, a similar approach is adopted. Thus, a search for the cost models of the majority of the components of an offshore wind farm is done. As a result of this search, the cost models are selected or developed, and for some of the components, an optimization is first carried out using a computational tool. The majority of these cost models can be expressed in terms of the rotor diameter and/or the turbine rated power. Since the optimal combination of power and diameter differs for different scales, it is decided to consider both parameters as independent variables. Subsequently, an energy yield model is established that along with the

cost models enable the calculation of the cost of energy for different wind turbine scales in each of the cases. The combination of power and diameter that results in the lowest cost of energy is the optimum wind turbine size.

Furthermore, since the optimum turbine size is not the same for all situations, two case studies of offshore wind farms with diverse conditions are set. One case is a large, far offshore farm, while the other is a small, near shore farm. Thus, the cost models and the energy yield model are coupled through the LPC function and implemented in each case to find the optimum turbine scale.

Finally, a sensitivity analysis is performed because it is appropriate to determine which are the components that have the largest effect on the optimum turbine scale in each of the two cases. Besides, this analysis is necessary to verify the robustness of the model.

1.5. Document Outline

The outline of the project report is as follows:

Chapter 2 presents the theoretical framework and describes the methodology followed.

Chapter 3 explains how the cost models of the turbines, support structure, electrical infrastructure and O&M are developed. Furthermore, it is introduced the computational tool used in the design and optimization of these components but the turbines.

Chapter 4 describes how the energy produced by a wind turbine is calculated and defines the energy yield model used in this project.

Chapter 5 analyzes and discusses the results obtained from the model of the optimum turbine size for the two case studies.

Chapter 6 presents the sensitivity study performed over the computational model developed to determine which components have the greatest impact on the calculation of the optimum wind turbine size.

Chapter 7 provides the conclusions of the project and the recommendations for a future work.

2. Theoretical Framework and Methodology

2.1. Overview of the chapter

This chapter treats with the methodology and the theoretical framework in which the project is built on.

Since this work intends to evaluate the effect of upscaling of wind turbines to analyze optimal size, the term 'size' has to be defined first. Subsequently, an objective function needs to be established to determine the optimal size. The components that constitute this objective function must be modeled, however, considering that an offshore wind farm consists of many components, only the most important are treated. Therefore, upscaling methods are employed to approach the modeling of these components. Furthermore, two cases are established to analyze the optimum turbine size for specific conditions. Finally, the robustness of the model and the reliability of the results have to be evaluated, for instance, through a sensitivity analysis.

2.2. Defining wind turbine size

The rotor diameter and the rated power have been for a long time fundamental parameters to describe a wind turbine. When a new turbine is released into the market, the manufacturers introduce the new model in terms of the diameter and the power. For instance, the latest Vestas turbine models the V136-4MW and the V164-8MW are some examples of the above mentioned. Therefore, it is reasonable to define the turbine size in terms of these two variables.

In this project, the cost models that are developed are a function of the diameter, or the power, or both. However, the rotor diameter and the rated power are not strictly correlated. Hence, it is appropriate to treat these two as independent parameters. At different scales different power densities may be optimal, in addition, the power density is in many cases site dependent. A high power density is preferred on sites with high wind speeds, while for sites with low wind speeds a low power density is selected.

Nevertheless, a correlation between these two parameters might be expected as observed in Figure 2, where the blue squares represent data collected from wind turbines currently in operation. According to the trend described by these data, the power P is proportional to the diameter D to the power of 1.8. However, it might be

possible than when using other data, this proportionality of P to $D^{1.8}$ changes. Moreover, assuming a constant power density, or a constant rated wind speed also gives a correlation between diameter and power for different scales. In Figure 2 the data is scattered along the trend. This dispersion is caused by the fact that in the industry there is not a fixed turbine power density. As an example, the power density showed by the collected data ranges from 305 to 497W/m^2.

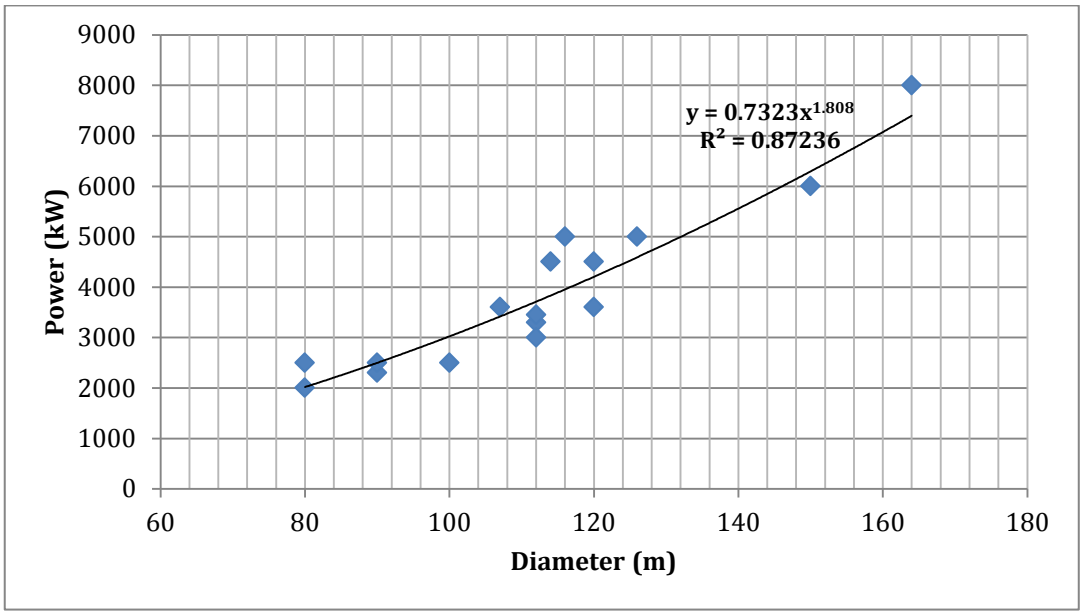

Figure 2. Turbine power as a function of the rotor diameter

2.3. LPC definition

The Levelized Production Cost (LPC) is considered to be a suitable parameter when evaluating the feasibility of an energy generation project. It is defined as the cost price of production per unit of energy, given in actualized nominal currency. The smaller the value of LPC for a certain project, the more beneficial, optimal, and achievable it is. Therefore, the current project takes the LPC as the objective function.

The mathematical expression of LPC is declared in Equation 1 and complemented by Equation 2 and Equation 3.

$$\textbf{Equation 1. } LPC = \frac{C_{investment}}{A*E_y} + \frac{C_{O\&M}}{E_y} + \frac{C_{decommissioning}*(1+r)^{-T}}{A*E_y}$$

$$\textbf{Equation 2. } A = \sum_{t=1}^{T}(1+r)^{-t} = \frac{1}{r}\left[1-\left(\frac{1}{1+r}\right)^{T}\right]$$

$$\textbf{Equation 3. } 1+r = \frac{1+i}{1+v}$$

where $C_{invetment}$ is the capital investment cost, $C_{O\&M}$ is the O&M cost, $C_{decommissioning}$ is the decommissioning cost, r is the real interest rate also referenced as discount rate, T is the project lifetime, A is the annuity factor, E_y is the energy yield per year, t is the index of year, i is the interest rate, and v is the inflation rate.

At the time of considering the definition of LPC given by Equation 1, several assumptions are made (Zaaijer M. , Economic Aspects, 2015):

- The wind farm starts operating after construction in year 0.
- Annual O&M costs are constant
- Decommissioning takes place in year T when the wind farm is shut down
- Annual energy production is constant

2.4. Determine LPC components

The LPC consists of two major components, which are the costs throughout the whole wind farm project and the energy yield during the entire operational project lifetime. Thus, this section treats the components that must be modeled to use properly the LPC function.

2.4.1. Costs

The total costs of a wind farm project are commonly split into three parts. According to Equation 1, these parts are the capital investment cost, the operation and maintenance cost (O&M), and the decommissioning cost. However, these three parts consist of other sub-elements. Despite the number of components in a wind farm is quite large, in this work just the most important are treated.

The capital investment cost is sub-divided in the following items:

- Support Structure
- Electrical Infrastructure
- Turbines
- Boat landing structure
- Offshore Platform
- Measuring tower
- Onshore premises
- Harbor use
- Warranty
- Transportation of the RNA onshore
- Installation of the RNA offshore
- Dune crossing
- Grid connection

- Transmission cable installation
- Infield cables installation
- Engineering
- Site assessment
- Management

The operation and maintenance cost is decomposed into the following components:

- Operation:
    - Administration
    - Grid charge
    - Bottom lease
    - Insurance
- Maintenance
    - Personnel
    - Access Vessels
    - Lifting Equipment
    - Subsea inspections
    - Consumables repair
    - Consumables service
- Management

The decommissioning cost is constituted by the following elements:

- Removal of the RNA's
- Removal of the foundations and scour protection
- Removal of the offshore platform and meteo tower
- Removal of the transmission cable
- Removal of the infield cables
- Site clearance
- Disposal of the RNA's
- Management

Regarding that the elements specified above still make a long list, not for all of them it is possible to do a detailed analysis to determine how their cost will behave when using different wind turbine sizes. According to Figure 3 the cost of the turbines, support structure, electrical infrastructure, and installation are about the 75% of the total capital expenditures for an offshore wind farm project. Moreover,

in the offshore wind industry O&M accounts for approximately the 23% of the total project expenses, and to 25 to 30% of the cost of energy generated. Thus, in this work, only a thorough analysis is performed for the support structure, the electrical infrastructure the turbines and the O&M cost. For the rest of the components listed above, cost models from different sources are used.

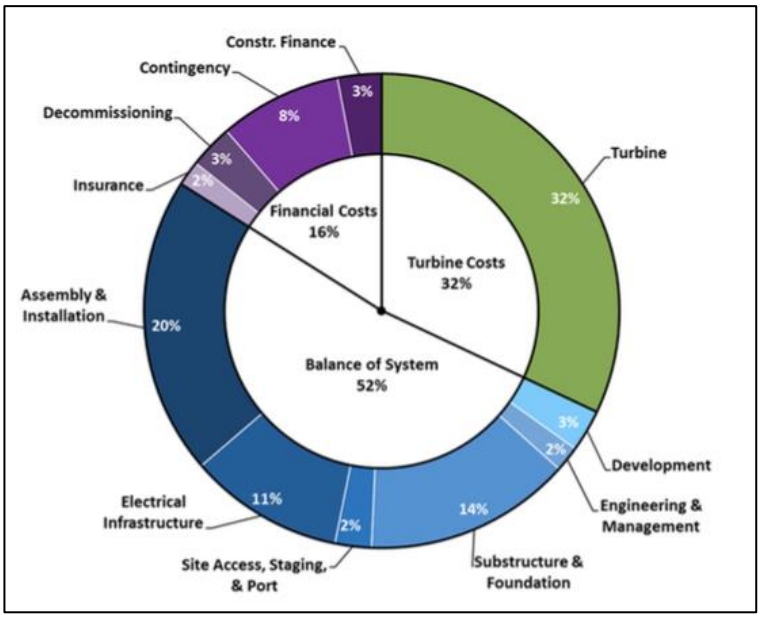

Figure 3. Capital expenditures for the 2013 offshore wind reference project (Moné et al., 2015)

2.4.2. Energy yield

It would be desirable that the energy yield in a wind farm would be simply the number of turbines times the energy produced by a single turbine. This would be the case if all the turbines produced the same amount of energy. However, the reality is more complex, and the energy yield is composed of the following factors:

- Individual turbine energy yield
- Wake efficiency
- Electrical losses
- Availability

Depending on the position that a turbine has in the wind farm layout, it produces more or less energy. This is caused by the wake effects, which lead to the variation of the wind speed induced by the influence of the turbines on each other. Therefore, not all the turbines are producing the same amount of electricity. The wake efficiency is then the ratio of the total energy output of the wind farm and the energy output of the total number of turbines if every single turbine is not affected by the neighboring turbines. Furthermore, electrical losses are present when the

infield cables and the transmission cables transmit the electricity from the wind farm to the onshore grid. Moreover, since the wind turbines present different kind of failures during the wind farm operation period, they are not continually available to produce energy.

2.5. Upscaling Approaches

There are multiple methods to estimate the effect of upscaling in fundamental performance parameters and components of wind turbines. This section introduces two classical upscaling methods, which are an analytic scaling law and an empirical approach.

2.5.1. Analytic Scaling Law

This first approach is also known as the square-cube law. It is based on the concept that when scaling the rotor diameter, all the other turbine components lengths scale linearly, all their surfaces increase quadratically as well as the power, and all the volumes, masses and costs increase with the cube of the dimensions. Figure 4 depicts the theory behind this approach. The main drawback of this method is that it does not take into account the technological advances that go hand-in-hand with increasing the turbine size like shown in Figure 5. Thus, it is not suitable when the parameter to be scaled plays a major role in the final result.

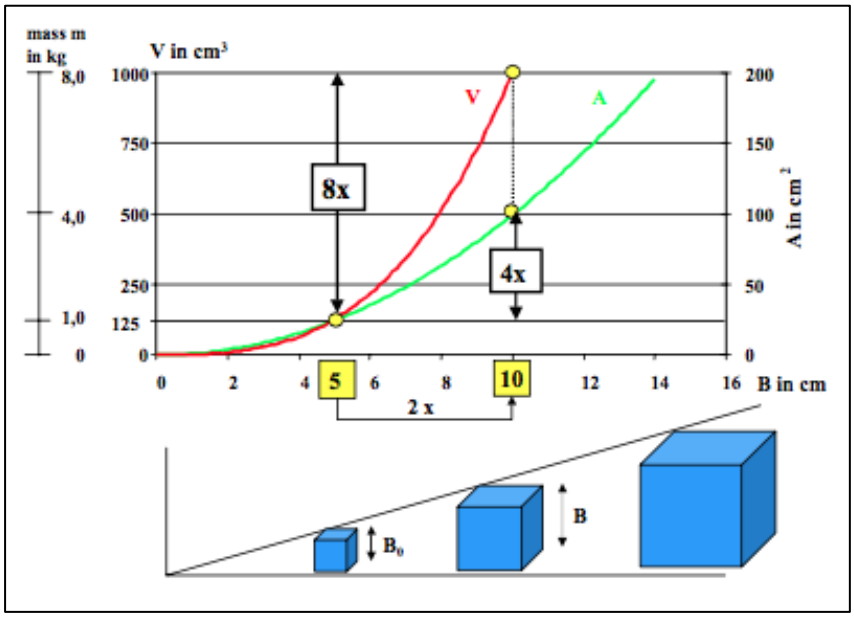

Figure 4. Analytical scaling law (Klinger et al, 2002)

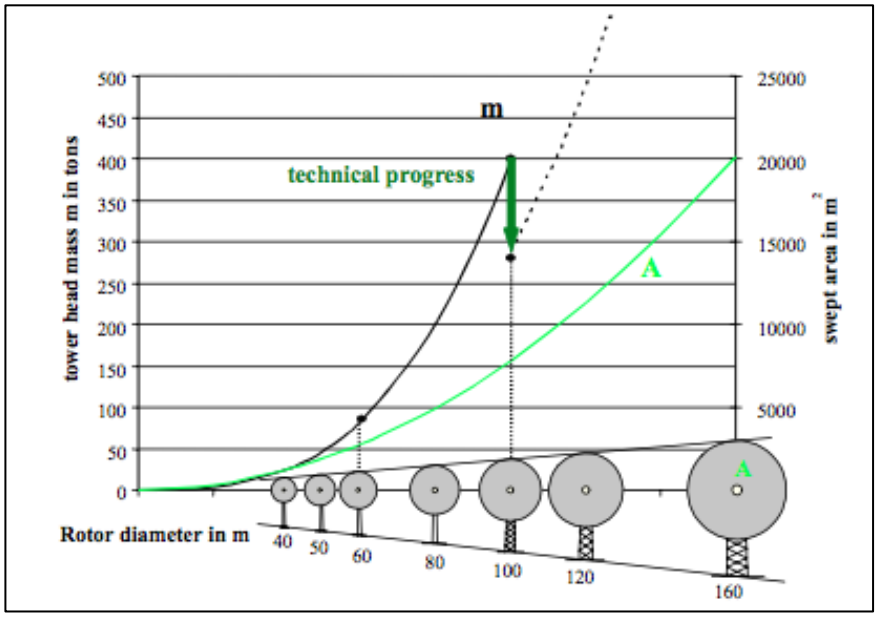

Figure 5. Technical progress in comparison to the analytic scaling approach (Klinger et al, 2002)

2.5.2. Empirical Approach

The second method is about gathering data of an individual parameter and fit a function, which can be either interpolated or extrapolated to predict the value of this parameter for a desired independent variable as the rotor diameter, the turbine rated power, etc. This approach does take account of the technological advances made by the industry. However, the gathered data might come from turbines with different design concepts, which induces scattering and leads to uncertainty. Likewise, when extrapolating beyond the collected data uncertainty is introduced. These two issues are regarded as the main drawbacks when applying this scaling approach (Ashuri et al., 2016).

Figure 6 shows the drawbacks of both scaling methods. The tower mass does not scale with a power factor of 3 as it suggests the square-cube law. And, in like manner, fitting a curve among scattered data leads to high uncertainties and little correlation between the dependent and independent variables.

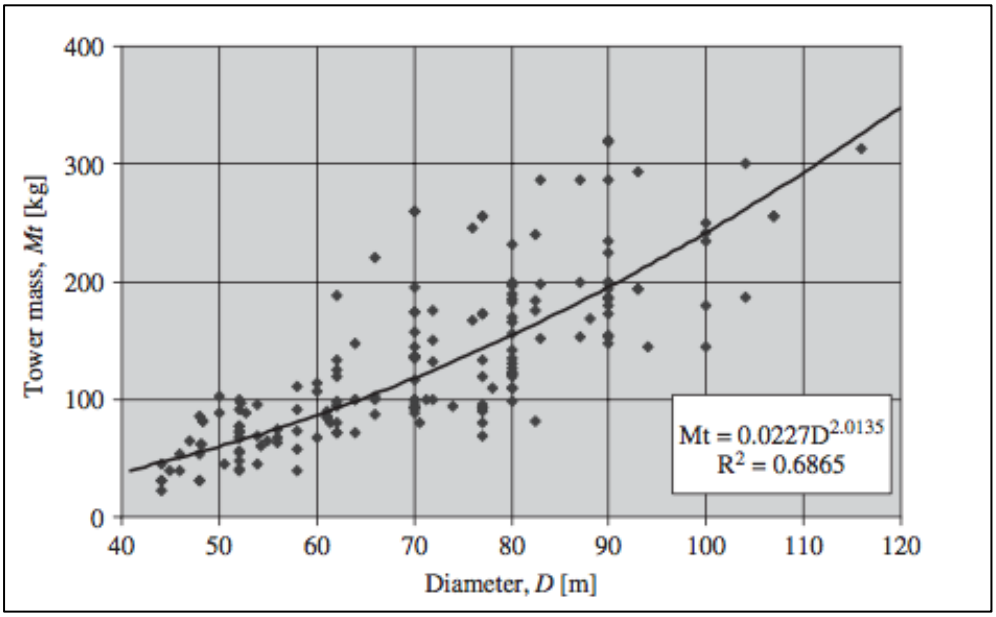

Figure 6. Tower Mass trends (Jamieson, 2011)

2.5.3. Remarks on the approaches

It is important to mention that these scaling methods do not always give the costs of the components or the energy yield. Nevertheless, they can be used to model intermediate parameters that can be used afterward in the cost models and the energy yield model.

For instance, when a turbine is upscaled, the power curve increases with the square of the increment in the rotor diameter if following the analytical approach. This could be used in the calculation of the energy yield for the upscaled turbine. Moreover, considering the empirical approach, the tower mass from Figure 6 can be used to find the cost of the tower.

2.6. Case Studies

As mentioned in section 1.2, the optimum wind turbine size differs depending on the situation; therefore, two cases for offshore wind farms with diverse conditions are established. It is intended that both cases contrast the different aspects that influence the optimum size of the wind turbine. Moreover, the two cases are meant to be potential locations for the development of offshore wind farms.

The first case is a large offshore wind farm in the North Sea that is located farther from the coast than most of the current offshore wind farms, which in average are located 25km from the shore. This case is considered because it is expected that in the future the wind farms are going to be built farther offshore in the North Sea

where more space and stronger winds are available. The second case is a small offshore wind farm in the Baltic Sea. This case is set because this region has an offshore wind potential of 40GW according to (Buljan & Durakovic, 2016). Besides, there are plans to construct more than 12GW of offshore wind install capacity in the south Baltic Sea (Hasager et al., 2011). Figure 7 shows the main characteristics of both cases; their references can be found in Appendix B.

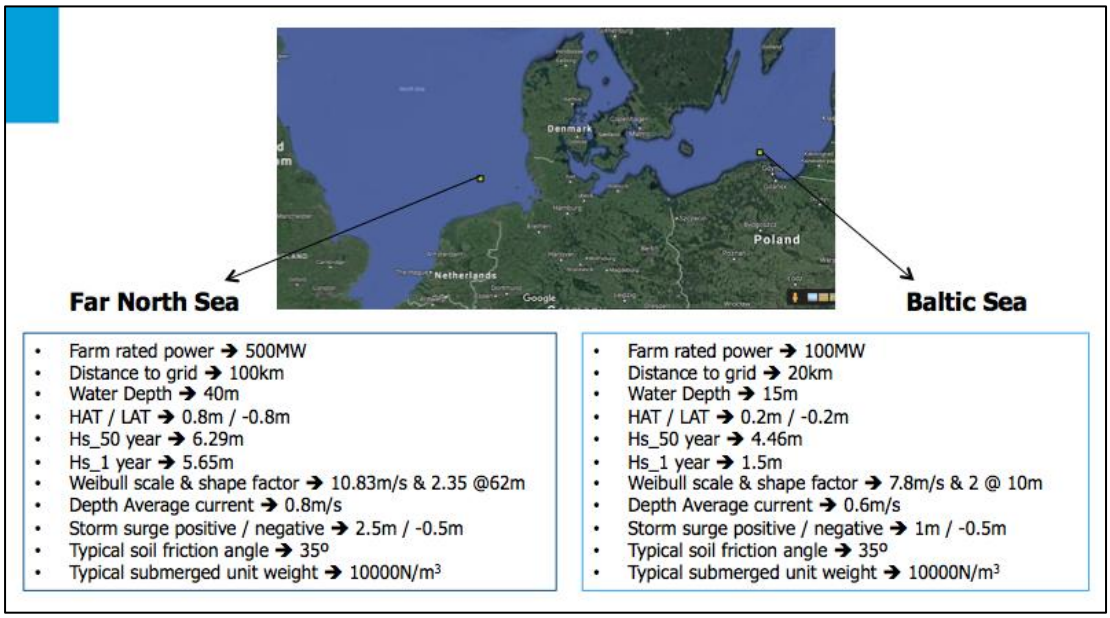

Figure 7. Main characteristics and potential locations for the two cases established

These cases allow the comparison between different conditions as shallow waters to deep waters, far offshore to near shore, large to small wind farm size and hard to soft wave conditions.

2.7. Sensitivity Study

A sensitivity analysis is a simulation analysis where key parameters are changed to judge their effect on the final outcome. It is used to identify significant factors with the aim of forecasting alternative results. In this project, the key parameters are the cost models, and the final outcome is the optimal wind turbine size.

There are several advantages of performing a sensitivity analysis. It permits the evaluation of the robustness of the complete model, thus, indicates how reliable are the results. Moreover, since the cost models present some uncertainty, performing a sensitivity study shows which components contribute the most to the uncertainty in the optimal size. Furthermore, it gives insight into the relationship between key parameters and the final result.

3. Cost Models

3.1. Chapter Introduction

As stated previously in section 2.4.1, in this project just the cost models for the turbines, the support structure, the electrical infrastructure, and the operation and maintenance are developed with more detail than the rest of the components that comprise an offshore wind farm. This chapter describes the development of the cost models of these components. Moreover, at the moment of estimating the cost models for the support structure, electrical infrastructure, and the operation and maintenance, a computational tool is utilized. This tool is outlined in the next section of this chapter.

3.2. The MZ tool

This computational tool is an offshore wind farm design emulator, developed by Dr.ir. Michiel B. Zaaijer, professor at the Delft University of Technology (Zaaijer M. B., 2013). The tool requires some inputs decided by the user to design the offshore wind farm and to estimate the different costs involved in its configuration. These inputs are detailed in Table 1.

Category	Description
Farms	The user specifies the layout of the farm setting the number of turbines in a row and the number of turbines in a column.
Sites	The user enters the parameters for the site where the wind farm is intended to be built. These parameters are related to wind climate, water levels, wave and current climate, water properties, geophysical properties, accessibility information and grid coupling point.
Turbines	The user introduces the parameters for the turbine model related to geometric properties, mass properties, aerodynamic load properties, power properties, electrical properties, operational properties and financial data. The tool only considers one turbine model for the whole wind farm.

Table 1. Tool parameter inputs

The tool works under some core concepts and configurations of wind farm hardware. The most relevant for this project are:

- The layout of the wind farm must be rectangular
- Equal spacing between the turbines in a row
- Equal spacing between the turbines in a column
- One support structure design for all positions
- The support structure is based on monopile foundation
- The electricity collection and transmission is three-phase AC
- One infield cable design for the collection system like observed in Figure 8

- Turbines in row connected to a string and each string is connected to the offshore platform as shown in Figure 8

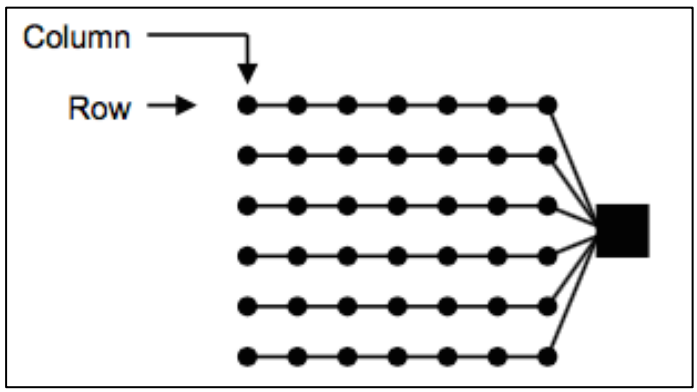

Figure 8. Layout of wind turbines and electrical collection system (Zaaijer M. B., 2013)

The objective function of the tool is the LPC. Thus, the tool gives the wind farm design that results in the lowest LPC for the input parameters introduced by the user. The tool separates the optimization problem into four disciplines. The sequence of disciplinary optimizations is depicted in Figure 9.

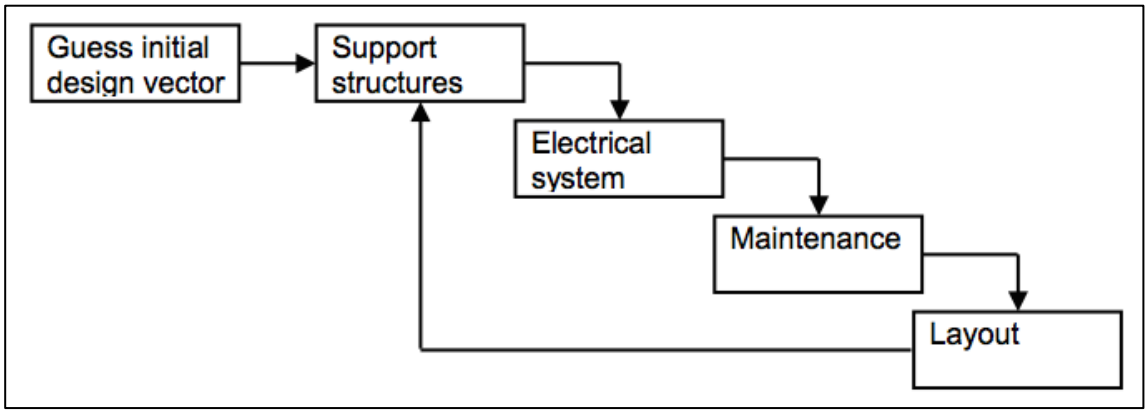

Figure 9. Sequence of disciplinary optimizations (Zaaijer M. B., 2013)

After introducing all the input parameters and running the tool, the outputs generated that constitute the design of the wind farm are specified in Table 2.

Category	Description
System	Estimation of the levelized production cost and the energy yield
Support Structures	Technical data of the design of the support structure components (monopile, transition piece, tower, scour protection) like dimensions and masses.
Layout	Spacing inside column and rows, wake efficiency, and total area used
Electrical system	Technical data of the design of the electrical infrastructure components (transformers, transmission cable, infield cable, shunt reactors) like the dimensions, voltage and current levels for the cables, the transformers winding ratios, and the power losses on each of these components.
Maintenance	Results for crew deployment, facilities, availability, downtime and total number of failures
Cost Details	Detailed estimation of the cost of the elements that compose the total capital costs, the operation and maintenance costs, and the decommissioning costs.

Table 2. Tool outputs

3.3. Turbine Cost Model

3.3.1. Overview of turbine cost components

There are many components involved in the operation of a wind turbine. Figure 10 shows some of the most relevant of these components. According to this figure, the rotor blades contribute with the 22% percent of the total cost of the wind turbine. Thus, they are the component with the second largest contribution to the total turbine cost after the tower. In this work, the tower is not part of the turbine, but it is of the support structure, which cost model is described in section 3.4. Hence, a thorough analysis is done to estimate the cost of the blades when increasing in size because they have the largest impact on the total turbine cost. This blade cost analysis is explained in the next section. For the rest of the parts that compose a wind turbine, their cost models are taken from (L. Fingersh et al., 2006), and presented in Appendix A. These parts are:

- Power converter
- Cooling system
- Nacelle cover
- Control system
- Direct drive generator
- Brake system
- Pitch mechanism
- Nose cone
- Main shaft
- Main bearing
- Yaw
- Mainframe

- Hub

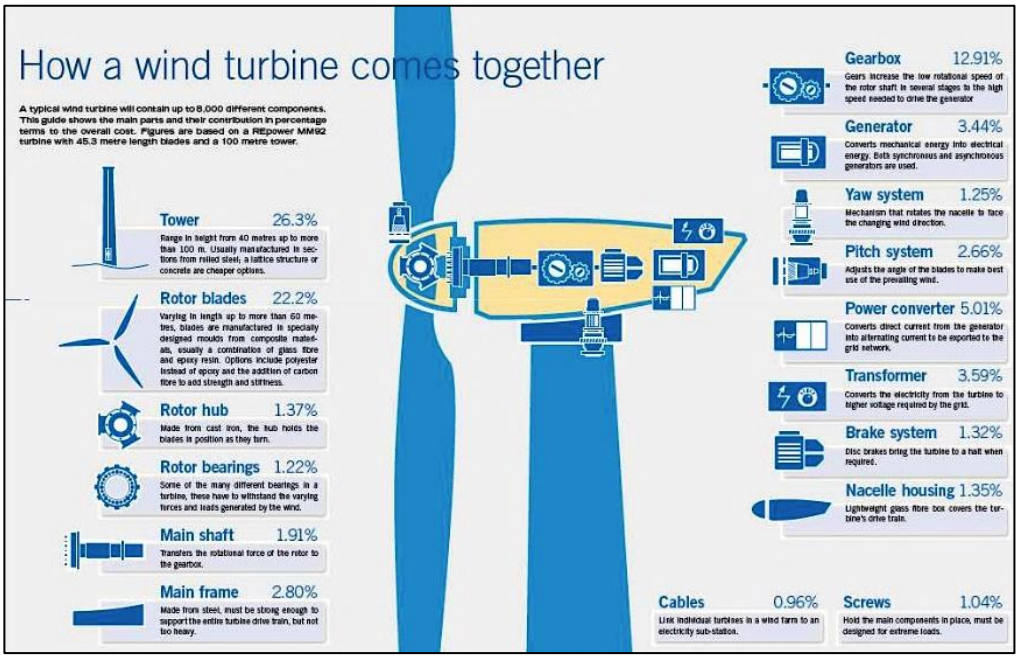

Figure 10. Main components of a wind turbine and their respective percentage contribution to the turbine total cost (EWEA, 2009)

The transformer inside the turbine is not considered in this analysis because it makes part of the electrical infrastructure cost model, which is explained in section 3.5. In addition, the gearbox system is not contemplated because it is expected that in the coming years the offshore turbines will implement a direct drive system. The reason is that wind turbines are planned to improve their reliability, and the gearbox is one of the components with the most number of failures.

3.3.2. Blade Cost Model

In order to develop a model that reasonably gives a cost estimate for the blades, especially for currently non-existing large rotor sizes, past trends in scaling, technology development, and material use are evaluated.

At the beginning of the 1980's first blades were attempted to be built in steel, but were rejected as they were too heavy, aluminum was also into consideration, but its low yield and maximum stresses brought uncertainty within the manufacturers regarding the performance of the blades against fatigue loads (Jamieson, 2011). Polyester resin reinforced with glass fiber (GI/P), came up to be the solution for both the weight and the load problem of steel and aluminum blades. The manufacturing of wind turbine blades has been dominated since then by composite materials. Nevertheless, there has been some evolution in the manufacturing and the material technology. The labor-intensive hand lay-up method was first used, but as the size of the blade increased, manufacturing automation was desired, and resin injection manufacturing methods were settled.

Likewise, epoxy resin composites present better properties than polyester resin leading to newer blades made mainly of glass fiber composed epoxy (GI/Ep). In the last years, hybrid glass-carbon blades have appeared as a solution for longer and heavier blades (Lekou, 2010). Figure 11 depicts how the mass of the blades has evolved for different materials and manufacturing methods.

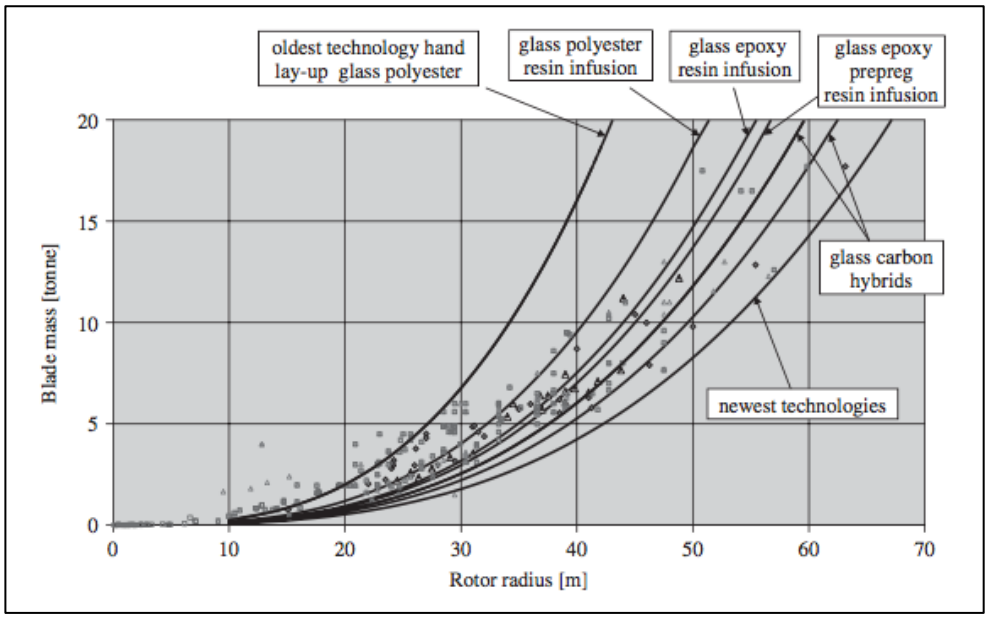

Figure 11. Blade mass scaling related to blade technologies (Jamieson, 2011)

To start with the blade cost model, data of rotor diameter and blade mass from wind turbines used in the industry is searched and plotted; results can be seen in Figure 12. Along with this data, it is plotted as well some results obtained by NREL (L. Fingersh et al., 2006) of some trends of blade mass when increasing the rotor diameter. The NREL Baseline Design gives the cost of a hand lay-up manufactured fiberglass blade. The LM-glassfiber blade model is characterized by a lower-weight root design. Moreover, the NREL Final Design provides an estimate of the blade mass if carbon fiber is incorporated into the blade. It can be observed in Figure 12 how the blade mass has changed in the last years compared to the trends forecasted. This is noticed as the industry trend gives the impression to start following the NREL Baseline Design, and as the diameter keeps increasing, the industry trend follows the LM glassfiber and the NREL Final Design trends. This shows how the technological advances of lighter root weight and the inclusion of carbon fiber have enabled the manufacture of larger wind turbine blades without a significant increase in their weight. Moreover, from the industry data, it is observed that the blade mass increases with an exponent factor of 1.82 and not with one of 3, as the square cube law suggests. This fact is expected since the square cube law does not take into account the technological advances.

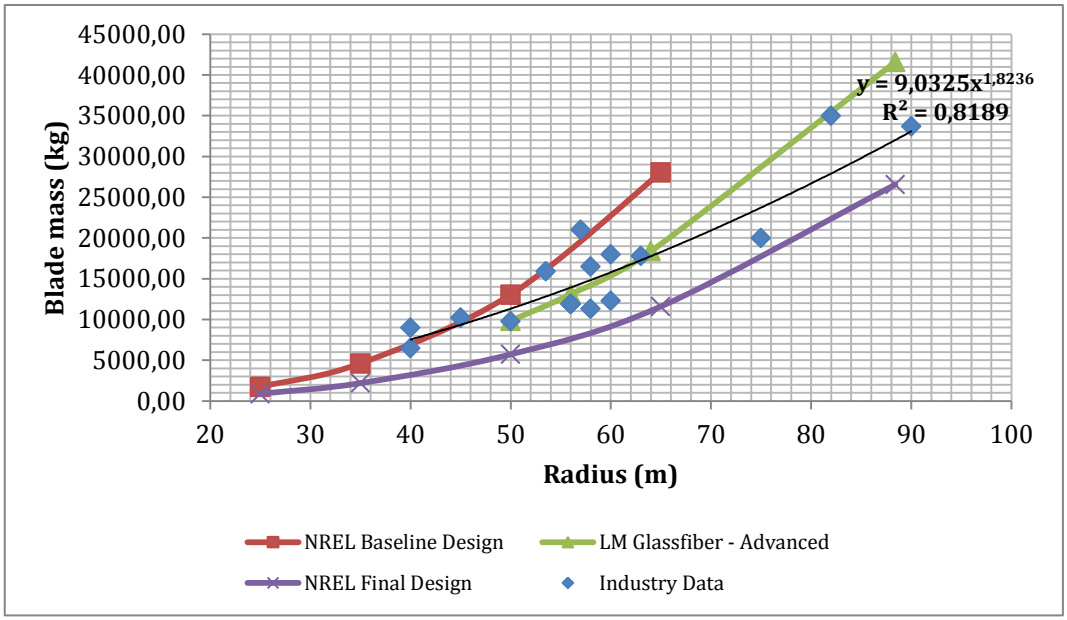

Figure 12. Blade mass as a function of the rotor radius

In Figure 13 it is plotted (green triangles) a forecast of the blade mass for wind turbines with rated powers of 10, 15 and 20MW according to the trend followed by the industry data in Figure 12 assuming a 400W/m^2 power density. In this chart, it is indicated as well the maximum and minimum rotor radius and blade mass that these 10, 15 and 20MW turbines would have for a range in power density from 300 to 500W/m^2.

Furthermore, it is observed in Figure 13 that the industry trend approaches the NREL Final Design as the rotor diameter increases. This tendency is expected because a reduction in the mass of the blades is necessary for large rotors to decrease the bending moment at the root of the blades. More use of carbon fiber in the spar of wind turbine blades is foreseen to reduce their weight. In addition, it also stiffens the blade, which is convenient since the larger the blades, the stiffer they have to be to avoid large tip deflections.

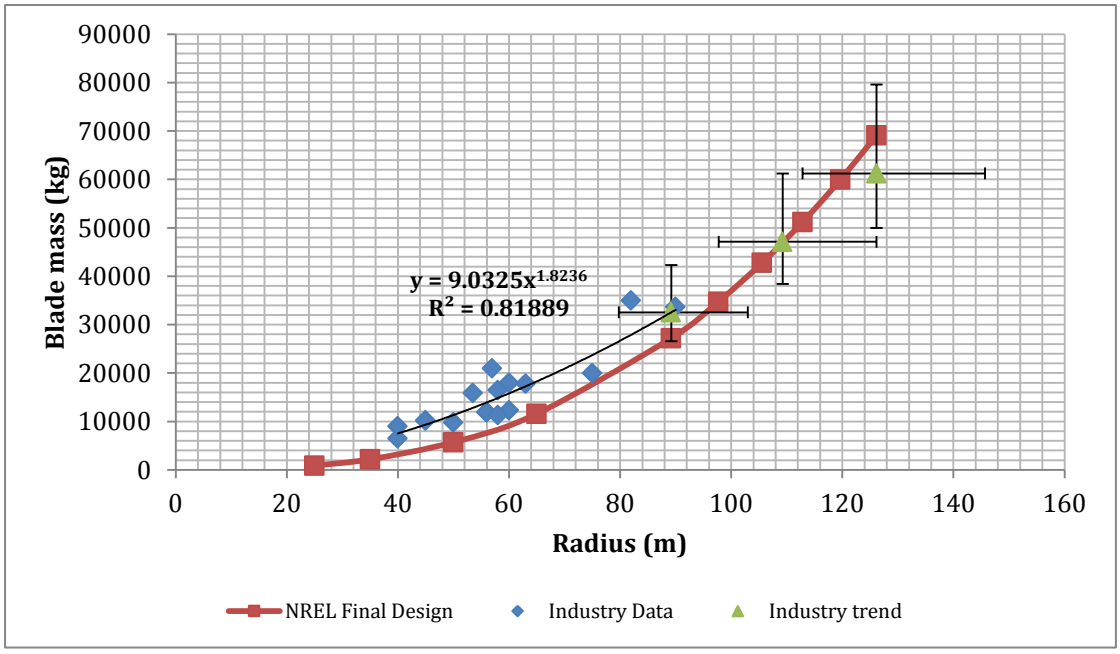

Figure 13. Blade mass forecast for wind turbines of 10, 15 and 20MW

According to (Wood, 2012), carbon fiber is currently used in the spar of wind blades larger than 45m. Besides, Figure 12 details how the industry trend (black line) follows the NREL Baseline Design up to a rotor radius of approximately 45m and then starts to separate from this later one. This separation is assumed to be the beginning of the incorporation of carbon fiber in the spar of the blade. The difference in mass between the industry trend and the NREL Baseline Design gives a weight ratio between a hybrid glass-carbon blade and an entire glass fiber blade. Calculating the weight ratio between these two trends for different rotor diameters and using Equation 4, the volume ratio between carbon and glass fiber used for a particular rotor diameter can be estimated. This volume ratio is then used in Equation 5 to calculate the material cost ratio. This material cost ratio practically means how much more a hybrid glass-carbon blade would cost than a blade entirely made of fiberglass considering the same size and axial stiffness. Later from Equation 6, it is possible to calculate the total cost ratio for a hybrid glass-carbon wind turbine blade. This total cost ratio is comprised of the material cost ratio, the labor cost ratio, and the profit & overhead cost ratio. The labor cost ratio is 1.14 as reported by (Lekou, 2010) that is how much more a wind turbine blade would cost when changing from the hand lay-up to the resin injection manufacturing method. It is assumed that the cost ratio for the profit & overhead cost when going from fiberglass to hybrid carbon-glass blades is equal to 1. The 0.3, 0.42 and 0.28 constants are the percentage contribution of labor, materials, and profit & overhead costs to the total cost of a wind turbine blade (Sandia National Laboratories , 2003).

$$\textbf{Equation 4. } r_w = \frac{1+(Volc_{/g} * S_c/S_g)}{1+(Volc_{/g} * E_c/E_g)}$$

$$\textbf{Equation 5. } r_{mc} = \frac{1+(Volc_{/g} * S_c/S_g * \$_c/\$_g)}{1+(Volc_{/g} * E_c/E_g)}$$

$$\textbf{Equation 6. } r_{tc} = 0.3 \cdot r_{lc} + 0.42 \cdot r_{mc} + 0.28 \cdot r_{p\&o}$$

where r_w is the weight ratio, r_{mc} is the material cost ratio, r_{tc} is the total cost ratio, r_{lc} is the labor cost ratio, $r_{p\&o}$ is the profit and overhead cost ratio, $Vol_{c/g}$ is the volume ratio between carbon fiber and glass fiber, S is the specific gravity, E is the axial modulus, and $\$$ is the price. The subscripts c and g relate to carbon fiber and glass fiber respectively.

The WindPACT blade cost model (L. Fingersh et al., 2006) presented in Figure 14, represents the cost of a blade made only with glass fiber employing the hand lay-up method. Therefore, the cost of a hybrid glass-carbon blade for any rotor size can be calculated when multiplying the total cost ratio by the WindPACT blade cost model. Subsequently, these blade costs are plotted as a function of the rotor radius, and a function is fitted through these points. The result is a blade cost model like the ones shown in Figure 14.

The price of carbon fiber is around 10$/lb (Plastics News, 2014), which translates into ~ 21.1€/kg. The price of glass fiber is around 2.1€/kg (de Oliveira & Fernandes, 2012), resulting in a price ratio between carbon and glass fiber of approximately 10. However, it is expected that the price of carbon fiber will decrease in the next years; therefore, it is pertinent to show blade cost models for different carbon and glass fiber price ratios. Figure 14 shows the blade cost models for a price ratio between carbon and glass fiber of 10, 7.5 and 5. As expected, the lower this price ratio, the lower the cost of a hybrid blade. Figure 15 presents the blade cost of turbines from 10MW to 20MW using the cost models depicted in Figure 14 assuming a power density of 400W/m^2. The blade cost happens to be highly sensitive to the cost ratio between carbon and glass fiber. Furthermore, the larger the rotor size, the greater this sensitivity.

The blade cost model used for the calculation of the total turbine cost is then the one described by the blue markers in Figure 14, which corresponds to a price ratio between carbon and glass fiber of 10. The total turbine cost is the sum of the blade cost according to this blade cost model and the costs of the other turbine components described in the previous section. Moreover, the other blade cost models presented in Figure 14 will be useful at the moment of performing the sensitivity analysis.

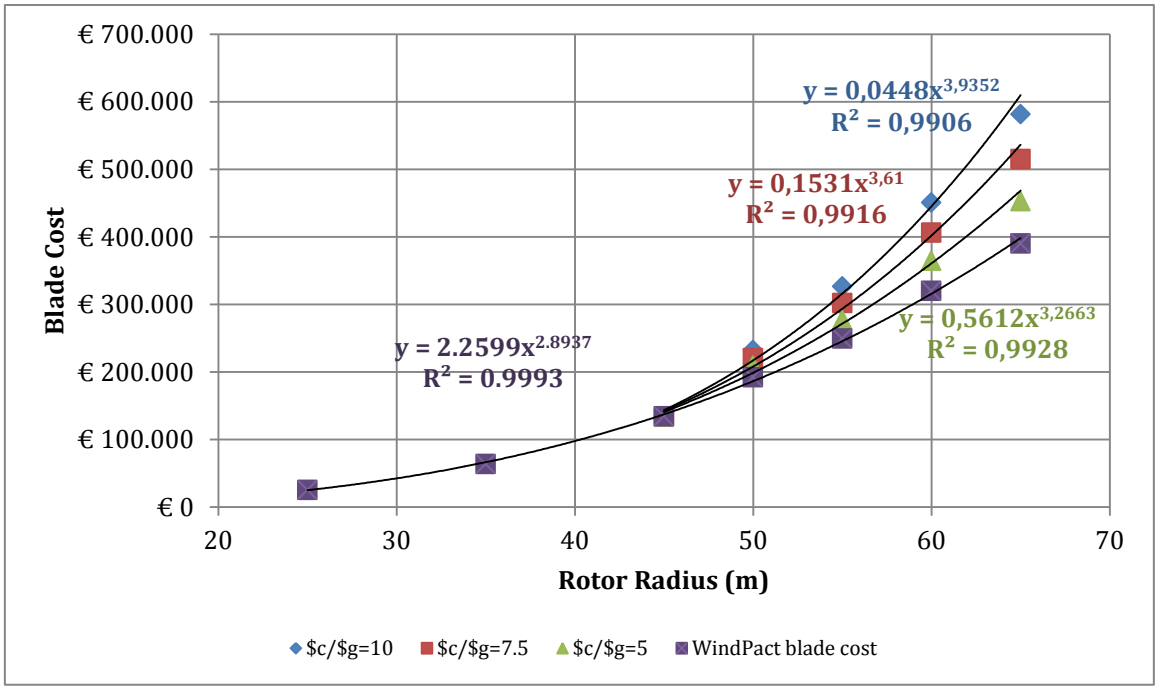

Figure 14. Blade cost as a function of rotor diameter

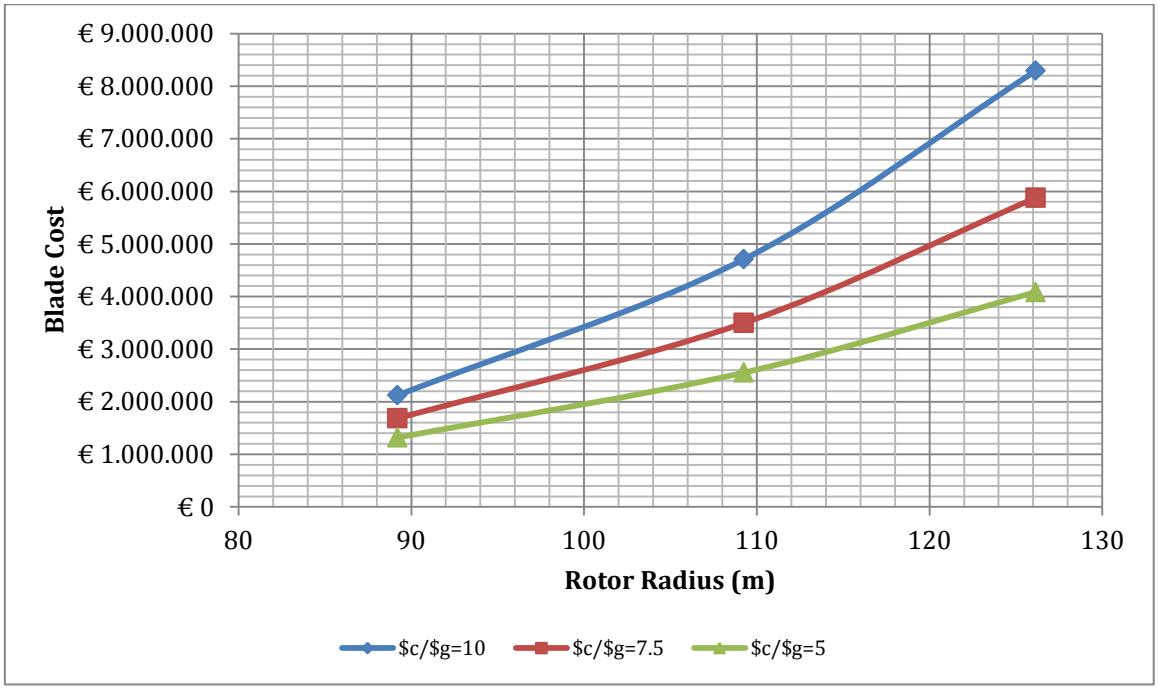

Figure 15. Sensitivity of blade cost to the price ratio between carbon and glass fiber. The markers show the blade cost of turbines of 10MW (left), 15MW (middle) and 20MW (right) for a power density of 400W/m²

3.4. Support Structure Cost Model

The support structure accounts for all the elements that from the seabed to the hub height carry the rotor-nacelle assembly. In the offshore wind industry, there are several types of foundations as monopile, gravity base, and multimember structures such as jackets or tripods. In this project, the support structure cost

model is only developed for monopiles foundations as they are currently the most preferred among the wind farm developers (EWEA, 2016). The aforementioned is because monopile structures are easy to fabricate and install. However, the water depth of the site where the wind farm is planned to be built limits their use. According to (Rosenauer, 2014), monopiles are suitable for water depths up to 30m. Nevertheless, in practice, monopiles have been used for 35 and a 36-meter water depth, as it is the case for the Gemini and the EnBW Baltic II offshore wind parks respectively. A picture of a support structure using monopile foundation can be observed in Figure 16.

In this cost model, the input is parameterized to obtain the cost of the support structure as a function of the rated power and the rotor diameter of the turbine. Moreover, the MZ tool is used to compute the support structure cost for different turbine scales.

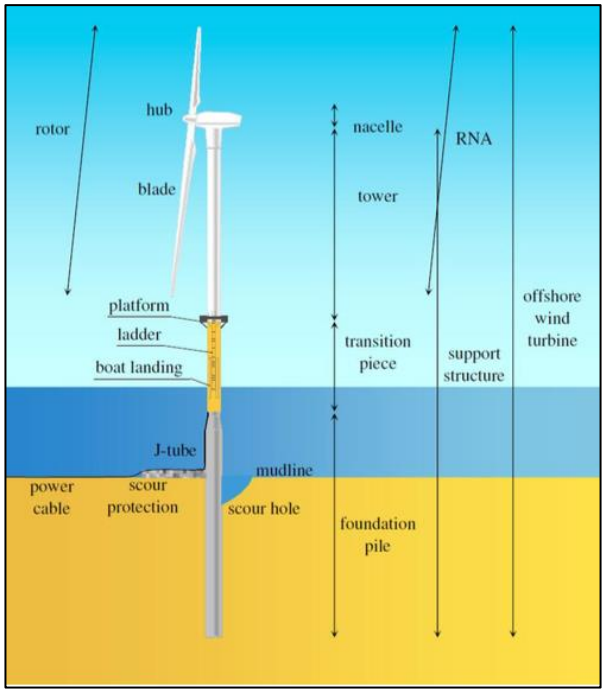

Figure 16. Offshore Wind Turbine (Velarde, 2016)

To begin with, the cost of a support structure depends on many parameters; the most significant are the water depth, the thrust force and the 50-year extreme significant wave height (Hs_50). From these three parameters, just the thrust force does not depend on the location of the wind farm but on the turbine characteristics. Both the turbine rated power and the rotor diameter are key parameters in determining the maximum thrust. Thus, it is suitable to write an expression that leaves the thrust as a function of these two parameters. In order to obtain this expression, it will be assumed that the scaled wind turbine, also referred to as the new turbine, has the same power coefficient as the reference turbine at rated power. Thus, taking Equation 7 for both the reference turbine and

the new turbine, and by setting the power coefficient equal for both, Equation 8 is reached.

$$\textbf{Equation 7.}\quad \boldsymbol{P = \frac{\pi}{8} * \rho * D^2 * V^3 * C_P}$$

$$\textbf{Equation 8.}\quad \boldsymbol{\frac{V_{new}}{V_{ref}} = \left(\frac{P_{new} * D_{ref}^2}{P_{ref} * D_{new}^2}\right)^{1/3}}$$

where P is the turbine rated power, ρ is the air density, D is the rotor diameter, V is the wind speed, and C_P is the power coefficient. The subscripts *ref* and *new* relate to the reference turbine and the new turbine respectively.

Subsequently, Equation 9 is used assuming that the new turbine has the same thrust coefficient at rated power as the reference turbine to obtain to Equation 10. Then, Equation 8 is inserted into Equation 10 to reach an expression for the thrust as a function of the power and diameter of the reference and new turbines. Equation 11 shows this expression.

$$\textbf{Equation 9.}\quad \boldsymbol{Th = \frac{\pi}{8} * \rho * D^2 * V^2 * C_T}$$

$$\textbf{Equation 10.}\quad \boldsymbol{Th_{new} = \frac{V_{new}^2 * D_{new}^2}{V_{ref}^2 * D_{ref}^2} * Th_{ref}}$$

$$\textbf{Equation 11.}\quad \boldsymbol{Th_{new} = \left(\frac{P_{new}}{P_{ref}}\right)^{2/3} * \left(\frac{D_{new}}{D_{ref}}\right)^{2/3} * Th_{ref}}$$

where Th is the thrust force, ρ is the air density, D is the rotor diameter, V is the wind speed, and C_T is the thrust coefficient. The subscripts *ref* and *new* relate to the reference turbine and the new turbine respectively.

The V80-2MW turbine is selected as the reference turbine, and from this turbine model, the cost of the support structure for the upscaled turbines is estimated. Technical data along with the power and thrust curves for this turbine can be found in Appendix C. In this project, the total cost of the support structure is composed of the following expenses:

- Tower
- Transition piece
- Grout
- Monopile
- Scour protection
- Installation Foundation

The MZ tool is used to estimate the cost of the support structure for the upscaled offshore wind turbines. For this purpose, only the part of the tool that designs the

support structure and computes its cost is used (see Figure 9). Since this cost only influences the numerator of the LPC, not affecting the energy yield, this approach can be done. To design the support structure elements, the tool uses different physical models to compute the loads, the clamping depth and the maximum weather conditions that drive the optimum design of a support structure. The tool comprises different cost models that determine each of the costs of the elements mentioned above of the support structure. To calculate the total cost, the tool needs different input parameters that define the site conditions where the wind turbine is planned to be erected. These inputs correspond to data of wind climate, water levels, wave and current climate, water properties, and geophysical properties. Some of these data are shown in Figure 7 for the locations to be analyzed and evaluated in this work.

Regarding the turbine characteristics that are the inputs required by the MZ tool to estimate the cost of the support structure, the most important are:

- Rotor radius
- Maximum operational thrust
- Yaw diameter
- Front area nacelle
- Tower top mass

The rotor radius is needed by the tool to calculate the hub height. Moreover, the rotor radius is also used in Equation 11 to calculate the maximum operational thrust force for the upscaled turbine. Besides, Equation 11 also needs the power of the upscaled turbine to find this thrust. Therefore, a rotor diameter is calculated for wind turbines with rated powers ranging from 2MW to 20MW in steps of 1MW. To compute these rotor diameter sizes, the empiric relationship between power and diameter that is displayed in Figure 2 is used. Subsequently, with the values of the rotor diameter and the turbine power for the upscaled turbines, it is possible to calculate now the maximum operational thrust, which is the second input for the MZ tool listed above. Since the last three parameters in the list do not have as much influence on the total cost of the support structure compared to the rotor radius and the maximum thrust, they are scaled in a simpler way. Thus, for every combination of power and diameter obtained to find the maximum operational thrust, the yaw diameter, the front area nacelle, and the tower top mass are calculated using the square cube law taking the V80-2MW turbine dimensions as the reference.

Having all the MZ tool inputs at hand, it is proceeded to estimate the cost of the support structure for the Far North Sea and the Baltic Sea locations for turbine rated powers ranging from 2MW to 20MW. Then, the support structure costs are plotted as a function of the thrust values used in their calculation, and a function is

fitted through the points. The mathematical expressions of the functions fitted are shown in Figure 17 and Figure 18. These two expressions represent the support structure cost models used in this project for the Far North Sea case and the Baltic Sea case respectively. According to Figure 17 and Figure 18, the cost of the support structure is larger for the Far North Sea case. The larger water depth and rougher wave conditions in this site clarify this result.

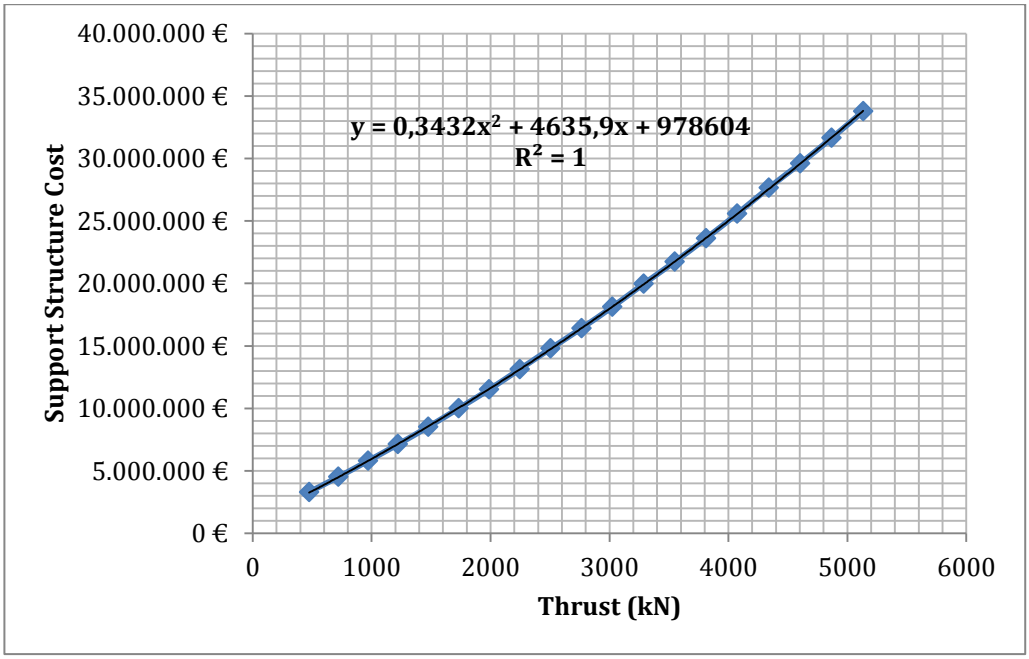

Figure 17. Support structure cost model for the Far North Sea case

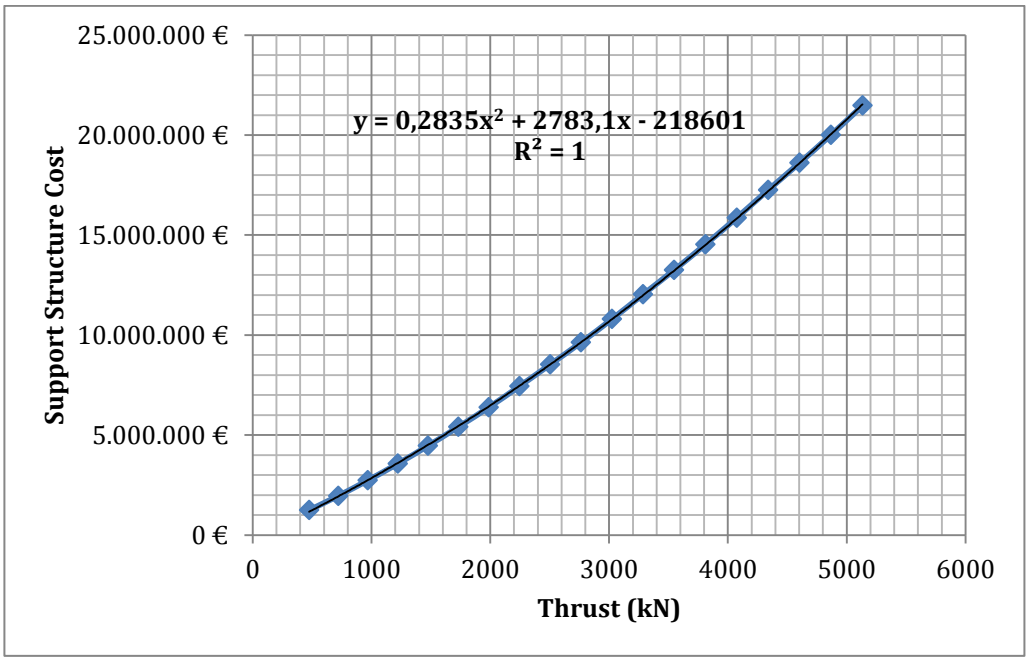

Figure 18. Support structure cost model for the Baltic Sea case

3.5. Electrical Infrastructure Cost Model

There are two ways in which electricity can be transported from the turbines at the offshore wind farm to the grid coupling point. The first one and most common is HVAC (High Voltage Alternating Current). This type of transmission is cost-effective up to 100km distance to shore because induction compensation requirements become difficult to meet (Schachner, 2004). Moreover, as AC cables produce reactive current, the capacity for transporting active 'real' power diminishes when the distance to shore increases. The second way of transmitting the electricity generated in the offshore wind farm to the grid is by HVDC (High Voltage Direct Current). This form of transmission has high initial costs as a result of AC/DC and DC/AC converters plus filters. Nonetheless, it is cost effective for distances larger than 100-120km from the wind farm to the shore because it does not need reactive power compensation (Rueda, 2016). Since most of the offshore wind farms actively working are not located farther than approximately 80km from the coast, this type of transmission is barely used. It is expected in the next years when offshore wind farms will be constructed farther from the coast in search of stronger winds, that HVDC transmission will be more used than HVAC.

In this project, the HVAC transmission is selected for both cases considering that the locations are within the optimal distance range. In the same way, as with the estimation of the support structure cost, the MZ tool is used to calculate the electrical infrastructure cost. Nevertheless, for this case, all disciplinary optimizations in Figure 9 need to be run because the cost and efficiency of the electrical infrastructure depend on the layout of the wind farm. There is a trade off made between electrical infrastructure cost and wake efficiency, which is determined by the layout of the wind farm. Therefore, the layout optimization also needs to be run. The electrical infrastructure cost model developed is only dependent on the rated turbine power. The reason behind this statement is explained in the paragraphs below.

The tool's design algorithm of the electrical infrastructure concentrates only on the elements that take part on the fundamental function of the system that is transmitting the electricity generated by the wind turbines to the grid. These most relevant parts are listed below:

- Infield cables
- Transmission cable
- Shunt reactor
- Onshore transformer
- Offshore transformer
- Turbine transformers
- Switch gear

Cost models for all these components are included in the tool, allowing the estimation of the cost of the electrical infrastructure for an offshore wind farm.

The MZ tool inputs that set the conditions for the design of the electrical infrastructure are:

- Distance to shore
- Voltage at grid coupling point
- Voltage of the turbine generator

The distance to shore is set to be 100km for the Far North Sea case and 20km for the Baltic Sea case. The voltage at the grid coupling point is settled as 400kV for both sites, considering that is a standard grid voltage used in northwestern European countries as Denmark and the UK. For the turbine generator voltage, a search of this value for wind turbines currently in operation is done, although not much information about it is found. Thus, an interpolation through the few data retrieved is done using the *interpolate.interp1d* function of scipy to estimate the generator voltage for different turbines. Although this way of calculating the generator voltage may not be highly accurate, it is enough for the calculation of the electrical infrastructure cost, as the effect of this voltage level is not significant in the estimation of this cost. Appendix D explains in more detail the procedure followed to calculate the generator voltages for the turbine rated powers considered in Table 3. The choice of turbine powers in Table 3 is explained in the next paragraph.

Far North Sea 500MW OWF		**Baltic Sea 100MW OWF**	
Turbine Power (MW)	**Generator Voltage (V)**	**Turbine Power (MW)**	**Generator Voltage (V)**
1.95	690	2.04	690
4.13	2300	4.00	2150
6.17	6600	6.25	6600
7.81	7580	8.33	7900
10.20	9035	11.11	9590
11.90	10070	12.5	10435
13.89	11280	16.67	12973
16.67	12973	25	18044
17.86	13700		
20.00	15000		

Table 3. Generator voltage for the turbines considered

The rated power of the turbine drives the total cost of the electrical infrastructure since the infield cable and the transmission cable are designed according to the

flow of current that passes through them, and these cables take the largest part of the total cost. Hence, to express the cost of the electrical infrastructure as a function of the rated power of the turbine a fixed rated power for the wind farm is established. As previously said, in the case of the Far North Sea case, this rated power is 500MW, and for the Baltic Sea case, it is of 100MW. The layout of the wind farm plays a significant role in the calculation of the electrical infrastructure cost. Thus, a square layout is set for different turbine rated powers. In this manner, it can be ensured that the layout does not significantly influence the estimated cost of the electrical infrastructure. However, layouts with an equal number of rows and columns lead to large gaps in turbine power for the higher powers, so a few layouts in which they deviate from equal numbers are added. The layouts with their corresponding turbine rated power used in each case are shown in Table 4.

Far North Sea 500MW OWF		**Baltic Sea 100MW OWF**	
Layout	**Turbine Power (MW)**	**Layout**	**Turbine Power (MW)**
16x16	1.95	7x7	2.04
11x11	4.13	5x5	4.00
9x9	6.17	4x4	6.25
8x8	7.81	3x4	8.33
7x7	10.20	3x3	11.11
6x7	11.90	2x4	12.5
6x6	13.89	2x3	16.67
5x6	16.67	2x2	25
4x7	17.86		
5x5	20.00		

Table 4. Layouts employed for the 500MW and 100MW offshore wind farms

After establishing the different layouts with their corresponding turbine power, the MZ tool is run to obtain the electrical infrastructure cost. At the moment of each run, the rotor diameter used for each turbine power is calculated according to the empirical trend depicted in Figure 2 like in the support structure cost calculation in section 3.4. The results obtained for the cost of the electrical infrastructure are shown in Figure 19 and Figure 20. In both charts, the blue and red points are the results estimated by the tool. However, in the case of the red points, a non-square layout was used, which influences the results and changes the trend in the cost. Therefore, these red points are not considered for the cost model in both case studies. The green points are plotted to project the behavior of the electrical infrastructure cost for different rated powers. These green points are calculated using the *interpolate.interp1d* function of scipy. For this function, the kind of interpolation chosen is quadratic because it showed to be the one that better fitted the data computed with the tool.

It is noticed that the cost of the electrical infrastructure for the Far North Sea case decreases rapidly in the 2−6 MW range, and then up to 15.5 MW, it keeps falling at a much lower rate. From 15.5 MW, where the cost seems to reach the minimum value, the cost slightly increases until 20MW. In the range of 10 to 20MW rated power, the cost variation is not more than 3.4%. Therefore, according to these results, it can be stated that the cost of the electrical infrastructure maintains relatively constant in this power range.

Concerning the Baltic Sea case, first, it must be said that a turbine rated power of 25MW have to be taken into account because there is not a different layout other than 1X5 or 5X1 to achieve a farm rated power of 100MW with 20MW turbines. Since the tool only works for layouts in which the number of rows and columns is bigger than one, a layout of 2X2 using 25MW turbines is used.

As in the Far North Sea case, it is observed in Figure 20 that the cost of the system decreases with a steep rate in the range of 2 to 6MW. Moreover, the cost continues falling smoothly until ~ 17MW rated power. From that point, the cost increases until reaching 25MW. The cost of the system does not vary more than a 5% in the range from 11 to 20MW even though the curve does not look as smooth as in the case of the of the Far North Sea case. In the same way, it can be stated that the cost of the electrical infrastructure is nearly constant for this power range. Basically, the behavior of the electrical infrastructure cost as a function of the turbine rated power is the same for both locations. It decreases steeply at the beginning, then it comes to a minimum around 15-17MW and then slightly increases until 20MW. Additionally, the cost of the system is roughly 11 to 12 times larger for the Far North Sea than for the Baltic Sea site for the same rated power of the turbine.

Due to the shape of the trend that the computed data shows, it is not possible to do a curve fit on it to get a cost model function. Therefore, an interpolation is made to calculate the cost of the electrical infrastructure for any rated power in the range of 2 to 20 MW for the two cases.

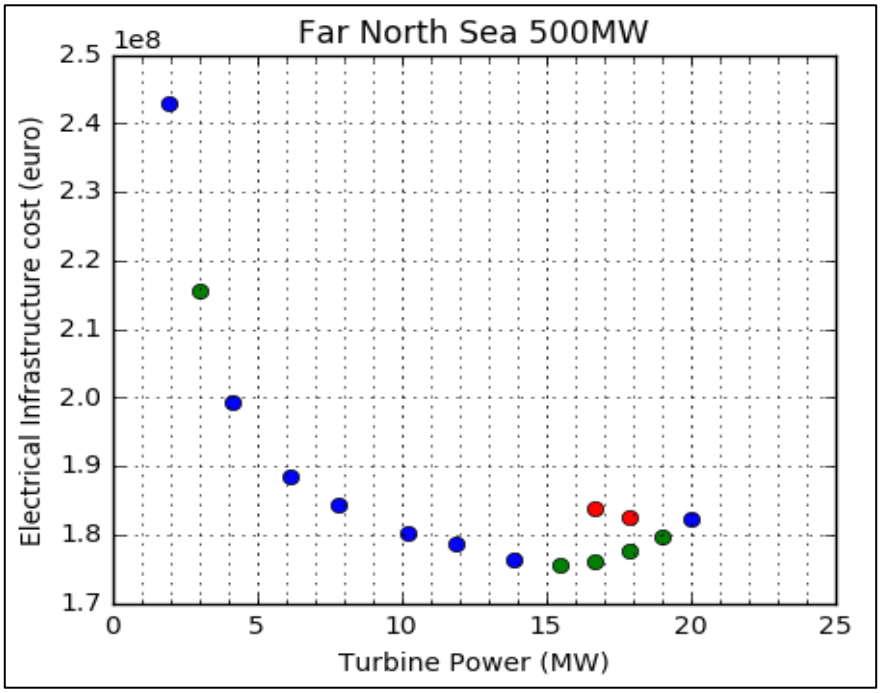

Figure 19. Electrical infrastructure cost for the Far North Sea case. The blue and red points are the results estimated with the MZ tool. The red points correspond to a non-square layout, which deviate from the electrical infrastructure cost trend. The green points are calculated using the *interpolate.interp1d* function of scipy

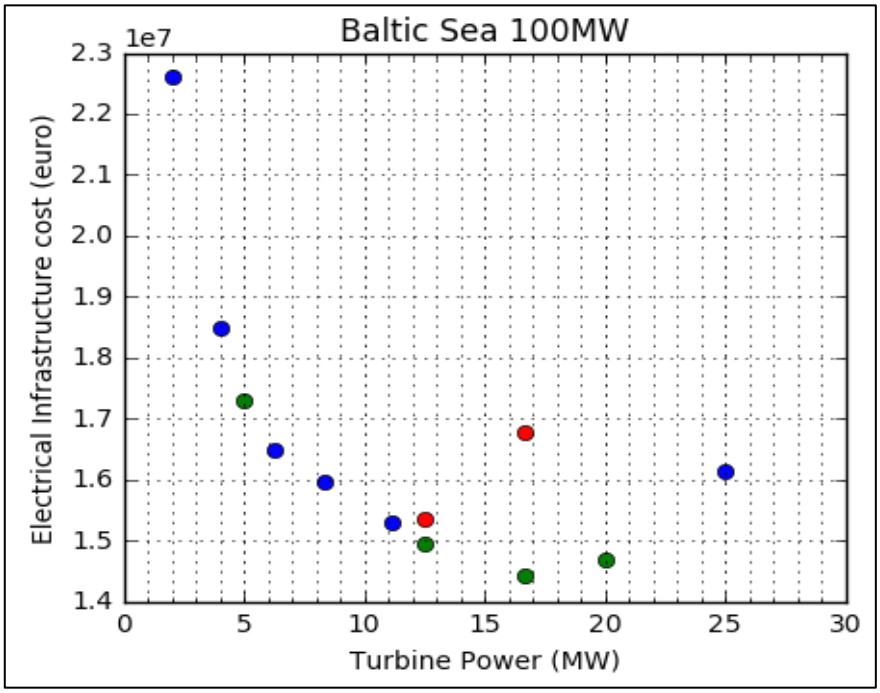

Figure 20. Electrical infrastructure cost for the Baltic Sea case. The blue and red points are the results estimated with the MZ tool. The red points correspond to a non-square layout, which deviate from the electrical infrastructure cost trend. The green points are calculated using the *interpolate.interp1d* function of scipy

3.6. O&M Cost Model

In the offshore wind industry O&M accounts for approximately the 23% of the total project expenses, and to 25 to 30% of the cost of energy generated. Moreover, according to (Ashuri, 2012) “Many cost elements such as operation and maintenance and infrastructure may decrease per rated MW capacity with fewer larger machines for the same installed capacity." Hence, for the realization of this project, it is important to estimate how this part of the LPC behaves for different wind turbine sizes. The O&M cost can be decomposed in some other subcomponent costs. Thus, to obtain a total O&M cost model several cost models that relate to these subcomponents are developed. As with the modeling of the electrical infrastructure cost, the MZ tool is used, and all the disciplinary optimizations shown in Figure 9 are run.

When comparing to onshore wind farms, the percentage of O&M in the cost of energy ranges between 5 to 10%. According to (Karyotakis & Bucknall, 2010), there may be two reasons to attribute such a difference in the O&M cost between offshore and onshore wind farms. First, to the impact of operating a wind turbine in a marine environment where the turbines are stressed in a harsher maritime climate, so the accessibility for maintenance and repair is reduced by sea-state and weather conditions. Second, it is more expensive to make a visit to a farm that is offshore because of the distance to shore and the costs for the special equipment needed. In the next years, it is foreseen that most of the wind turbines installed offshore will have a direct drive train instead of a gearbox. The gearbox is one of the parts of the wind turbine that wears out easier. The numerous wheels and bearings in a gearbox have to withstand huge stress from wind turbulence, and any defect in a component can cause the turbine to stop operating. As a consequence, the gearbox is the part of the turbine that needs more maintenance. When going for a direct-drive system, the number of failures in the turbine decreases improving its reliability. According to Henrik Stiesdal, chief technology officer of Siemens Wind Power, his estimation is that by 2021 all of the 6MW offshore wind turbines and up will incorporate a direct-drive system (Power Engineering, 2011).

To model the total O&M cost, first, it is necessary to differentiate between operation costs and maintenance costs. Each of these two components is made of other subcomponents. Furthermore, for each of them, it is appropriate to determine how their behavior is when considering different wind turbine sizes for the same offshore wind farm installed capacity. For operation costs, which cost models are described in Appendix A, the following items are taken into account:

- Administration cost, which is assumed as a fixed cost for the two cases, independent of the turbine size or the farm rated power.

- Grid charge cost, which depends on the energy yield per year of the wind farm.
- Bottom lease cost, which is proportional to the area of the wind farm.
- Insurance cost, which is proportional to the number of turbines and the cost of the RNA.

Regarding the maintenance costs the following elements are considered:

- Consumable repairs, which accounts for all the spare parts cost. The individual spare parts cost are proportional to turbine rated power. The consumable repairs cost is dependent on the number of failures and the number of turbines.
- Consumables service or preventive maintenance, this cost grows proportionally to wind turbine rated power. In this model, preventive maintenance is assumed to happen twice a year.
- Personnel costs and access vessels costs, which are highly dependent on the number of mobilizations and consequently on the number of turbines in the wind farm.
- Lifting equipment cost, which is dependent on the number of mobilizations and the number of wind turbines, but additionally on the hub height of the turbine.
- Subsea inspection cost, which is assumed to be a fixed cost per turbine regardless of the size of the turbine.

In order to estimate each of these costs but the grid charge, the MZ tool is used. The tool returns each of these subcomponents costs. The operational properties inputs of the turbine category in the tool are set according to the rated power of the turbine. These inputs are the preventive maintenance cost and the cost of the spare parts. The tool divides the spare parts into three categories: needs diagnosis, no diagnosis, needs lifting. These inputs mentioned above are assumed to increment linearly with the rated power of the turbine, taking as a reference the ones for the V80-2MW (Zaaijer M. B., 2013). The inputs of the reference turbine are shown in Table 5.

Component	Cost (€)
Preventive maintenance	1,250
Spare parts - needs lifting	210,000
Spare parts - needs diagnosis	1,100
Spare parts - no diagnosis	1,600

Table 5. Preventive maintenance and spare parts cost of the reference turbine

Generally, the cost of a wind turbine is estimated in terms of €/MW. Thus, it is reasonable to assume the costs depicted in Table 5 in terms of the rated power of

the wind turbine. For example, for a 4MW turbine these costs will double, and for a 20MW turbine, these costs are estimated to be ten times larger.

After running the tool for the different layouts presented in Table 4 for both cases, it is found that the costs of the preventive maintenance and the consumables repairs keep almost constant. For the Far North Sea case, these costs range between 6,686,924 € to 6,827,053 € for the consumable repairs and between 624,000 € to 625,125 € for the preventive maintenance. While for the Baltic Sea case, these costs range between 1,373,641 € to 1,384,255 € for the consumables repairs and between 124,950 € to 125,025 € for the preventive maintenance. These results were expected since when turbines start increasing in size, the cost of the consumable repairs and the preventive maintenance do as well, and the number of turbines for the same rated power wind farm decreases in the same proportion. For example, if 2MW wind turbines are used for a 500MW wind farm, it would be needed ten times fewer turbines when building this farm with 20MW turbines, but the costs of these consumable repairs and preventive maintenance increase ten times. Therefore, leading to an almost constant cost of these elements for the different turbine rated powers considered in each of the two cases. These constant costs are calculated as the average of the results and can be seen in Table 6.

Component	Case	Cost (€)
Preventive Maintenance	Far North Sea	624,795
	Baltic Sea	124,989
Consumables repairs	Far North Sea	6,807,362
	Baltic Sea	1,375,553

Table 6. Cost of the preventive maintenance and consumables repairs for the two cases

According to the results shown above it could be assumed that the cost of the consumables repair and preventive maintenance are a function of the farm rated power. Hence, the cost models of these two parameters are as expressed in Equation 12 and Equation 13.

$$\textbf{Equation 12. } C_{PM} = c_{pm} \cdot P_{farm}$$

$$\textbf{Equation 13. } C_R = c_r \cdot P_{farm}$$

where C_{PM} is the preventive maintenance cost, C_R is the consumables repairs cost, P_{farm} is the farm rated power, c_{pm} is the preventive maintenance cost coefficient equal to 1250€/MW/year for both cases, and c_r is the consumables repairs cost coefficient equal to 13615€/MW/year and 13755€/MW/year for the Far North sea case and the Baltic sea case respectively.

Regarding the elements left in the maintenance costs, the cost models proposed are depicted in Figure 21 and Figure 22 for the two cases. The data points in these

charts correspond to the same power ratings and layouts used for the electrical infrastructure cost modeling. Each of the components that make part of this cost model presents the same trend, however, not the same exponent value as registered in Table 7. From this table, it is noticed that the subsea inspection cost is the only one that is exclusively a function of the number of turbines. Moreover, it is noticed as well that for the Far North Sea case the components of personnel cost and access vessels cost have an exponent value close to -1. This means that these two elements are almost entirely a function of the number of turbines and thus inversely proportional to the turbine rated power. Furthermore, with respect to the lifting equipment cost, it was stated previously that it is dependent on the number of mobilizations and the hub height of the wind turbine. The exponent value of this component is around -0.6, which evidently shows the effect of the hub height in the cost. For simplicity of the model, these four elements are coupled as one cost and as a function of just the turbine power. Even though these components are influenced by other variables, the curve fit shows a high correlation between their cost and the turbine power, which is illustrated in Figure 21.

Concerning the Baltic Sea case, it perceived that the first three components have an exponent value in the range of -0.45 to -0.65. Taking into account that in this case, the number of turbines is five times lower, the influence of the number of turbines decreases as well, and the exponent values get farther from -1. Thus, this outcome is coherent. Likewise, for this case, the four components are added up and assumed as a function of only the turbine power. The result is depicted in Figure 22 from where it is observed that the correlation between the cost and the turbine power is high as well.

Component	Case	Exponent
Personnel	Far North Sea	-0.913
Access Vessels	Far North Sea	-0.92
Lifting Equipment	Far North Sea	-0.583
Subsea Inspections	Far North Sea	-1
Personnel	Baltic Sea	-0.456
Access Vessels	Baltic Sea	-0.55
Lifting Equipment	Baltic Sea	-0.65
Subsea Inspections	Baltic Sea	-1

Table 7. Exponent factors for the different components and cases

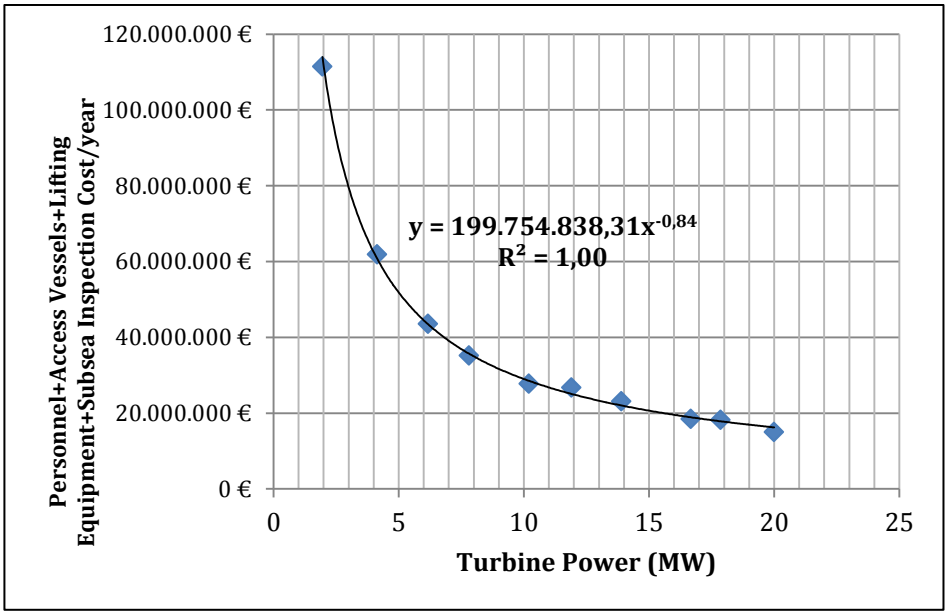

Figure 21. Cost model for the Personnel, Access Vessels, Lifting Equipment and Subsea Inspections for the Far North Sea case

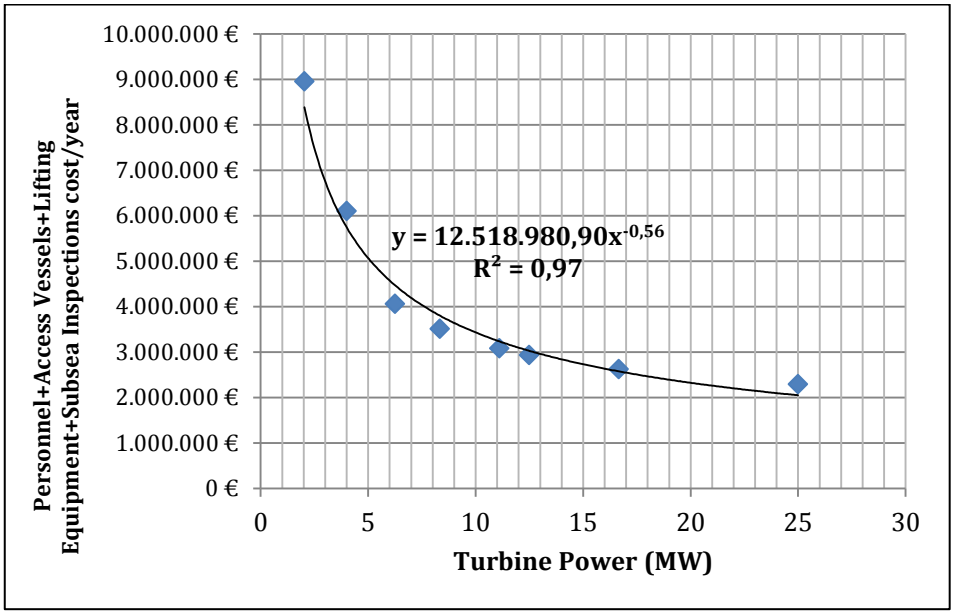

Figure 22. Cost model for the Personnel, Access Vessels, Lifting Equipment and Subsea Inspections for the Baltic Sea case

Concerning to the operational costs, the insurance cost is constant for every layout considered because it is purely a function of the RNA cost and the number of turbines as shown in Appendix A. The RNA cost is assumed to scale with the ratio of the upscaled turbine rated power to the reference turbine rated power. Thus, the increment in the cost of the RNAs is compensated to the same amount by the reduction in the number of turbines for every layout. The cost of the reference turbine is 1,500,000€ (Zaaijer M. B., 2013). In like manner as in the preventive maintenance cost model and the consumables repairs cost model, the insurance

cost model can be expressed as a function of the farm rated power. Equation 14 express this cost model.

Equation 14. $C_I = c_i \cdot P_{farm}$

where C_I is the insurance cost, P_{farm} is the farm rated power and c_i is the insurance cost coefficient equal to 7500€/MW/year.

Considering the bottom lease cost, it is only a function of the area used by the wind farm according to its cost model presented in Appendix A. The results obtained with the tool showing the variation in the area used for different turbine rated powers are depicted in Figure 23 and Figure 24 for the Far North Sea case and the Baltic Sea case respectively. It is noticed that the larger the turbine rated power, the lesser area used for the offshore wind farm. This result is consistent with the fact that the higher the turbine rated power, the fewer number of turbines needed for a wind farm with a fixed rated power. Moreover, if the number of turbines is small, the wake effects are small as well. Therefore, less area usage is demanded. Nevertheless, the extent of the area used is not highly dependent on the number of turbines as it is shown by the exponent of the mathematical expressions depicted in both charts. These exponents show the influence that has the wake effects on the amount of area used. For the Baltic Sea case, this influence is lower due to the smaller size of the wind farm with respect to the Far North Sea case. Hence, it is coherent that the exponent value is much closer to -1 for this case. Furthermore, the area used is also dependent on the rotor diameter of the turbine because it would be expected that for a larger rotor, the area used would be larger as well. However, to get a function of the area used that is also dependent on the rotor diameter would require running the MZ tool many times. Thus, for simplicity, it is assumed that the area used is only dependent on the turbine rated power. Since the bottom lease cost is around the 10% of the total O&M cost, this assumption does not have an appreciable effect on the calculation of the LPC and consequently in the final results of this project. The rotor size for the power ratings depicted in Figure 23 and Figure 24 is calculated according to the empirical trend shown in Figure 2. The area of the farm is calculated then as a function of the turbine rated power with the expressions shown in Figure 23 and Figure 24. Subsequently, the area computed is entered in the bottom lease cost model to obtain the cost.

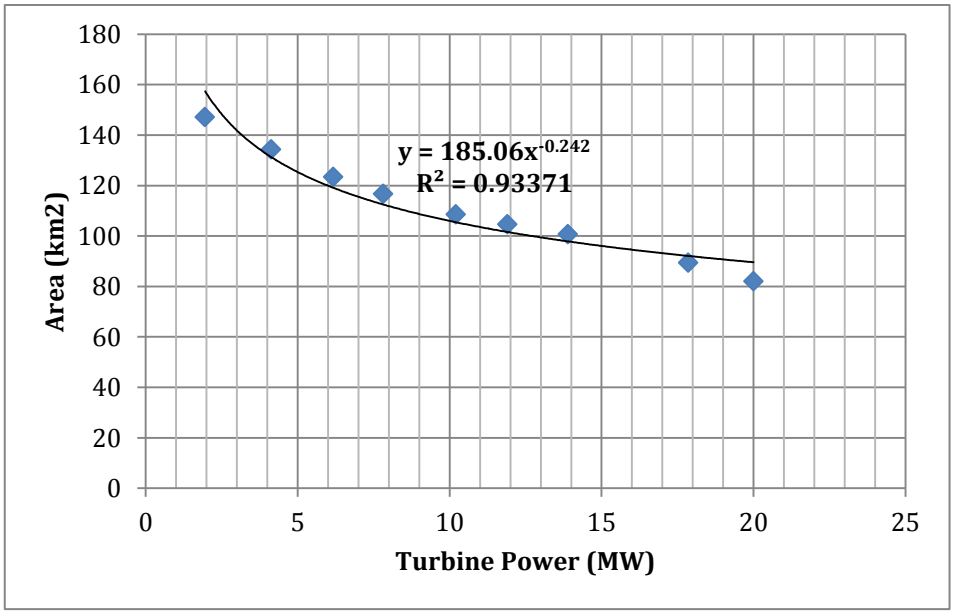

Figure 23. Area used for different turbine rated powers in the Far North Sea case

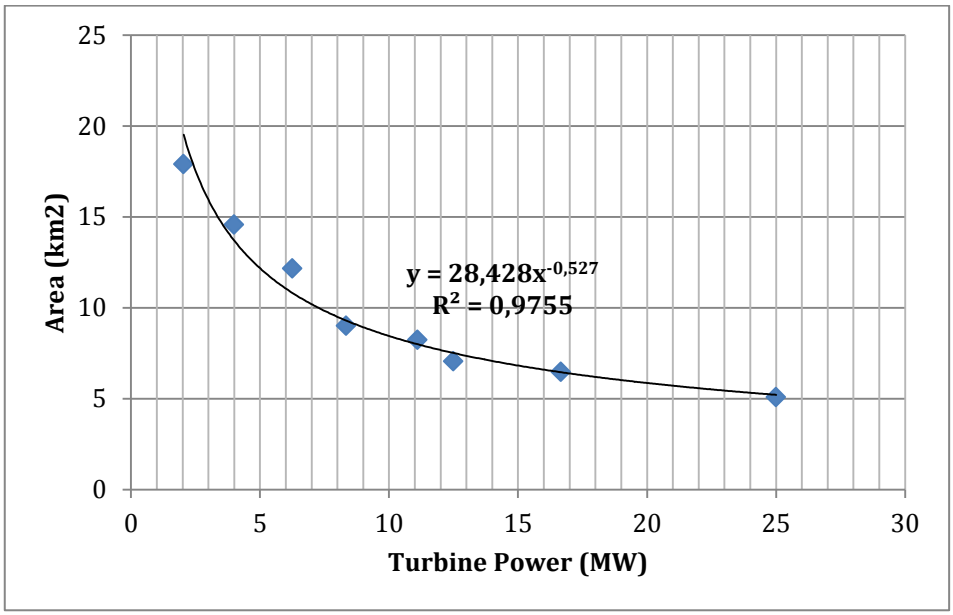

Figure 24. Area used for different turbine rated powers in the Baltic Sea case

The grid charge cost is solely a function of the energy yield produced per year as indicated by its cost model presented in Appendix A. The calculation of the energy yield is explained in the next chapter. In addition, O&M management cost is estimated to be 3% of the total O&M cost per year.

4. Energy Yield Model

4.1. Chapter overview

This chapter first explains how the energy yield in a wind turbine is calculated. Then, since the energy yield depends on the power curve of the turbines, it is later explained how the power curve is estimated for different turbine scales. The energy yield model is then a function of the rotor diameter and the turbine rated power. Later, it is described how the wind speed is computed for different turbine hub heights for each case study. Finally, the calculation of the wind farm energy yield for every turbine scale is defined. Besides, as stated in section 2.4.2, some other components affect the farm energy yield apart from the individual turbine energy output, which are the wake efficiency, the electric losses, and the availability. These components are not taken into account in the energy yield model developed in this project for the reasons given at the end of this chapter.

4.2. Energy Production

The energy yield that a wind turbine produces per year can be determined from Equation 15.

$$\textbf{Equation 15. } \boldsymbol{E_y = T_{hr} \cdot \int_{V_{in}}^{V_{out}} P(U) \cdot f(U)\, du}$$

where E_y is the energy yield, T_{hr} is the number of hours in a year, V_{in} is the cut-in wind speed, V_{out} is the cut-out wind speed, $P(U)$ is the power that the wind turbine generates at a wind speed U according to its power curve, and $f(U)$ is the Weibull probability density function.

Figure 25 shows the power curve of the V80-2MW turbine. For this turbine, it is observed that its cut-in and cut-out wind speeds are 4 and 25m/s respectively. The cut-in speed is the wind speed at which the turbine starts moving and generating electricity, while the cut-out speed is the wind speed at which the rotor is brought to a halt to protect the wind turbine structure from excessive loading. Furthermore, Equation 16 expresses the Weibull probability density function. This function just needs the scale factor and the shape factor to reproduce the wind speed distribution at a particular site. Figure 26 depicts the Weibull distribution for the wind regime at Horn Rev at a reference height of 62m (Zaaijer M. B., 2013). The probability that the wind speed U occurs within the range du is calculated as $f(U) \cdot du$.

Equation 16. $$f(U) = \frac{k}{a} \cdot \left(\frac{U}{a}\right)^{k-1} \cdot e^{\left(-\left(\frac{U}{a}\right)^{k}\right)}$$

where k is the shape factor, a is the scale factor, and U is the wind speed.

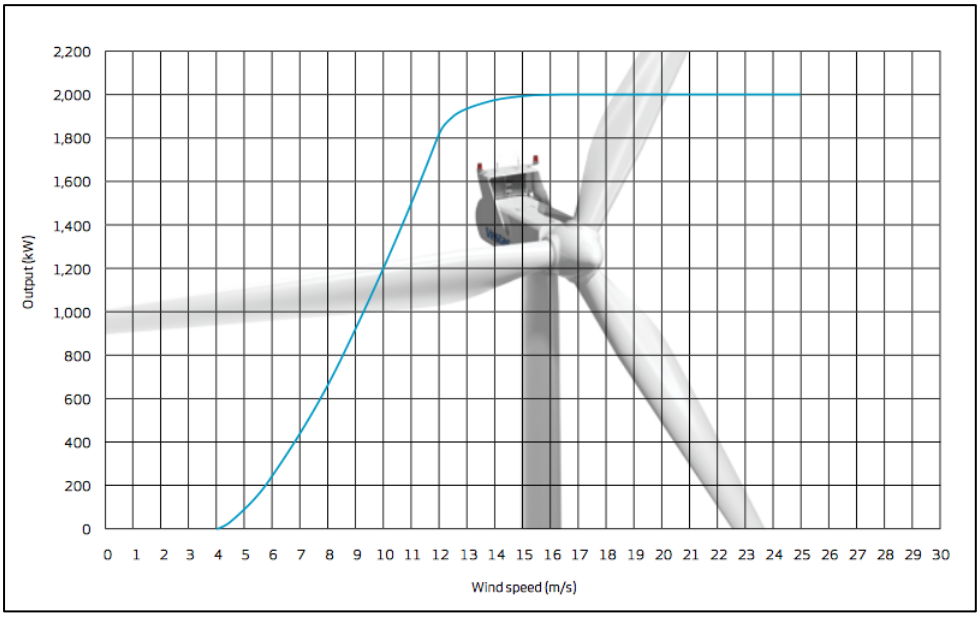

Figure 25. V80-2MW power curve (Vestas)

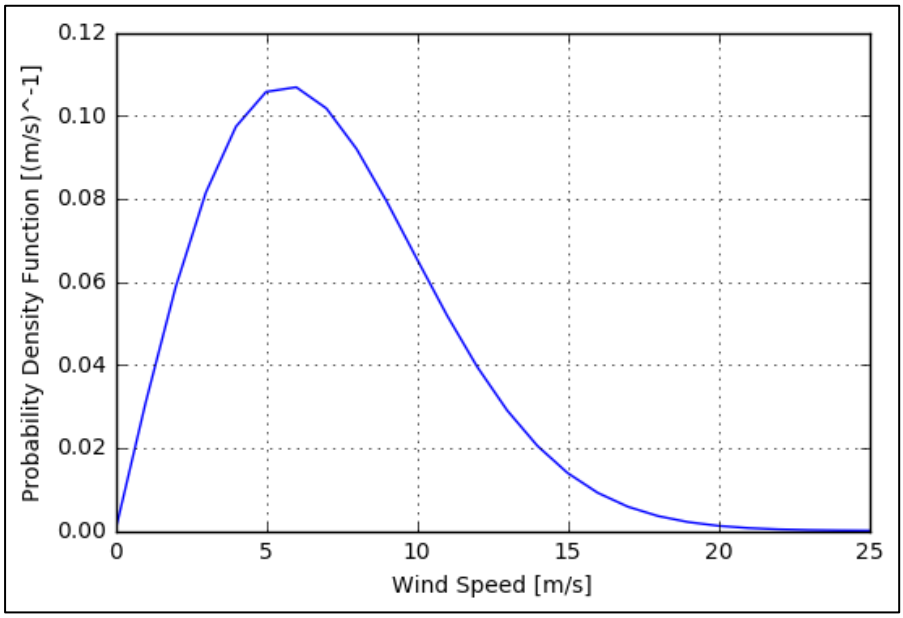

Figure 26. Weibull distribution at Horn Rev at a reference height of 62m, *k* and *a* equal to 2 and 10.83 respectively

4.3. Energy yield model

The MZ tool gives an estimate for the energy yield for each of the layouts and power ratings considered in Table 4. The tool also takes into account the wake effects, the electricity losses, and the availability within the farm. Figure 27 shows

the results for the energy yield calculated with the tool for the layouts and turbine powers evaluated in the Baltic Sea case. It is perceived that the larger the turbine rated power, the higher the energy yield for the same wind farm rated power. This is explained by the fact that a large turbine rated power translates to a less number of turbines in the wind farm, and therefore in a reduction of the wake effects. The lesser the wake effects, the higher is the energy yield of the offshore wind farm. In this chart it is only shown the effect of the turbine rated power on the energy yield, ignoring the influence that the rotor diameter has on this calculation.

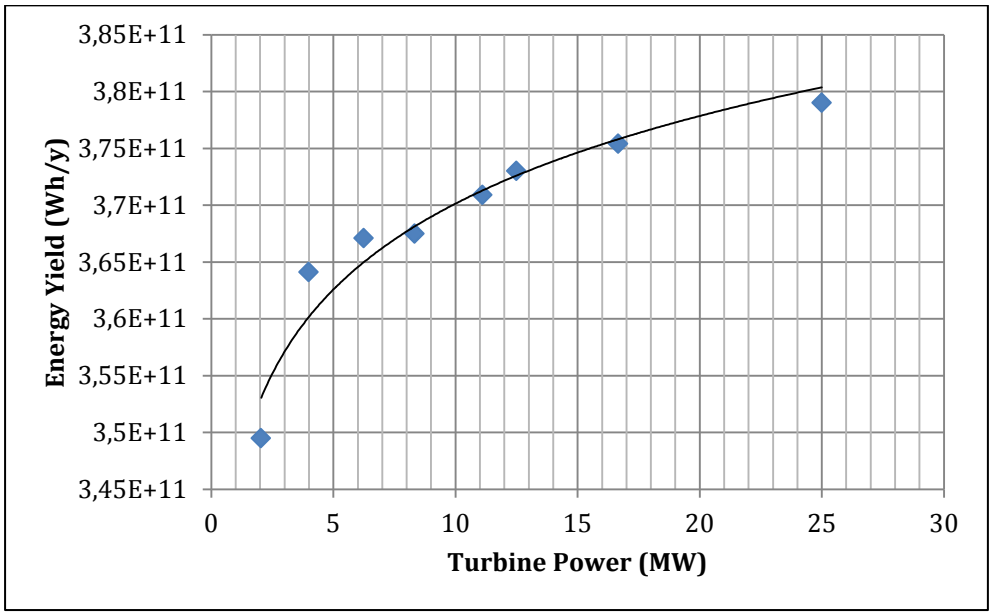

Figure 27. Energy yield for the Baltic Sea case computed with the MZ tool

It would take a lot of time to run the tool for different rotor diameters at the same turbine rated power for all the layouts and power ratings considered in Table 4 to obtain a function for the energy yield that is dependent on the power and the diameter. Hence, in this project, the energy yield is calculated according to Equation 15. First, to calculate the power curve for different turbine scales, the condition that the same power coefficient of the reference turbine can be obtained for the upscaled turbine at rated wind speed is assumed. Therefore, using Equation 8, the wind speed axis can be adjusted according to the power and diameter of the upscaled turbine. Subsequently, introducing this wind speed in Equation 7, and using the same power coefficient values that the reference turbine has, the power can be obtained for that wind speed. Thus, a new power curve can be calculated for every wind turbine size when repeating this procedure for a wind speed range of 0 to 25m/s. For all the turbine scales, the cut-out wind speed is set at 25m/s. In a similar way as in the calculation of the electrical infrastructure cost, the interpolation function *interpolate.interp1d* of scipy is used to calculate the power of the turbine given a certain wind speed. However, in this case, the kind of

interpolation selected is linear because it fits the best with the values estimated for the new power curves.

The Weibull probability density function stated in Equation 16 is used for the two case studies taking the respective values of shape factor and scale factor of Figure 7. Since these two factors are related to a particular height, the wind speed must be scaled for different hub heights. Equation 17 and Equation 18 refer to the Power Law wind profile and the Logarithmic wind profile respectively. The Power Law wind profile is suitable to estimate the wind speed above 60m, while the logarithmic wind profile works better in the range of 0 to 60m height. Regarding that the values of shape factor and scale factor for the Baltic Sea case represent the wind regime at 10m height, Equation 18 has to be used first to determine the wind speed at 60m height. Subsequently, Equation 17 is used to estimate the wind speed at hub heights above 60m. For the North Far Sea case, Equation 17 is enough considering that the shape factor and the scale factor are referenced for a 62m height.

$$\textbf{Equation 17.}\quad U(h) = U(h_{ref}) * \left(\frac{h}{h_{ref}}\right)^{\alpha}$$

$$\textbf{Equation 18.}\quad U(h) = U(h_{ref}) * \frac{Ln(\frac{h}{z_0})}{Ln(\frac{h_{ref}}{z_0})}$$

where U is the wind speed, h is the height at which the wind speed U is desired to be calculated, h_{ref} is the reference height, α is the wind shear exponent and z_0 is the surface roughness length. The surface roughness length and the wind shear exponent are taken as $2X10^{-4}$ m and 0.1 respectively for an open sea environment (Zaaijer M. , Wind climate and energy production, 2015).

The total wind farm energy output for every turbine size is then the energy yield of a single turbine calculated with Equation 15 multiplied by the number of turbines required to meet the total power installed capacity of the wind farm depending on the case study. The number of turbines required is computed as the farm rated power divided by the turbine rated power according to the turbine size. As stated at the beginning of this chapter, the wake efficiency, the electricity losses and the availability are not considered in the energy yield model developed. With respect to the electrical losses, from the runs made with the MZ tool for the layouts and power ratings shown in Table 4 these losses are around 3% of the total energy yield of the farm. Thus, as they are minimal, they can be neglected because they do not have a significant effect at the moment of finding the optimum wind turbine size. Moreover, regarding wake efficiency, this component may have an impact on the results. However, due to lack of time, the modeling of this factor for different turbine scales is not done. In section 6.4, the impact of not considering the wake efficiency in the results is analyzed. Finally, the availability of the wind farm is

affected by the turbine rated power and by the location of the wind farm. The number of failures per turbine per year is proportional to the number of turbines since the more number of turbines, the larger number of failures. Therefore, for the same wind farm rated power the availability of the wind farm is higher when using less number of turbines with a high rated power. Moreover, the availability is also affected by the wind farm location since reaching a site that is farther offshore takes longer than reaching one closer to shore. Thus, if a turbine fails and stops operating, the time to repair it will vary with respect to the distance between the wind farm and the shore. In addition, the sea-state and weather conditions affect the accessibility to the wind farm. For a harsh maritime environment, the accessibility decreases leading to a reduction in the availability of the farm. The availability is then not considered in the energy model because of its modeling complexity and the lack of time for carrying out such work.

5. Analysis and Discussion on the Model Results

5.1. Description of the chapter

In this chapter, the analysis and discussion of the results obtained with the computational model for the two cases is carried out. First, the boundaries and conditions to run the model are explained. Then, the optimal turbine scale for each case is presented. Afterward, the optimal combination of power and diameter according to the model is shown for every power rating in the range from 2MW to 20MW taking 1MW steps. Therefore, it is possible to make an analysis of the optimum turbine size while the turbine scale increases. Subsequently, the components that have a substantial percentage contribution in the LPC function are identified. Finally, the behavior of each of these components is analyzed along the optimum turbine sizes in the power range established. Thus, it can be determined how the coupling of these components results in the optimum turbine size of each case.

5.2. Setting the model boundaries and conditions

After placing all the components cost models along with the energy yield model in the LPC function expressed in Equation 1, it is possible to find the LPC value for every rated power and rotor diameter combination for each case. The rated power range considered to run the model is from 2 to 20MW in steps of 1MW. In addition, the rotor diameter range is determined for a power density range of 200 to 600W/m^2. Therefore, the total rotor diameter range for all rated powers from 2 to 20 MW then becomes from 66 to 356 m in steps of 1m. Moreover, the discount rate is taken as 10% and the project lifetime as 20 years. Now, the model is ready to calculate the LPC for each power-diameter combination, and this output can be used to determine the turbine scale with the lowest LPC value.

5.3. Model results

5.3.1. Far North Sea case – 500MW OWF

Figure 28 shows the LPC as a function of the power and the rotor diameter for this case study. From this chart, it is perceived that small rated powers in combination with small rotor diameters lead to a high LPC. Likewise, high rated powers combined with large rotor diameters drive to a high LPC. Besides, it is observed that every turbine power in the range of 2 to 20MW has an optimum rotor

diameter size, which is inside the power density range established in the previous section. However, the values of power, diameter, and LPC are not clearly distinguished in the chart for the optimum sizes. Hence, the results of the optimum turbine size for all the power ratings in the range of 2 to 20MW are shown in Table 8. With respect to this case, the model outcome for the optimum wind turbine size is a turbine of 11MW rated power and 176m diameter.

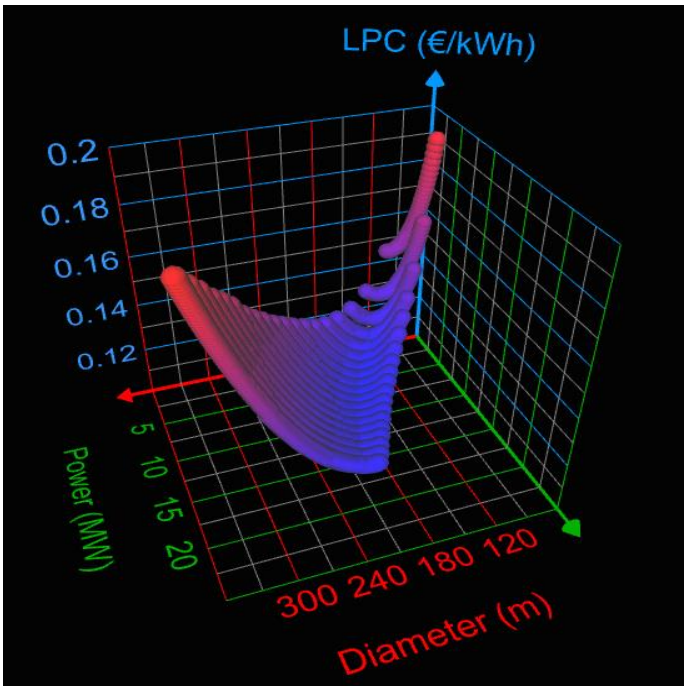

Figure 28. LPC as a function of the power and the rotor diameter for the Far North Sea case

The data in Table 8 not only shows the optimum turbine size for every rated power, but it also shows the LPC and the power density for each turbine. Considering the power density values, for turbines with low rated powers, it is optimal to have a low power density, thus a large rotor. On the other hand, for turbines with high rated powers, it is optimal to have a high power density, thus a small rotor. Moreover, to have a better look at the behavior of the LPC values for the different turbine scales of Table 8, the LPC is plotted as a function of the power. The plot is depicted in Figure 29. From this chart it is appreciated a steep decrease in the LPC between the 2MW and the 6MW turbine, then the LPC keeps decreasing but gradually up to the 11MW turbine. From this point, the LPC starts increasing slightly up to the 20MW turbine. From the chart, it is observed that in the range of 10 to 13 MW the LPC has a minimal variation, which causes the plot to seem flat over this power range.

Power (MW)	Optimum Diameter (m)	LPC (€¢/kWh)	Power Density (W/m²)
2	110	14.948	210
3	122	13.388	257
4	132	12.609	292
5	140	12.177	325
6	146	11.914	358
7	149	11.781	401
8	160	11.705	398
9	165	11.642	421
10	171	11.615	435
11	176	11.607	452
12	180	11.610	472
13	187	11.628	473
14	188	11.656	504
15	190	11.694	529
16	197	11.740	525
17	199	11.789	547
18	203	11.845	556
19	207	11.908	565
20	210	11.977	577

Table 8. Optimum turbine size of every rated power in the range of 2 to 20MW for the Far North Sea case. The optimum size of the case is highlighted in yellow

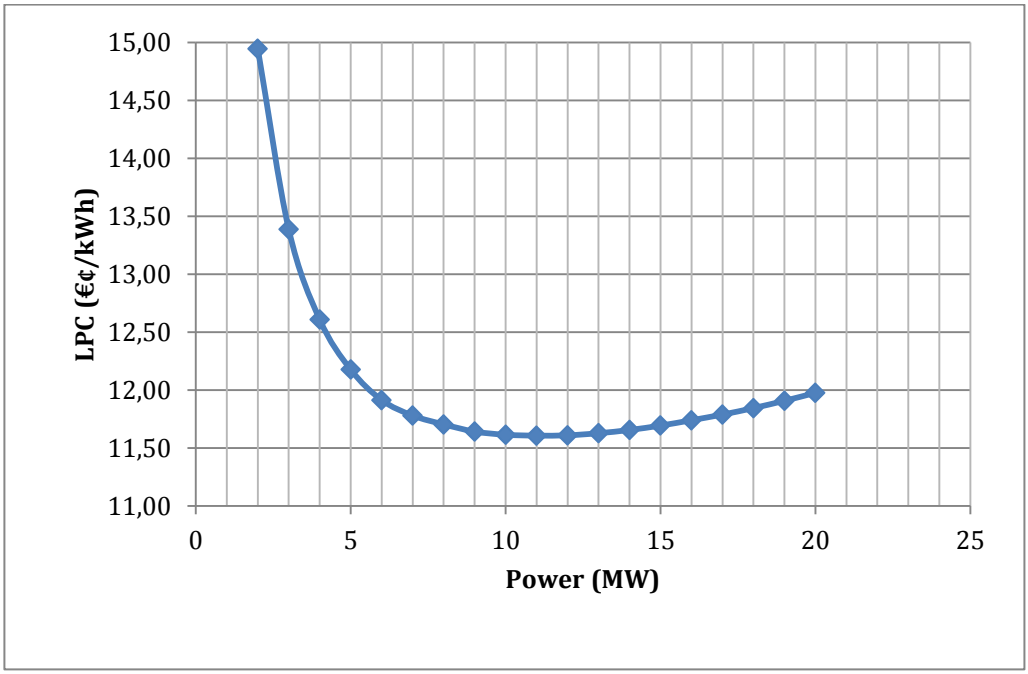

Figure 29. LPC as a function of the turbine power for the optimum turbine sizes shown in Table 8

To get a better understanding of the behavior of the LPC function depicted in Figure 28 and Figure 29, and the results shown in Table 8, the components that have a substantial percentage contribution to the LPC are determined, and then their contribution to the LPC is analyzed along the power range. First, this percentage contribution is computed for the capital investment, the O&M, and the decommissioning. Table 9 shows these percentages, which are calculated for the optimum turbine size of the lowest and the highest of the power ratings considered, plus the optimum turbine size result for this case study. From this table, it is observed that the capital investment has the largest contribution of the three elements for the three turbine sizes. In addition, as the turbine scale increases, this contribution increases from a 60% to 77.5%. The O&M has a large percentage contribution in the case of the smallest turbine size, but as the scale increases the percentage decreases from 33% to 16.5%. This result is expected, since the O&M cost is proportional to the number of turbines, therefore, inversely proportional to the turbine rated power. Moreover, the percentage contribution of the decommissioning keeps practically constant through the turbine scales.

Turbine Size	Capital Investment (%)	O&M (%)	Decommissioning (%)
2MW-110m	60.30	33.16	6.55
11MW-176m	73.49	20.08	6.43
20MW-210m	77.46	16.53	6.01

Table 9. Percentage contribution of the capital investment, the O&M, and the decommissioning in the LPC of different turbine scales for the Far North Sea case

After identifying that the capital investment has the largest contribution to the LPC, it is decomposed to determine which elements have the largest influence on it. Table 10 shows the results, from where it is noticed that the support structure has the largest percentage contribution to the capital investment, followed by the turbines, the electrical infrastructure, and the transportation & installation of the RNA.

Turbine Size	Support Structure (%)	Electrical Infrastructure (%)	Turbines (%)	Transportation & Installation RNA (%)
2MW-110m	41.23	10.41	25.33	8.14
11MW-176m	36.25	9.72	30.32	3.24
20MW-210m	39.21	10.79	34.11	2.56

Table 10. Percentage contribution to the capital investment of different turbine scales for the Far North Sea case

To elaborate a better analysis for the results shown in Table 10, it is appropriate to see the behavior in the contribution to the LPC of the support structure, the electrical infrastructure, the turbines, and the transportation & installation of the RNA for all the turbine sizes shown in Table 8. This contribution is calculated taking as reference Equation 1. Hence, the costs of these components are individually

computed for every turbine size in Table 8 and divided by the annuity factor expressed by Equation 2, and by the total wind farm energy yield, calculated as explained in section 4.3. The behavior of the contribution to the LPC of these elements is illustrated in Figure 30. In addition, the same behavior is depicted in this chart for the O&M, the decommissioning, and the energy yield to get a wider picture of what is going on in the model. In the case of the O&M and the decommissioning, their contributions to the LPC are calculated like the last two terms on the right side of Equation 1.

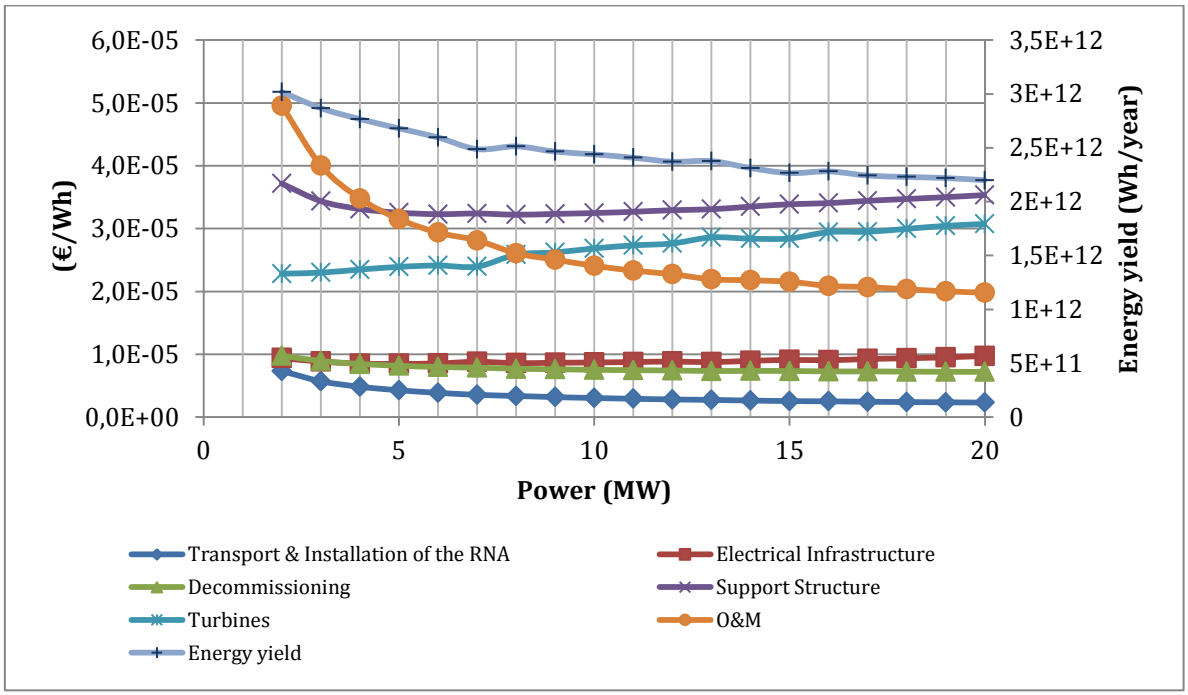

Figure 30. Behavior in the contribution to the LPC for different components plus the energy yield trend for the turbine sizes in Table 8

First, the transportation & installation of the RNA is from the components depicted in Figure 30, the one with the lowest contribution to the LPC for all the power ratings. Moreover, its contribution to the LPC decreases as the turbine power increases. This means that even though the costs for the transportation & the installation of the RNA increase for large diameters, this increase is outweighed by the reduction in the number of turbines like observed in Table 11. With respect to the decommissioning, its contribution to the LPC behaves similarly as the one for transportation & installation of the RNA. Likewise, the decrease in the number of turbines outweighs the increment in the decommissioning costs for large turbine scales like shown in Table 11. Furthermore, concerning the electrical infrastructure, its contribution to the LPC seems almost constant along the power range according to Figure 30. However, there is a difference of 15% in this contribution between the maximum point and the minimum point of the curve. Besides, this curve is not smooth and has some local bumps that due to the scale of the axis in this chart

cannot be noticed. Thus, as these bumps are tiny, they are not relevant for the final results of the optimum turbine size.

Turbine Size	Transportation & Installation (€)	Decommissioning (€)
2MW-110m	188,583,098	251,430,798
11MW-176m	59,784,834	152,977,982
20MW-210m	43,222,502	134,756,154

Table 11. Transportation & Installation, and decommissioning costs for different turbine scales in the Far North Sea case

According to Figure 30, the support structure, the turbines, and the O&M have the largest contribution to the LPC and therefore, are the elements that have the biggest impact on it. From the chart, it is observed that the turbines contribution to the LPC increases along the power range, moreover, the curve is not smooth and different gradients can be noticed. Since the turbines cost seems to not vary significantly along the optimum turbine scales as shown in Table 12, the increment in the turbines contribution to the LPC seen in Figure 30 is mainly due to the reduction in the energy yield as the turbines increase in size, which is also depicted in Figure 30. With respect to the support structure contribution to the LPC, it decreases between the 2MW and the 6MW turbines. Therefore, the reduction in the number of turbines for using higher turbine powers outweighs the increment in the support structure cost per turbine in this power range. Nevertheless, the previous statement also applies to the rest of the power range like suggests Table 12. Furthermore, in the range between the 6MW and the 10MW turbines, the contribution to the LPC maintains almost constant, for this reason, the curve seems flat in this region. This means that in this range the support structure cost and the energy yield are declining almost at the same rate. In addition, from the 10MW power rating onwards, the contribution to the LPC increases gradually. Nevertheless, this increase is driven by the reduction in the energy yield and not because of an increment in the support structure cost. Finally, about the O&M contribution to the LPC, it presents a sharp decrease in the range of 2 to 13MW, and from 13MW it decreases gradually. Therefore, along the complete power range, the benefit in the reduction of the number of turbines when using turbines with higher powers becomes evident to reduce the O&M costs. However, this benefit is less visible and significant as the turbine power increases, which is noticed in Figure 30 and Table 12. This is because for high power ratings the O&M percentage contribution to the LPC is smaller than for low power ratings as observed in Table 9.

Turbine Size	Turbines (€)	Support Structure (€)	O&M (€/year)
2MW-110m	586,663,256	954,971,586	149,608,220
11MW-176m	560,154,701	669,804,413	56,133,395
20MW-210m	575,628,178	661,733,013	43,548,587

Table 12. Turbines, support structure and O&M costs for different turbines scales in the Far North Sea case

To understand the model results, it is also appropriate to analyze the behavior that the energy yield presents. From Figure 30, it is noticed that the energy yield decreases as the turbine scale increases. This can be attributed to the increment in the power density from the smallest to the largest turbine scale shown in Table 8. The high power density, especially for large turbine sizes is due to the increment that the support structure cost and the turbines cost undergo when the rotor increases in size. Thus, for the large turbine scales, increasing the rotor diameter to generate more energy does not compensate for the cost increment of the turbines and the support structures. To get a better understanding of the previous statement, Table 13 shows the percentage increase of the support structure cost and the turbines cost plus the percentage increase in the energy yield when going from a power density of 400 to 300W/m^2. From this table, it is appreciated that the percentage increase of the support structure cost and the turbines cost is much larger for a 20MW turbine than from a 2MW turbine, while the percentage increase in the energy yield is even higher for the 2MW turbine than for the 20MW turbine. Besides, the turbine cost presents the largest increase, which is explained by the fact that the larger the rotor diameter, the larger blades are required, therefore, a higher amount of carbon fiber in the blade is needed. Since the blade cost increases to the power of 3.93 as the blade length increases as shown in Figure 14, this huge increase in the turbine cost for a 20MW turbine when going from a power density of 400 to 300W/m^2 is a sensible result.

Rated Power (MW)\Parameter	Support Structure cost (%)	Turbines cost (%)	Energy yield (%)
2	7.1	19.7	12.9
20	12.2	53.7	10.9

Table 13. Increment when going from 400 to 300W/m^2

The previous analysis is helpful to understand the behavior of the components that have the largest impact on the LPC when the wind turbines are upscaled according to the model developed. However, it may not be enough to understand the optimum turbine scale result for the case, which is an 11MW-176m turbine. Therefore, in Figure 31 the cumulative contribution to the LPC for the same components analyzed previously is plotted. The purpose of this chart is to determine how the coupling of the contributions to the LPC of these elements ends up in this optimum turbine size of 11MW-176m.

The addition of the contributions to the LPC of the transportation & installation of the RNA, and of the decommissioning has the lowest value in the 20MW turbine. Since these two costs are proportional to the number of turbines, this result is reasonable. Then, after the addition of the contribution to the LPC of the electrical infrastructure, the minimum LPC moves to the 13MW turbine. Since the electrical infrastructure curve in Figure 30 has the lowest value at the 5MW turbine, it is rational that it moves the optimum to a lower turbine scale. Furthermore, the fact that this curve has a local minimum at 13MW may lead to this outcome. After the addition of the support structure contribution to the LPC, the optimum turbine size relocates in the 10MW turbine. This may be explained by Figure 30 since it shows that the curve of the contribution to the LPC of this component has the lowest value at the 6MW turbine and from there it keeps almost constant up to 10MW from where it starts increasing again. Later, the optimum turbine scale is pushed to the 7MW turbine with the addition of the turbines contribution to the LPC. Regarding that after the 7MW turbine the contribution to the LPC of this component increases with a higher gradient according to Figure 30, this result is sensible. In addition, although the turbines contribution to the LPC is lower for the turbines with lower power ratings than 7MW, the fact that for smaller turbine scales than 6MW the support structure contribution to the LPC increases significantly also influences this optimum value of 7MW up to this point. Finally, after the addition of the O&M contribution to the LPC, the optimum turbine size moves to the turbine of 12 MW. Since this contribution of the O&M presents a behavior contrary to the one of the support structure and turbines, it is reasonable that it moves the optimum to a large power rating. However, even though the contribution to the LPC of the O&M keeps decreasing after the 12MW turbine, the decrease becomes less significant and cannot compensate for the large increase in this same contribution of the support structure and turbines for the turbine scales larger than 12MW. The values of the cumulative contribution to the LPC up to the addition of the O&M show to be similar in the range of 11 to 13MW. Thus, this optimum size may be easily moved between this range. Since not all the components that constitute an offshore wind farm are shown in Figure 31, it is reasonable that the optimum turbine size is the 11MW-176m after the addition of the components left.

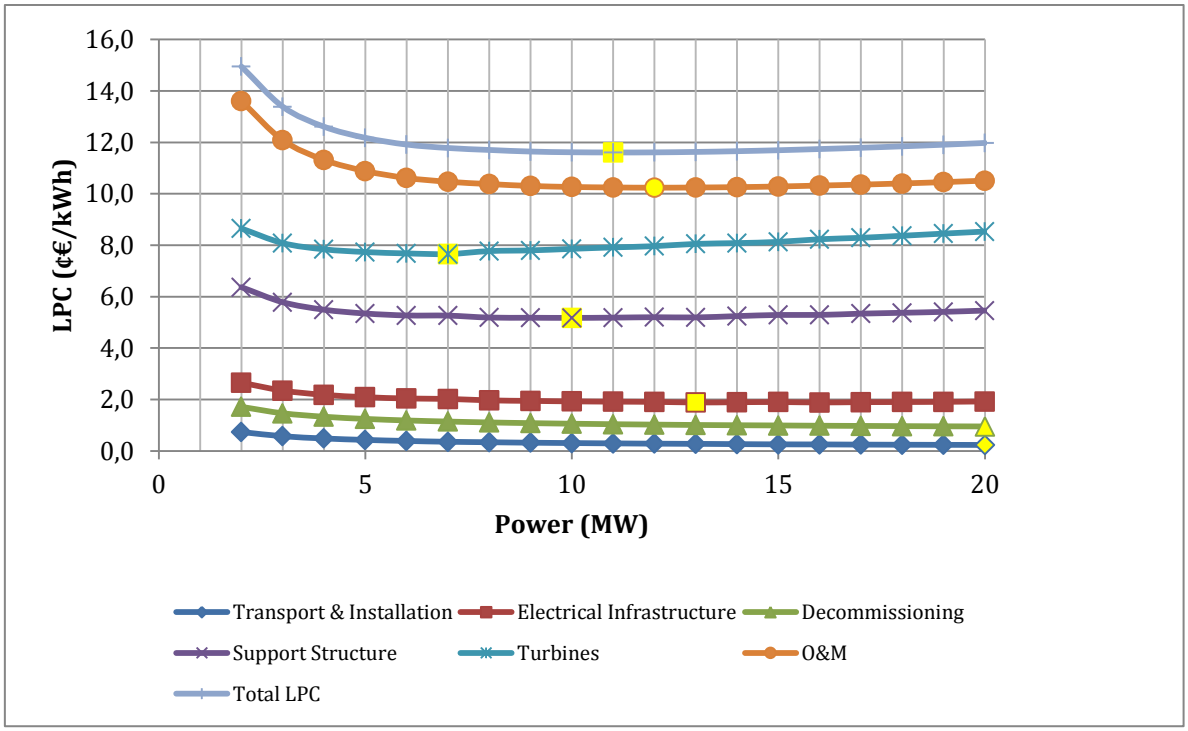

Figure 31. Cumulative contribution to the LPC for different components plus the total LPC. The optimum turbine size after each component addition is marked with yellow

5.3.2. Baltic Sea case – 100MW OWF

Figure 32 shows the LPC as a function of the power and the rotor diameter for this case study. From this chart, it is observed that for high rated powers in combination with large rotor diameters the LPC values are the highest. However, for low rated powers and small rotor diameters, the LPC values become high as well. Besides, it is observed that every turbine power in the range of 2 to 20MW has an optimum rotor diameter size, which is inside the power density range established in section 5.2. Nevertheless, the values of power, diameter, and LPC are not clearly distinguished in the chart for the optimum turbine sizes. Thus, the results of the optimum turbine size for all the power ratings in the range of 2 to 20MW are shown in Table 14. Regarding this case, the model outcome for the optimum wind turbine size is a turbine of 6MW rated power and 147m diameter.

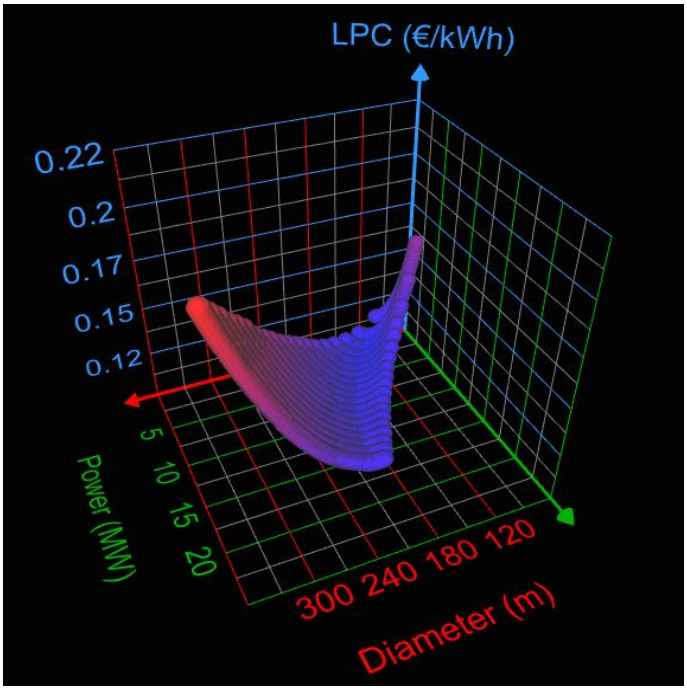

Figure 32. LPC as a function of the power and the rotor diameter for the Baltic Sea case

Power (MW)	Optimum Diameter (m)	LPC (¢€/kWh)	Power Density (W/m2)
2	109	12.095	214
3	120	11.510	265
4	132	11.269	292
5	140	11.180	325
6	147	11.161	354
7	149	11.229	401
8	161	11.305	393
9	170	11.385	397
10	171	11.465	435
11	173	11.550	468
12	180	11.635	472
13	184	11.723	489
14	189	11.814	499
15	193	11.908	513
16	199	12.007	514
17	204	12.117	520
18	209	12.224	525
19	214	12.334	528
20	211	12.438	572

Table 14. Optimum turbine size of every rated power in the range of 2 to 20MW for the Baltic Sea case. The optimum size of the case is highlighted in yellow

The data in Table 14 not only shows the optimum turbine size for every rated power, but it also shows the LPC and the power density for each turbine. Regarding the power density values, for turbines with low rated powers, it is optimal to have a low power density, thus a large rotor. On the contrary, for turbines with high rated powers, it is optimal to have a high power density, thus a small rotor. Furthermore, with the intention of having a better look at the behavior of the LPC values for the different turbine scales of Table 14, the LPC is plotted as a function of the power in Figure 33. From this chart it is noticed a steep decrease in the LPC between the 2MW and the 5MW turbine, then it slightly decreases to the 6MW turbine. From this point, the LPC starts increasing almost linearly up to the 20MW turbine. It is observed in Figure 33 that the optimum turbine size seems to concentrate in the range of 5 to 6MW, contrary to what is perceived in Figure 29 where this optimum seems spread inside the range of 10 to 13MW.

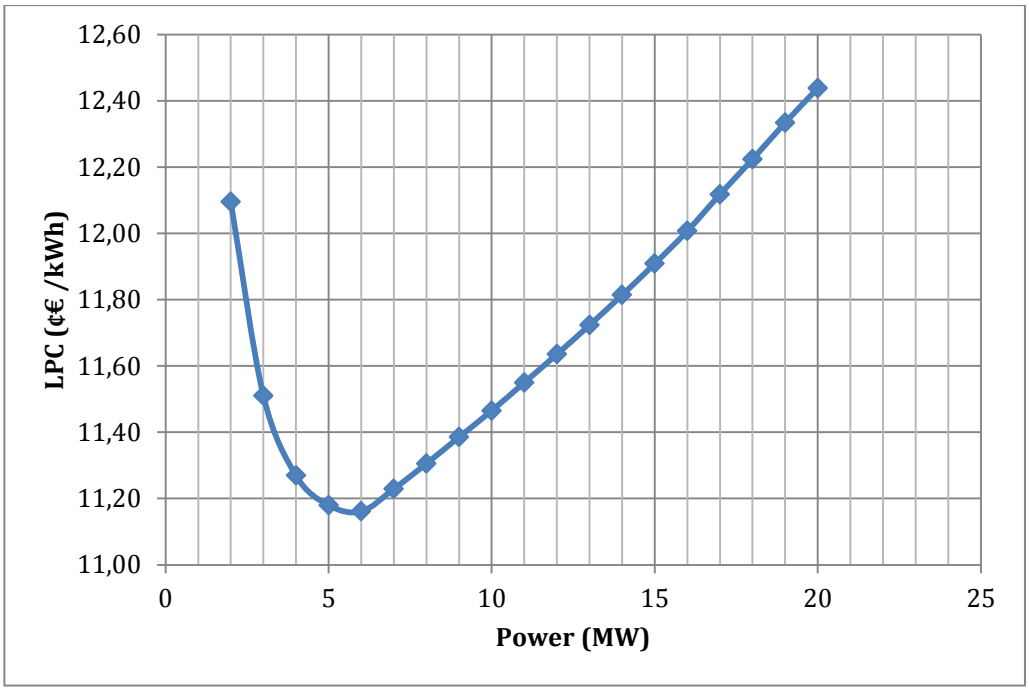

Figure 33. LPC as a function of the turbine power for the optimum turbine sizes shown in Table 14

To get some insight into the behavior of the LPC function depicted in Figure 32 and Figure 33, and the results shown in Table 14, the components that have a significant percentage contribution in the LPC are determined, and then their contribution to the LPC is analyzed along the power range. First, like in the Far North Sea case, this percentage contribution is computed for the capital investment, the O&M, and the decommissioning. Table 15 shows these percentages, which are calculated for the optimum turbine size of the lowest and the highest of the power ratings considered, plus the optimum turbine size result for this case study. From this table, it is observed that the capital investment has the largest contribution of the three elements for the three turbine sizes. In addition, as the turbine scale

increases, this contribution increases from a 66.5% to 77.3%. The O&M has a large percentage contribution in the case of the smallest turbine size, but as the scale increases the percentage decreases from 25.5% to 17.4%. This result is expected since the O&M cost is proportional to the number of turbines, thus, inversely proportional to the turbine rated power. The decommissioning percentage contribution slightly decreases as the turbine scale increases from an 8% to a 5.25%.

Turbine Size	Capital Investment (%)	O&M (%)	Decommissioning (%)
2MW-109m	66.55	25.48	7.97
6MW-147m	71.40	22.27	6.33
20MW-211m	77.33	17.42	5.24

Table 15. Percentage contribution of the capital investment, the O&M, and the decommissioning in the LPC for the Baltic Sea case

As well as in the Far North Sea case, the capital investment has the largest contribution in the LPC, so it is decomposed to determine which elements have the most considerable influence on it. Table 16 shows the results, where it is noticed that the turbines have the largest percentage contribution to the capital investment and not the support structure like in the Far North Sea case. After the turbines percentage contribution, the most significant contributions to the capital investment come from the support structure, the transportation & installation of the RNA, and the electrical infrastructure.

Turbine Size	Support Structure (%)	Electrical Infrastructure (%)	Turbines (%)	Transportation & Installation RNA (%)
2MW-109m	21.82	6.61	33.65	10.93
6MW-147m	26.91	5.81	37.88	6.02
20MW-211m	28.75	5.16	41.03	3.07

Table 16. Percentage contribution on the capital investment for the Baltic Sea case

To elaborate a better analysis for the results shown in Table 16, it is appropriate to see the behavior in the contribution to the LPC of the support structure, the electrical infrastructure, the turbines, and the transportation & installation of the RNA for all the turbine sizes shown in Table 14. Hence, the behavior of the contribution to the LPC of these elements is depicted in Figure 34. In addition, the same behavior of the O&M, the decommissioning, and the energy yield are shown, to get a broader picture of what is going on in the model. The contributions to the LPC of the components previously mentioned are computed in the same manner as for the Far North Sea case, which procedure is described in section 5.3.1.

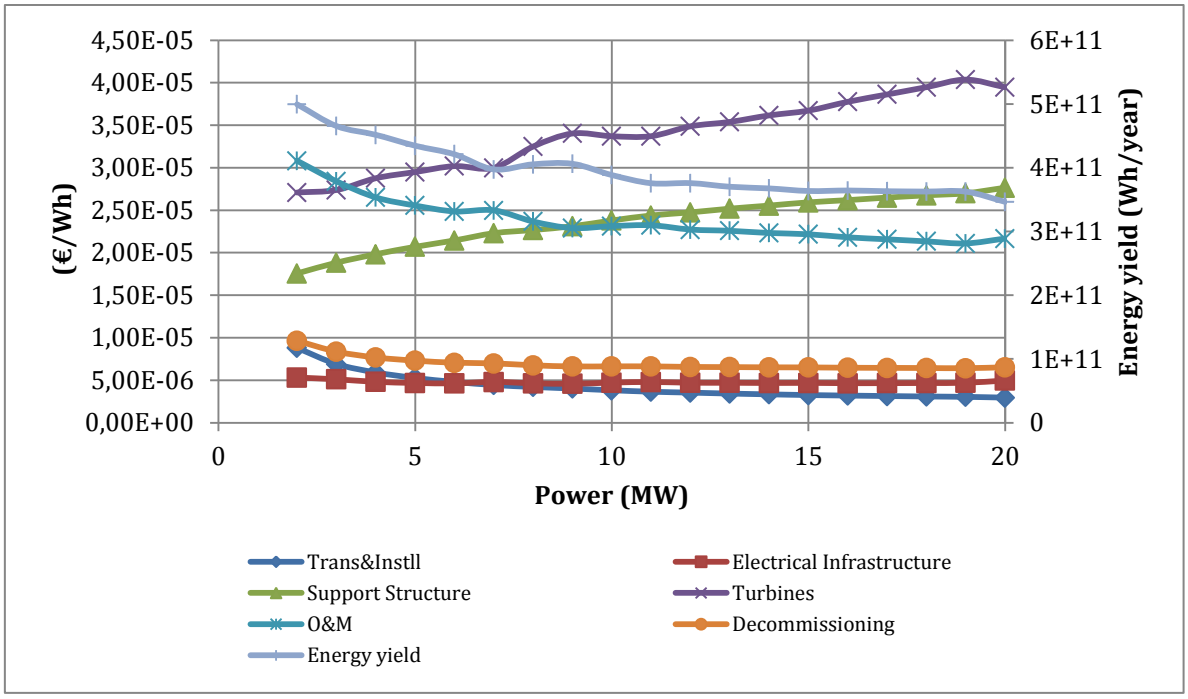

Figure 34. Behavior in the contribution to the LPC for different components plus the energy yield trend for the Baltic Sea case

First, the transportation & installation of the RNA and the electrical infrastructure are the components with the lowest contribution to the LPC. With respect to the former, its contribution to the LPC decreases as the turbine power increases. This means that even though the costs for the transportation & the installation of the RNA increase for large diameters, this increase is outweighed by the reduction in the number of turbines like observed in Table 17. Concerning the electrical infrastructure, its contribution to the LPC seems almost constant along the power range according to Figure 34. However, there is a difference of 16% in this contribution between the maximum point and the minimum point of the curve. Moreover, this curve is not smooth and has some local bumps that due to the scale of the axis in this chart cannot be perceived. Thus, as these bumps are tiny, they are not relevant for the final results of the optimum turbine size. With respect to the decommissioning, its contribution to the LPC behaves similarly as the one for transportation & installation of the RNA. Likewise, the decrease in the number of turbines outweighs the increment in the decommissioning costs for large turbine scales like shown in Table 17.

Turbine Size	Transportation & Installation (€)	Decommissioning (€)
2MW-109m	37,397,876	40,978,882
6MW-147m	17,211,617	25,312,534
20MW-211m	8,712,566	19,241,089

Table 17. Transportation & Installation, and decommissioning costs for different turbine scales in the Baltic Sea case

According to Figure 34, the turbines, the support structure, and the O&M have the largest contribution to the LPC and therefore, are the elements that have the greatest impact on it. The support structure contribution to the LPC gradually increases in the complete power range. This increase is principally due to decrease in the energy yield along the power range because Table 18 implies that the support structure cost slightly decreases as the turbine scale increases. With respect to the turbines contribution to the LPC, it can be said that this contribution practically increases along the complete range of power ratings as it suggests the trend depicted. Furthermore, the increment in the turbines contribution to the LPC is not smooth and different gradients, and bumps can be noticed. Since the turbines cost seems to not vary significantly along the optimum turbine scales as shown in Table 18, the increment in the turbines contribution to the LPC seen in Figure 34 is mainly due to the reduction in the energy yield as the turbines increase in size, which is also depicted in this chart. Finally, about the O&M contribution to the LPC, it presents a steep decrease in the range of 2 to 6MW and keeps almost constant until the 7MW turbine. From this point, the contribution to the LPC drops gradually up to 20MW. Hence, along the complete power range, the benefit in the reduction of the number of turbines when using turbines with higher powers becomes evident to reduce the O&M costs. However, this benefit is less visible and significant as the turbine power increases, which is observed in Table 18 and in Figure 34 where different gradients that this curve has are noted. This is because for high power ratings the O&M percentage contribution to the LPC is smaller than for low power ratings as observed in Table 15.

Turbine Size	Support Structure (€)	Turbines (€)	O&M (€/year)
2MW-109m	96,997,217	115,165,631	15,389,978
6MW-147m	82,779,587	108,222,745	10,467,476
20MW-211m	84,769,393	116,421,116	7,508,856

Table 18. Support structure, turbines, and O&M costs for different turbines scales in the Baltic Sea case

However, to understand the model results, it is not enough to analyze the behavior of the costs, but also the one that the energy yield shows. From Figure 34, it is noticed that the energy yield decreases as the turbine scale increases. This can be explained by the increment in the power density from the smallest to the largest turbine size shown in Table 14. In the same way, as in the Far North Sea case, the high power density, especially for large turbine scales is due to the increment that the support structure cost and the turbines cost have when the rotor increases in size. Therefore, for the large turbine scales, increasing the rotor diameter to generate more energy does not compensate for the cost increment of the turbines and the support structures.

The previous analysis is helpful to understand the behavior of the components that have the largest impact on the LPC when the wind turbines are upscaled according to the model developed. However, it may not be enough to understand the optimum turbine scale result for the case, which is a 6MW-147m turbine. Thus, in Figure 35 the cumulative contribution to the LPC for the same components analyzed previously is plotted. The purpose of this chart is to determine how the coupling of the contributions to the LPC of these elements ends up in this optimum turbine size of 6MW-147m.

The transportation & installation of the RNA has the lowest contribution to the LPC at the 20MW turbine. Since this cost is inversely proportional to the turbine rated power, this outcome is reasonable. Then, after the addition of the electrical infrastructure contribution to the LPC, the lowest LPC moves to the 19MW turbine. This is expected because the electrical infrastructure contribution to the LPC increases from 19 to 20MW, and this increase is higher than the decrease in the same contribution of the transportation & installation of the RNA for the same power range. Later, when the decommissioning contribution to the LPC is added, the optimum turbine size keeps in the 19MW turbine. This means that the decrease of this contribution for the decommissioning in the range of 19 to 20MW is outweighed by the increment in the electrical infrastructure contribution to the LPC in the same range. After the addition of the support structure contribution, the optimum turbine size moves considerably to a lower turbine scale, which is the 6MW turbine. Moreover, up to this point, the LPC of the 5MW turbine is 0.01 larger than the LPC of the 6MW turbine. Therefore, it can be said that the optimum turbine size lies in the range of 5 to 6MW. Furthermore, what it is happening is that for the turbines larger than 6MW the increment in the support structure contribution to the LPC becomes high to a point where outweighs the decrease in this same contribution of the sum of the previous three components. On the other hand, for turbines smaller in scale than the 5MW turbine, even though the support structure contribution to the LPC is lower, it is influenced by the added contributions of the three previous components, which have the largest LPC values for the small power ratings. Subsequently, after the addition of the turbines contribution to the LPC, the optimum turbine size relocates at the 3MW turbine. This outcome is sensible since the turbines are the component that has the largest contribution to the LPC in this case study, and this contribution increases along the power range, so it moves the optimum towards the smallest turbine size. Finally, after the addition of the O&M contribution to the LPC, the optimum turbine size is pulled to the turbine of 6 MW. Since the O&M contribution to the LPC presents a behavior contrary to the one of the support structure and turbines, it is reasonable that it moves the optimum to a large power rating. However, even though the contribution to the LPC of the O&M keeps decreasing after the 6MW turbine, the decrease becomes less significant and cannot compensate for the large increase in this same contribution of the support structure and the turbines for the turbine

scales larger than 6MW. The values of the cumulative contribution to the LPC up to the addition of the O&M show to be similar in the range of 5 to 6MW like shown in Figure 35. Thus, this optimum size may be easily moved between this range. Since not all the components that constitute an offshore wind farm are shown in Figure 35, it is reasonable that the optimum turbine size lies in the 6MW and not in the 5MW after the addition of the components left. Some of these components decrease in cost due to the reduction in the number of turbines as the infield cable installation and the boat landing. The rest of the expenses keep almost constant for all the turbines scales like the costs of the offshore platform, the harbor use, the dune crossing, etc.

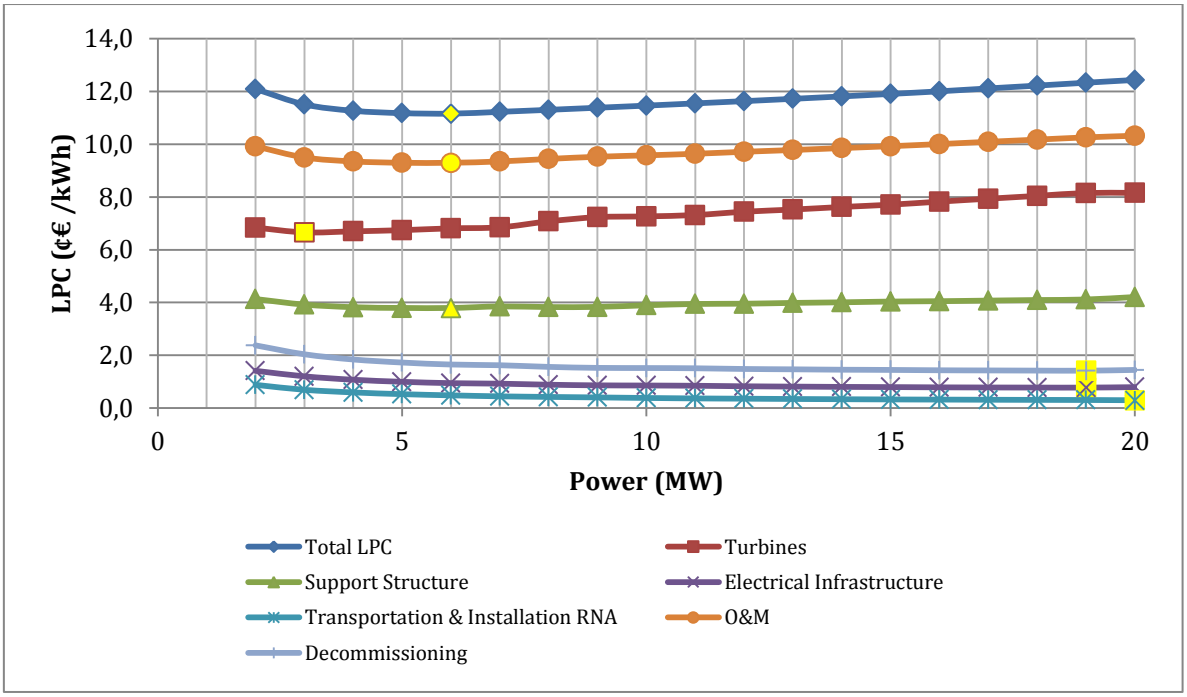

Figure 35. Cumulative contribution to the LPC for different components plus the total LPC. The optimum turbine size after each component addition is marked with yellow

5.4. Analysis of the gradients of the contributions to the LPC curves in Figure 30 and Figure 34, and their role in the optimum turbine size in each case study

In both cases, the contributions to the LPC of the turbines, the support structure, and the O&M are the largest. Therefore, it can be said that these three components costs seem to dominate the optimum turbine size. Furthermore, from Figure 30 and Figure 34 it is observed that the curves of the contributions to the LPC of these three components increase and decrease with different gradients along the power range. In the two case studies, the turbines and the support structure contributions to the LPC increase along the major part of the power range, while this same contribution

of the O&M decreases. Figure 36 and Figure 37 shows the sum of the gradients of the support structure curve and the turbine curve along with the absolute value of the gradient of the O&M curve for the Far North Sea case and the Baltic Sea case respectively.

On the assumption that the cost of the turbines, the support structure, and O&M dominate the results of the optimum turbine size, then when the two gradients cross each other, it should be at the optimum turbine power or close to it as not all the components that constitute an offshore wind farm are included. Concerning the Far North Sea case, it is observed in Figure 36 that this two gradients cross at the 11MW turbine power, which is the optimum turbine power in this case. On the other hand, regarding the Baltic Sea case, it is approximately at 2.6MW where the two gradients cross each other, while the optimum turbine power of this case is 6MW. Therefore, it can be said that for the Far North Sea case, the costs of the turbines, the support structure, and the O&M dominate the optimum turbine size. Besides, from Figure 36 it is observed that the O&M gradient is larger than the gradient of the addition of the turbines and the support structure contribution to the LPC up to 11MW. This means that according to the model, for this case study, it is cost effective to increase the turbine rated power to have less number of turbines and reduce the O&M costs up to 11MW. For higher power ratings than 11MW, the O&M gradient becomes lower than the addition of the other two elements gradients. Thus, it is not cost effective anymore to keep reducing the number of turbines, because the increment in the contribution to the LPC of the support structure and the turbines when going for higher power ratings is greater than the reduction in this same contribution of the O&M. Regarding the Baltic Sea case, the gradient of the O&M curve is larger up to 2.6MW than the gradient of the sum of the support structure and the turbines contribution to the LPC curves as shown in Figure 37. This means that since the optimum turbine rated power of this case is 6MW, the addition of the gradients of the contribution to the LPC curves of the components left moves the optimum turbine power towards 6MW. Thus, as the contributions to the LPC of the decommissioning, the electrical infrastructure, and the transport & installation of the RNA also decrease along the power range, the gradients of their curves are added to the one of the O&M, and the result is observed in Figure 37. The gradient of the electrical infrastructure contribution to the LPC curve in Figure 34 is minimal in comparison to the gradient of the curves of the other elements, and thus it does not have an impact on the results of the model in this case study. However, the gradients of the decommissioning and the transport & installation of the RNA are significant in this case study for the results of the optimum turbine size because they shift the red curve considerably in Figure 37 upwards leading to the green curve. In addition, it is noticed that especially in the range of 2 to 8MW, the decommissioning and the transport & installation of the RNA have a large gradient since after 8MW the red and the green curve almost overlap each other. Moreover, in the Far North Sea case, the gradients of the

components left, move to red curve in Figure 36 just slightly upwards since the two curves already cross around the optimum power of 11MW. Therefore the decrease or increase in the contribution to the LPC of the electrical infrastructure, the transport & installation of the RNA, and the decommissioning have a minimal impact on the outcome of the model in this case study.

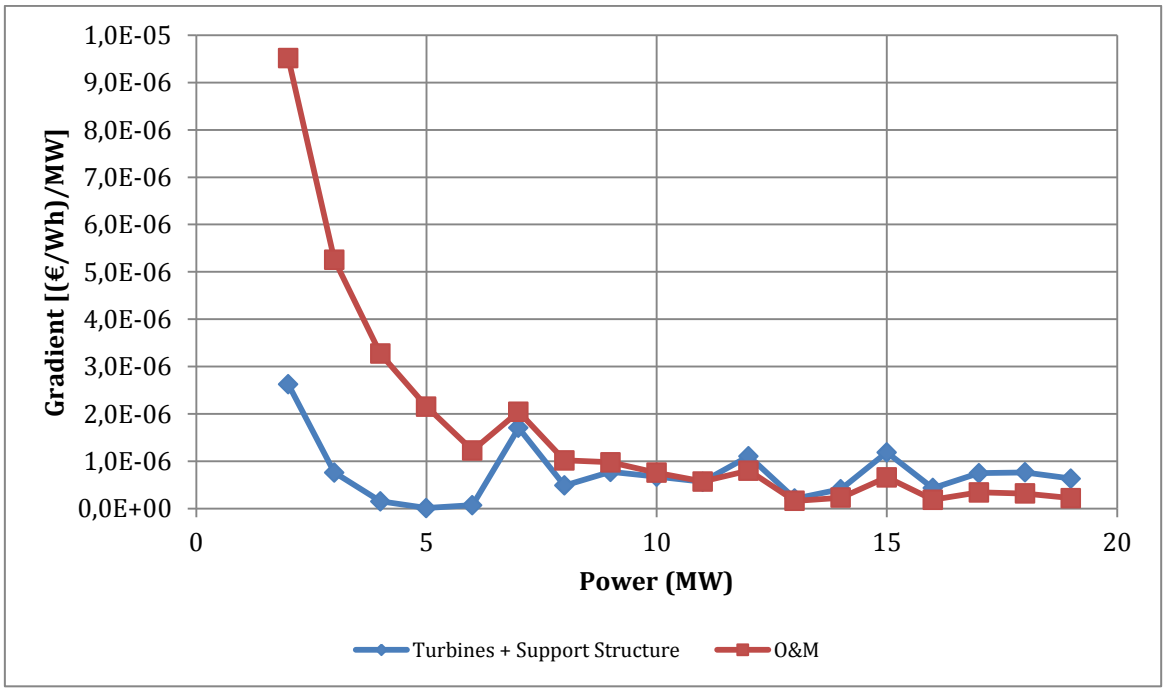

Figure 36. Gradients comparison of the dominant components in the model results for the Far North Sea case

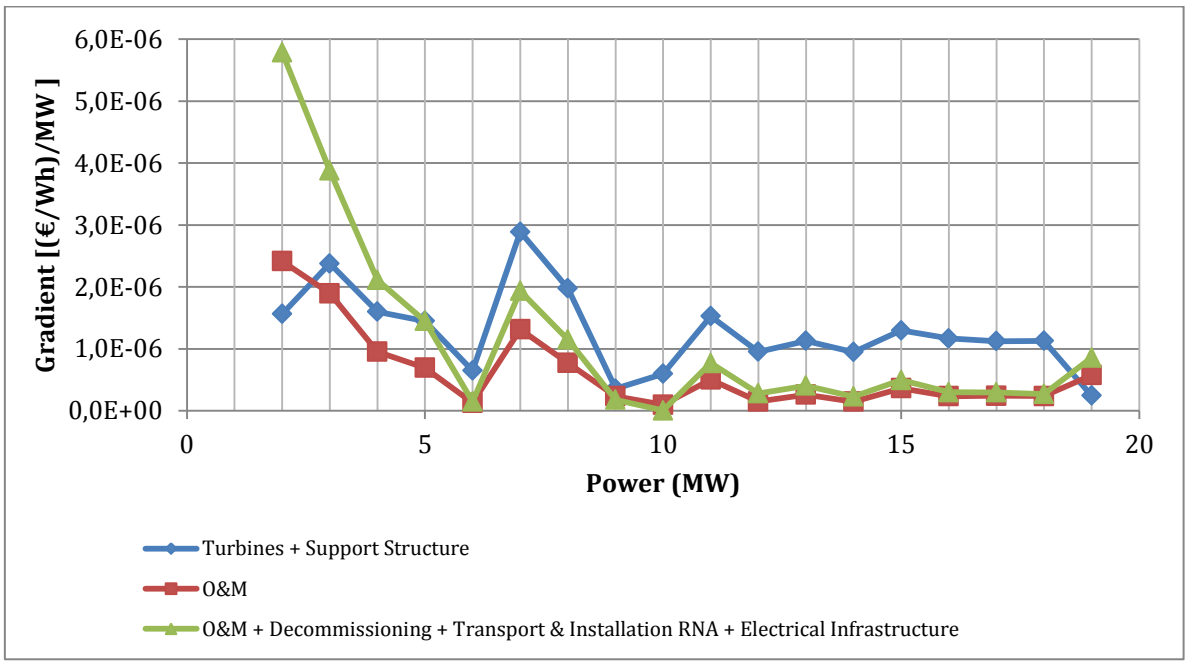

Figure 37. Gradients comparison of the dominant components in the model results for the Baltic Sea case

5.5. Remarks about the previous analyses for both case studies

One of the important differences between the results obtained in the two case studies is that in the Far North Sea case the largest contribution to the LPC comes from the support structures, while in the Baltic Sea case comes from the turbines. The fact that in the Baltic Sea case the water depth is 15m while in the Far North Sea case is 40m, and that the wave environment is softer in this case than in the Far North Sea, leads to smaller support structures in length, diameter, and thickness, especially for the monopile design. Thus, the support structure cost in the Baltic Sea case is much cheaper than in the Far North Sea case.

Moreover, according to Table 8 and Table 14, the lowest power ratings have the lowest power densities, and the highest power ratings have the highest power densities. The reason for these outcomes is that for small turbine scales is cost effective to increment the rotor diameter to generate more energy and compensate for the high O&M costs. Besides, the O&M expenses hardly rise when the rotor diameter increases for the same turbine rated power, and the support structures and turbines cost increment is not that high that it is overweighed by the benefits of producing more energy. On the other hand, following the same reasoning, there is not the need to increase the rotor diameter to produce more energy for large turbine scales since the O&M costs are low. Furthermore, for large turbine sizes, increasing the rotor diameter to generate more energy does not compensate for the high increment in the cost of the support structures and the turbines like shown in Table 13. This analysis is also related to the shape of Figure 28 and Figure 32, where low turbine powers in combination with small rotors lead to high LPC values and high turbine powers in combination with large rotors result in high LPC values.

From the analysis made in section 5.4, it is noticed that more than the value of the contribution to the LPC of the different components, what drives the optimum turbine size are the gradients at which these components contribution to the LPC decrease or increase along the power range. The optimum turbine size converges at the point where the gradients of the components which contribution to the LPC rises as the turbine size increases are equal in magnitude as the gradients of the components which contribution to the LPC decreases as the turbine size upscales.

6. Sensitivity Analysis

6.1. Purpose of the Analysis

In this chapter, a sensitivity study is performed with the intention of verifying in what magnitude the optimum turbine scale changes when the components that have the largest impact in the LPC are varied. Moreover, this study shows which components have the greatest effect in the optimum scale depending on each case study. Furthermore, this analysis is helpful to determine how reliable are the results obtained and how robust is the model developed.

6.2. Far North Sea case

First, the sensitivity of the model at the moment of varying the capital investment cost, the O&M cost, and the decommissioning cost is computed and depicted in Figure 38. The percentage variation in the costs is done for a range of -90% to 100% in multiples of 10% steps. However, it is not expected that for instance, the capital investment cost could reduce in a 90% or that the decommissioning cost could increase by 100% percent. Thus, this percentage variation range is chosen to have a wider view of the change in the optimum turbine scale. Furthermore, due to the resolution of the model, the changes in the optimum turbine power occur in 1MW steps. Thus, when the optimum turbine power is constant along a percentage variation range, a change on it of 0.99MW or less may be going on, but the model does not capture it. Moreover, the optimum power could have changed for a variation of a component cost in multiples of 1%, but the change is presented in multiples of 10%. However, the resolution of the model is enough to realize the components that have the largest impact on the results.

It is observed in Figure 38 that when increasing the capital investment cost, the optimum turbine size moves towards a turbine size with a lower power rating and when decreasing this same cost, the optimum turbine size goes towards a turbine scale with a higher power rating. In contrast, the opposite situation happens for the O&M cost, an increment in the O&M cost leads to an optimum turbine size with a higher rated power, and a decrease in the O&M cost leads to a lower turbine rated power. One way to understand these results is relating to the analysis made in section 5.4. When the O&M costs are multiplied by a factor larger than 1, its gradient of the contribution to the LPC curve is multiplied by the same factor. Therefore, the negative gradient of the O&M keeps larger than the positive gradient of the capital investment up to higher powers. The opposite happens when the capital investment costs are multiplied by a factor greater than 1, as its positive gradient becomes larger than the negative gradient of the O&M at a lower turbine rated power. For the decommissioning cost, the model has a very low

sensitivity to the cost variation of this component since with the used 1 MW resolution a change in optimum power only becomes visible with a variation of 70%. Regarding that the cost contribution of this model accounts for approximately the 6% in the Far North Sea case this low sensitivity is expected. Since a variation of 10% in the capital investment cost or the O&M cost changes the optimum turbine power in 1MW, it can be stated that for this case study the sensitivity of the model output to a variation in these two costs is high.

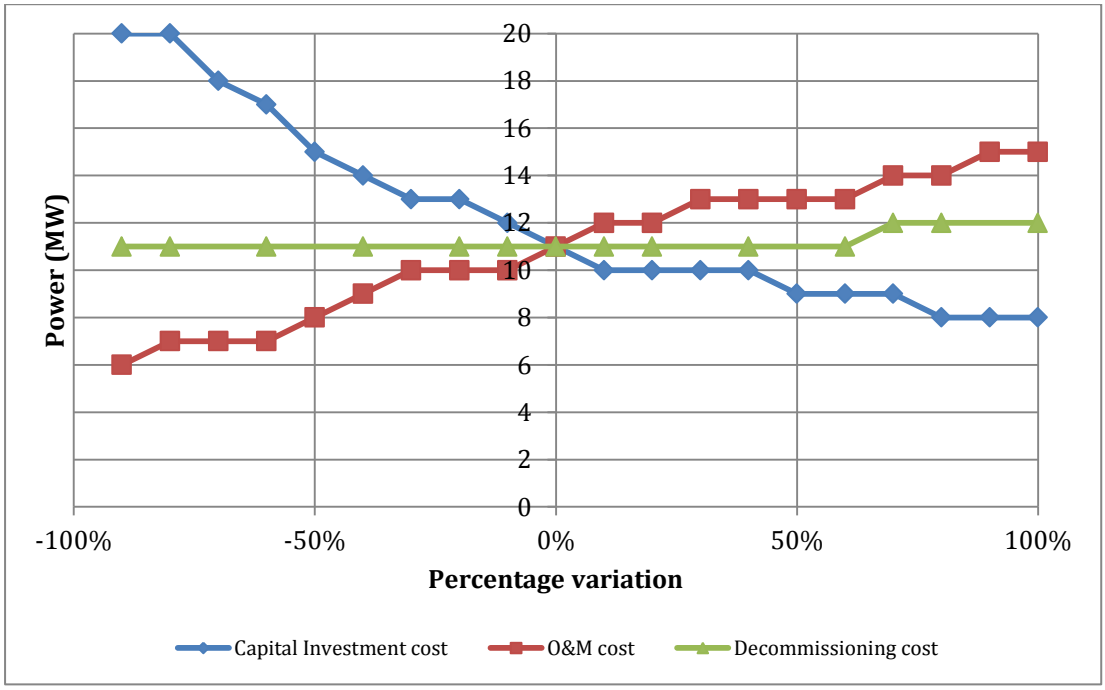

Figure 38. Sensitivity of the model when varying the costs of the capital investment, the O&M and the decommissioning in the Far North Sea case

Recognizing the high sensitivity of the model to a variation in the capital cost and the O&M cost, it is appropriate to determine with more precision, which components of the capital investment and the O&M have the largest influence on this sensitivity. First, the components of the capital investment to be analyzed are the same ones of the analysis in section 5.3. According to Figure 39, the optimum turbine size has the highest sensitivity to a variation of the turbines cost since with the used 1MW resolution a decrease or increase of 10% moves the optimum turbine power 1MW higher or lower respectively. The model outcome is also sensitive to the support structure cost variation as a decrease of 20% moves the optimum turbine power 1MW higher and a further decrease of 90% 3MW higher. Moreover, the optimum turbine power becomes 10MW after an increase of 50% in the support structure cost. Therefore, the model is more sensitive to a decrease in this cost than to an increase of it. Furthermore, the model results are robust upon a variation in the electrical infrastructure cost since according to the resolution of the model the optimum turbine power does not change for any increase or decrease in this cost, except for an increase of 100%, which moves the optimum

size to a higher power rating. Finally, an increment of 30% in the transport & installation cost of the RNA causes the optimum turbine power to move towards a higher power rating and a decrease of 60% towards a lower power rating according to the model resolution. Since the transport & installation cost of the RNA is proportional to the number of turbines, so the gradient of the contribution to the LPC curve of this component is negative like for the O&M, this behavior in the optimum size is expected.

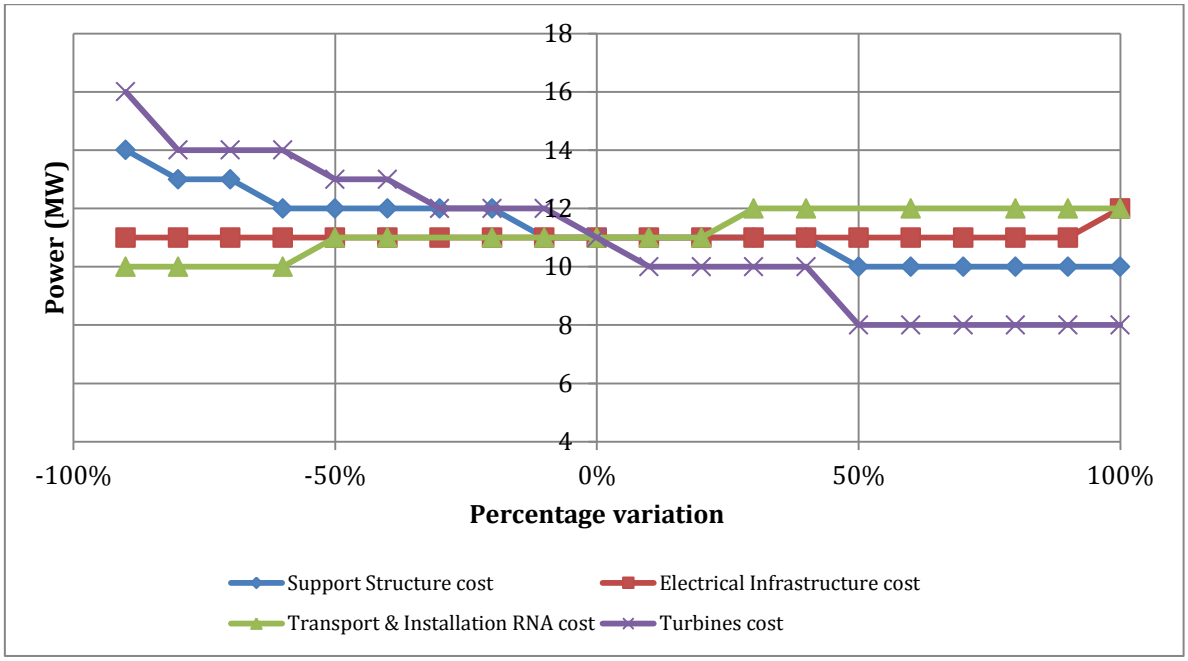

Figure 39. Sensitivity of the model when varying the costs of the support structure, the electrical infrastructure, the turbines and the transport & installation of the RNA in the Far North Sea case

The model exhibits a high sensitivity to a variation in the O&M costs, which is noticed in Figure 38. Thus, it is decomposed to see with more detail the components that have the greatest effect on the optimum turbine size. According to Figure 40, the model outcome has the largest sensitivity when the cost model that groups the expenses of the personnel, access vessels, lifting equipment and subsea inspections is varied. Upon an increase or decrease of 10% in this cost model, the optimum turbine size moves 1MW higher or lower respectively under the model resolution. These maintenance costs were grouped since they are a function of mostly the number of turbines, while the consumables repairs and consumables maintenance costs are a function of the farm rated power in this project. Moreover, the model is robust to a variation in the operation costs or the repair consumables costs since with the used 1MW resolution the optimum turbine power keeps constant when either one of these two costs increases or decreases along the percentage variation range established.

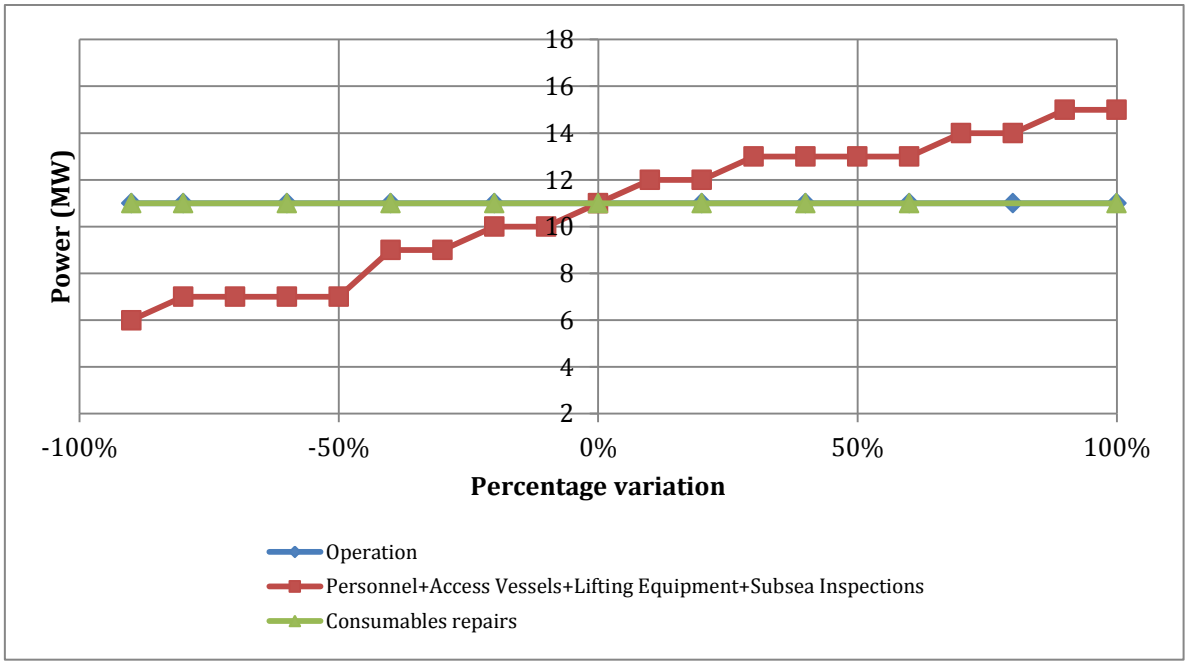

Figure 40. Sensitivity of the model when varying the costs of operation, repair consumables, personnel, access vessels, lifting equipment and subsea inspections in the Far North Sea case

Other factors can cause the optimum turbine size to change apart from a variation in the cost of different components. Some of these other factors taken into account in this sensitivity study are the discount rate, the price ratio between carbon fiber and glass fiber, and the exponent at which the consumables repairs cost upscales to the turbine rated power, which is equal to 1 in the model.

Table 19 shows the effect that the discount rate has in the optimum turbine size. It is appreciated that for a discount rate of 7.5% the optimum turbine size moves to 12MW-182m and in the case of 5% to 13MW-188m. Thus, the optimum turbine scale is sensitive to a variation in the discount rate since it increases if the discount rate decreases. It is noticed as well that the power density of the optimum turbine sizes for the power ratings of 12MW and 13MW in Table 19 is smaller than for the optimum turbine sizes of the same rated powers shown in Table 8. This means that for lower discount rates the cost-effectiveness of increasing the rotor diameter to generate more electricity increases as well. The results in Table 19 can be explained since a lower discount rate reduces the weight of the capital investment cost in Equation 1, leading then to a decrease in the gradients of the contribution the LPC curves of the capital investment components depicted in Figure 30. Hence, relating to the analysis in section 5.4, the absolute value of the negative gradient of the O&M keeps larger than the sum of the gradients of the turbines and the support structure up to higher power ratings. Moreover, a further rise in the costs of the turbines and the support structure due to an increment in the rotor diameter can take place before the added gradient of these two components becomes larger and crosses with the absolute value of the O&M gradient. For that reason, the power densities of the optimum turbine sizes in Table 19 are lower than the ones of Table 8.

Discount rate (%)	Optimum Diameter (m)	Optimum Power (MW)	LPC (€/kWh)	Power Density (W/m²)
10	176	11	0.116	452
7.50	182	12	0.101	461
5	188	13	0.086	468

Table 19. Effect of the discount rate in the optimum turbine size in the Far North Sea case

In section 3.3.2 it was said that it is expected that in the next years the price ratio between carbon fiber and glass fiber will reduce. Thus, the effect of the decrease in this cost ratio is shown in Table 20. Similarly, to the discount rate, a drop in the price ratio between carbon fiber and glass fiber increases the optimum wind turbine size. According to the model, if this price ratio is 7.5 the optimum turbine size increases to 13MW-190m and if it is 5, the optimum turbine size becomes 14MW-210m. Moreover, in the hypothetical case that no carbon fiber would be needed to manufacture longer blades and only glass fiber would be used to fabricate them, this optimum turbine size increases even more and comes to 15MW-224m. These results were obtained using the blade cost models presented in Figure 14.

Therefore, it can be said that the sensitivity of the model to this price ratio and the material used in the blades is high. In addition, it is noticed that the power densities of the optimum turbine sizes in Table 20 are lower than the ones for the optimum turbine sizes with the same rated power shown in Table 8. Hence, the factor that is limiting the most the increment of the rotor diameter for the turbine to have a higher power density and therefore higher energy yield in the model is the blades cost. The results in Table 20 can be understood by taking a look at the exponent values that the blades cost models have in Figure 14. Since these exponents get lower for a decrease in the price ratio between carbon and glass fiber and the use of only glass fiber in the blades (WindPACT blade cost model), the gradient of the contribution to the LPC curve of the turbines drops. Moreover, the smaller the value of these exponents, the lower the turbine gradient. Thus, in like manner as in the explanation of the discount rate results, the absolute value of the O&M gradient keeps larger than the sum of the gradients of the turbines and support structure up to higher power ratings, and a further increase in the rotor diameter can take place.

$c/$g ratio	Optimum Diameter (m)	Optimum Power (MW)	LPC (€/kWh)	Power Density (W/m²)
10	176	11	0.116	452
7.5	190	13	0.112	459
5	210	14	0.108	404
WindPact	224	15	0.104	381

Table 20. Effect of the price ratio between carbon fiber and glass fiber, and the use of just glass fiber in the blades to the optimum turbine size in the Far North Sea case

One of the assumptions made in the model, specifically for the O&M cost model in section 3.6, was to state that the consumables repairs cost scales linearly with the ratio of the upscaled turbine rated power to the reference turbine rated power. Because of this assumption is that the consumables repairs cost keeps constant for all the turbine scales and it is expressed in Equation 13 as a function of only the farm rated power. Thus, it is suitable to determine whether this assumption has a significant role in the calculation of the optimum turbine size. To ascertain the relevance of this assumption, the consumables repairs cost is set to scale with the ratio of the upscaled turbine rated power to the reference turbine rated power to the power of a number larger than one, thus not linearly. Therefore, the cost model of the consumables repairs becomes like expressed in Equation 19.

$$\textbf{Equation 19. } C_R = N_{turbines} \cdot c_{r*} \cdot \left(\frac{P_{new}}{P_{ref}}\right)^b$$

where C_R is the consumables repairs cost, c_{r*} is the consumables repairs cost per turbine per year of the reference turbine calculated as the total consumables repairs cost in the farm computed with Equation 13 divided by the number of turbines needed to meet the farm power installed capacity resulting in 26,591€/year, $N_{turbines}$ is the number of turbines in the wind farm computed as the farm rated power divided by the turbine rated power, b is an exponent that takes the value of 1.1, 1.2, 1.3, 1.4 and 1.5, and P is the rated power of the turbine. The subscripts *ref* and *new* relate to the reference turbine and the new turbine respectively. In section 3.4 the reference turbine is introduced as the V80-2MW.

From Equation 19 it is noticed that this cost is not constant anymore for a fixed farm rated power, but it rises as the rated power of the upscaled turbines used in the farm increases. After replacing the cost model of the consumables repairs given by Equation 13 for the one expressed by Equation 19 in the model, the results presented in Table 21 are obtained. From this table, it is observed that the optimum turbine size maintains constant with the used 1MW resolution until the exponent increases to 1.2 and the optimum size becomes 10MW-171m. A further increase in the exponent to 1.5 changes the optimum size to 9MW-167m. As this exponent increases, the optimum turbine scale decreases. The results in Table 21 are sensible since the consumables repairs cost now becomes larger as the turbine rated power

increases. Thus, following the analysis in section 5.4, the gradient of this cost is positive and adds to the gradients of the support structure and turbines, balancing with the absolute value of the negative gradient of the O&M up to lower power ratings. Moreover, the larger the exponent used in this cost model, the greater its gradient. In addition, based on these results it can be said that this assumption does influence the optimum turbine size.

Exponent equal to	Optimum Diameter (m)	Optimum Power (MW)	LPC (€/kWh)	Power Density (W/m²)
1	176	11	0.1161	452
1.1	176	11	0.1166	452
1.2	171	10	0.1173	435
1.3	171	10	0.1180	435
1.4	171	10	0.1188	435
1.5	167	9	0.1197	411

Table 21. Effect of the variation in the exponent of the assumption that the consumables repairs scales with the increment in rated power

6.3. Baltic Sea case

In this case study, it is also analyzed first the sensitivity of the model output to the variation in the costs of the capital investment, the O&M and the decommissioning. It is observed in Figure 41, that with the used 1MW resolution the optimum turbine power does not change for an increment in the cost of the decommissioning or the O&M, except for an increase of 100% in the O&M cost, which moves the optimum 1MW higher. However, when the O&M cost decreases 30%, the optimum lowers 1MW, and when the decommissioning cost decreases 80% the optimum power drops 1MW as well. In the case of the capital investment cost, an increment of 30% in this cost moves the turbine optimum power 1MW lower. In addition, the optimum turbine power increases to 8MW when a decrease in the capital investment cost of 50% takes place. Therefore, the model results seem more robust to an increase in the cost of these three components than to a decrease in the cost of them.

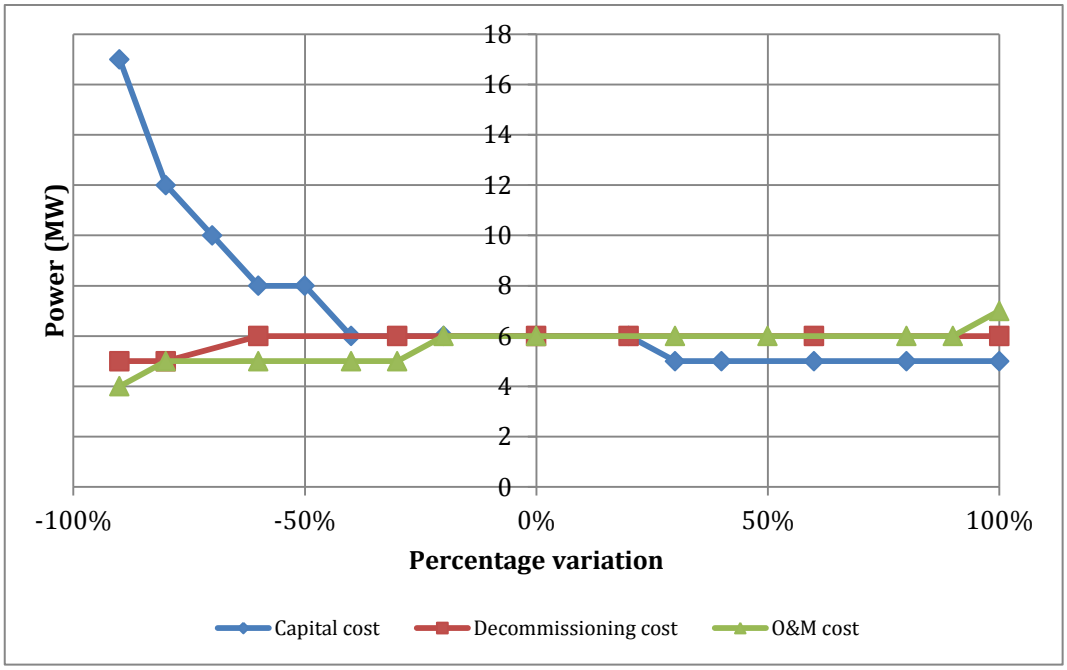

Figure 41. Sensitivity of the model when varying the costs of the capital investment, the O&M and the decommissioning in the Baltic Sea case

Even though a variation in the capital investment cost seems to have a small influence on the optimum turbine size, especially when this cost increases, its components appear to have a greater influence in this optimum when varied separately, which is noticed in Figure 42. The optimum turbine size remains unchanged with the used 1MW resolution until a decrease of 40% or an increase of 30% in the turbines cost, which is the component of the capital investment with the largest effect on the optimum turbine size. Moreover, the optimum turbine power is not influenced by a decrease or increase in the electrical infrastructure cost, as it keeps constant throughout the percentage variation range according to the model resolution. Furthermore, the model is also robust to a change in the support structure cost since the optimum turbine power lowers 1MW for an increase of 70% in this cost. Finally, concerning the transport & installation of the RNA cost, the optimum size moves to a lower power rating when this cost decreases 40%. From Figure 42 it is perceived that when the turbines cost increases the optimum power lowers and the opposite happens when the turbines cost decreases. This outcome is reasonable taking into account the analysis made in section 5.4 because a rise in the turbines cost causes the gradient of the contribution to the LPC curve of the turbines depicted in Figure 34 to increase. Thus, the sum of the gradients of the turbines and the support structure illustrated in Figure 37 becomes larger than the sum of the gradients of the O&M, decommissioning, electrical infrastructure, and transport & installation of the RNA at a lower power rating. A similar result would be expected for an increment or a decrease in the support structure cost. However, Figure 42 shows that the optimum turbine power keeps constant for almost the complete percentage variation range according to the used 1MW resolution of the model. The smaller contribution to

the LPC of the support structure in comparison with this same contribution of the turbines in this case study, clarify this result.

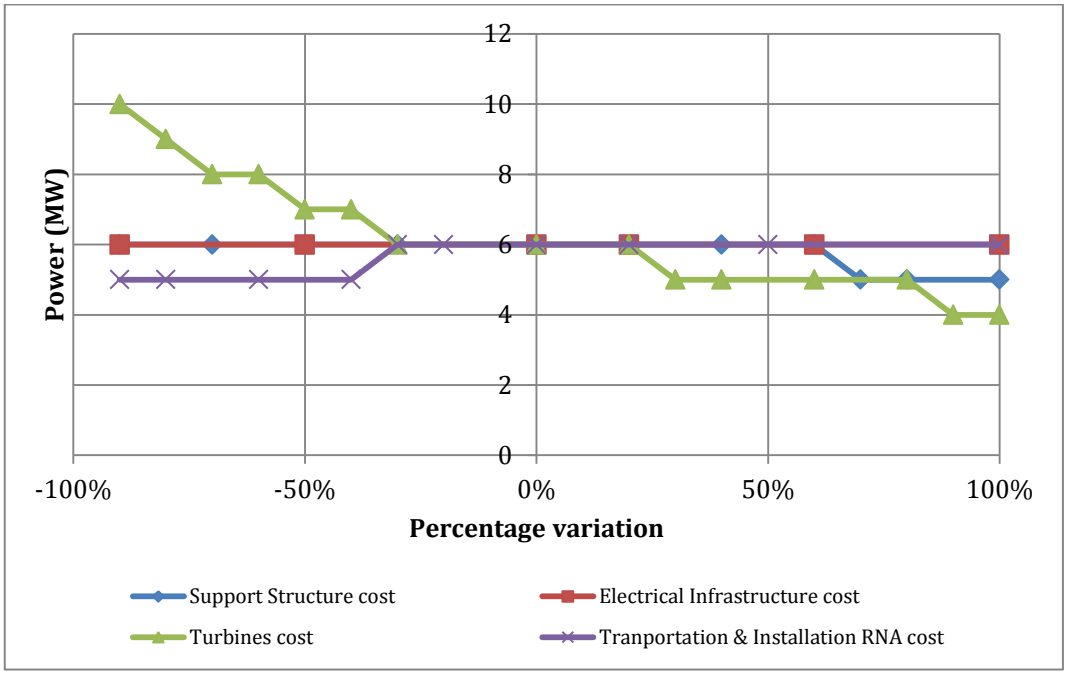

Figure 42. Sensitivity of the model when varying the costs of the support structure, the electrical infrastructure, the turbines and the transport & installation of the RNA in the Baltic Sea case

The sensitivity of the model to a variation in the components costs of the O&M is depicted in Figure 43. The change in the optimum turbine power shown in Figure 41 when the O&M cost decreases in 30% is entirely due to the reduction of 30% in the cost model that groups the expenses of the personnel, access vessels, lifting equipment and subsea inspections. In addition, the optimum turbine power maintains constant with the used 1MW resolution when a variation in the operation costs or the consumables repairs cost takes place along the percentage variation range. The fact that the optimum turbine power decreases when the O&M costs are reduced is sensible because following the analysis made in section 5.4 the O&M gradient drops, so it is higher than the sum of the gradients of the support structure and the turbines up to lower power ratings.

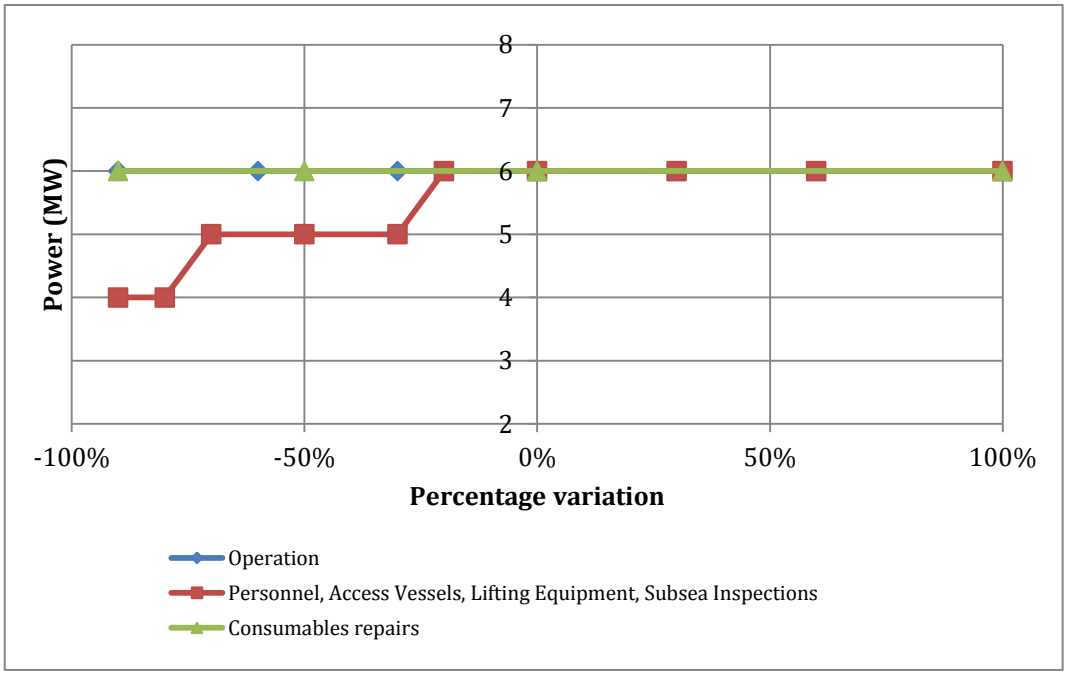

Figure 43. Sensitivity of the model when varying the costs of operation, repair consumables, personnel, access vessels, lifting equipment and subsea inspections in the Baltic Sea case

As previously explained in section 6.2, other factors can cause the optimum turbine size to change apart from a variation in the cost of different components. Thus, in this sensitivity study it is also treated the change in the optimum turbine size due to a change in the discount rate, the price ratio between carbon fiber and glass fiber, and the exponent at which the consumables repairs cost upscales to the turbine rated power, which is equal to 1 in the model.

According to Table 22, there is a minimal influence of the discount rate in the optimum turbine size in this case study. When the discount rate decreases to 7.5% or 5%, the optimum turbine power stays constant according to the used 1MW resolution while the optimum rotor diameter increases just one meter. The results presented in Table 22 can be explained relating to the analysis performed in section 5.4. When the discount rate decreases, the annuity factor given by Equation 2 becomes larger causing a reduction in the weight of the capital investment and the decommissioning in the LPC according to Equation 1. Therefore, the gradients of the support structure and the turbines drop, but so do the negative gradients of the decommissioning and the transport & installation of the RNA. This causes the curve that gathers the gradients of the O&M, the decommissioning, the electrical infrastructure, and the transport & installation of the RNA to shift down along with the curve that groups the turbine and the support structure gradients. Thus, both curves, which are depicted in Figure 37, drop to a level where the optimum turbine size maintains the same as in the base case.

Discount rate (%)	Optimum Diameter (m)	Optimum Power (MW)	LPC (€/kWh)	Power Density (W/m²)
10	147	6	0.112	354
7.50	148	6	0.097	349
5	148	6	0.084	349

Table 22. Effect of the discount rate in the optimum turbine size in the Baltic Sea case

From Table 23 it is observed that when the price ratio between carbon fiber and glass fiber is 7.5 the change in the optimum turbine size is minimal since with the used 1MW resolution only the rotor diameter increases 2m. However, when the price ratio becomes 5, a larger change in the optimum turbine power takes places as the turbine scale changes to 8MW-179m. In addition, in the hypothetical case that only glass fiber is used in the blades, the optimum turbine size increases to 10MW-201m. These results are obtained using the blade cost models presented in Figure 14.

Hence, it can be said that the model is sensitive to the material used in the blades and to a decrease in the price ratio of carbon fiber to glass fiber. Taking a look on the optimum power densities shown in Table 23, they are larger than the ones for the optimum turbine sizes with the same rated power shown in Table 14. Thus, in like manner as in the Far North Sea case, the factor that is limiting the most the increment of the rotor diameter for the turbine to have a higher power density and therefore a higher energy yield in the model is the blades cost. Furthermore, the difference in the values of the power densities also means that for lower price ratios of carbon fiber to glass fiber the cost-effectiveness of increasing the rotor diameter to generate more electricity increases as well. Similarly, as on the Far North Sea case, the results in Table 23 can be interpreted by taking a look at the exponent values that the blades cost models have in Figure 14. Since these exponents get lower for a decrease in the price ratio between carbon and glass fiber and the use of only glass fiber in the blades (WindPACT blade cost model), the gradient of the contribution to the LPC curve of the turbines drops. Moreover, the smaller the value of these exponents, the lower the turbine gradient. Hence, the absolute value of the O&M gradient keeps larger than the sum of the gradients of the turbines and support structure up to higher power ratings, and a further increase in the rotor diameter can take place.

$c/$g ratio	Optimum Diameter (m)	Optimum Power (MW)	LPC (€/kWh)	Power Density (W/m2)
10	147	6	0.112	354
7.5	149	6	0.109	344
5	179	8	0.106	318
WindPact	201	10	0.101	315

Table 23. Effect of the price ratio between carbon fiber and glass fiber, and the use of just glass fiber in the blades to the optimum turbine size in the Baltic Sea case

Like stated in the previous section it is appropriate to check the impact on the optimum turbine size when the exponent at which the consumables repairs cost scales is changed. Therefore, the cost model of the consumables repairs expressed in Equation 13 is replaced from the one in Equation 19. The exponent *b* is varied in a range between 1 and 1.5 in steps of 0.1, and the results are shown in Table 24. It is observed from this table that the optimum turbine size decreases to a 5MW-140m for an exponent change in the range of 1.3 to 1.5 under the used 1MW resolution. In like manner as in the Far North Se case, the results in Table 24 are sensible because the consumables repairs cost now becomes larger as the turbine rated power increases. Hence, following the analysis in section 5.4, the gradient of this cost is positive and adds to the gradients of the support structure and turbines, balancing with the absolute value of the negative gradients of the O&M, the decommissioning, and the transport & installation of the RNA up to lower power ratings. In addition, the larger the exponent used in this cost model, the greater its gradient. Thus, it can be said that there is an impact on the optimum turbine size for a variation on this exponent. However, the effect appears smaller than for the Far North Sea case.

Exponent equal to	Optimum Diameter (m)	Optimum Power (MW)	LPC (€/kWh)	Power Density (W/m²)
1	147	6	0.1116	354
1.1	147	6	0.1120	354
1.2	147	6	0.1124	354
1.3	140	5	0.1128	325
1.4	140	5	0.1132	325
1.5	140	5	0.1136	325

Table 24. Effect of the variation in the exponent of the assumption that the consumables repairs scales with the increment in rated power

6.4. Remarks on the Sensitivity Study

From the analysis performed, it is noticed that in both case studies the model has the largest sensitivity to a variation in the turbines cost. Furthermore, based on the results of the model when the price ratio of carbon fiber to glass fiber is reduced, it can be said the high sensitivity of the model to the turbines cost is mainly due to the blades cost model. After the turbines cost, the component of the capital investment that has the largest impact in the optimum turbine size is the support structure cost. This is noted especially in the Far North Sea case where this cost has a larger percentage contribution to the LPC than in the Baltic Sea case due to the higher water depth and rougher wave environment. In both cases, the model is

robust to a variation in the electrical infrastructure cost and the decommissioning costs, which is expected because of their low contribution to the LPC.

A variation in the O&M cost has a greater impact on the optimum turbine size result in the Far North Sea case than in the Baltic Sea case. This is reasonable since the O&M cost has a larger contribution to the LPC in the former case due to the higher number of turbines. Furthermore, the gradient of the contribution to the LPC curve of the O&M depicted in Figure 30 for the Far North Sea case is larger than the one in Figure 34 for the Baltic Sea case. Thus, a variation in a larger gradient of the O&M has a greater effect on the optimum turbine size relating to the analysis performed in section 5.4. Moreover, considering the costs that compose the total O&M cost, a change in the operation costs has a minimal effect on the optimum turbine size. However, a variation in the cost model that gathers the expenses of the personnel, access vessels, lifting equipment, and subsea inspections, has a high impact on the model results, especially in the Far North Sea case. In addition, regarding the consumables repairs cost, the model is robust to an increment in this cost up to 100% for the two case studies. Nonetheless, when changing this cost model, and stating that the rise in this cost is not linear to the ratio of the upscaled turbine rated power to the reference turbine rated power, the model robustness to this cost reduces since the optimum turbine size changes.

In a more general perspective, it is perceived that the model results are more robust in the Baltic Sea case than in the Far North Sea case. In other words, the optimum turbine power keeps unchanged with the used 1MW resolution to a larger variation in the costs of the different components that constitute an offshore wind farm in the Baltic Sea case than in the Far North Sea case. This difference in robustness between the two cases is expected since for the latter case the optimum turbine size is concentrated around the 5 to 6MW range like depicted in Figure 33 while for the former case the curve in Figure 29 is smooth around the optimum turbine size.

Finally, in section 4.3 it is stated that the energy yield model does not consider the wake effects inside the offshore wind farm. Since any of the wind farm cases treated has area usage limitation, the turbines could be placed at any distance from each other so that the wake efficiency could be almost constant for every combination of rated power and rotor diameter of the upscaled turbines. Moreover, any increase or decrease in the electrical infrastructure cost because of the previous condition would hardly affect the model results considering the robustness shown by the model to a variation in the electrical infrastructure cost in both case studies. Therefore, it can be said that not considering the wake efficiency in the energy model does not impact the results obtained.

7. Conclusions and Recommendations

7.1. Conclusions

The optimum turbine size is the result of a trade-off between the components that their cost reduce and the components that their cost rise as the turbine scale increases. This trade-off is chiefly made between the O&M, and the turbines and support structure since are the components with the largest contribution to the LPC. Therefore, these three components dominate the optimum turbine size to be used in an offshore wind farm. The results of this project revealed that the optimum turbine rated power for a 500MW offshore wind farm is in the range of 10 to 13MW while for a 100MW offshore wind farm is in the range of 5 to 7MW. The difference in these optimum turbine size results is due to the greater reduction in the O&M costs that in a large wind farm can take place in comparison to a small farm.

The upscaling methods used, which were the analytic and the empirical approach, were useful for the calculation of intermediate parameters that in combination with the MZ tool resulted in the cost models of the support structure, the electrical infrastructure, and the O&M. The square cube law was convenient at the moment of estimating parameters in which not much data was found like the RNA mass, yaw diameter, and front area nacelle to model the support structure cost. Furthermore, the empirical approach was appropriate to upscale parameters in which some data was retrieved like it was the case of the rotor size used to obtain the support structure cost model and the generator voltage level to obtain the electrical infrastructure cost model.

The definition of turbine size in terms of the turbine rated power and the rotor diameter was appropriate since at different rated powers a different power density is optimal. Moreover, the cost models developed in this project of the rotor blades, the support structure, the electrical infrastructure, and the O&M could reasonably be parameterized in terms of the power and the diameter of the turbine. However, not all the cost models for the components mentioned above are a function of the two parameters since the influence that the rotor diameter and the turbine power have in these components cost differs among them. For instance, the electrical infrastructure cost was found to be mainly driven by the turbine power and the blades cost by the rotor diameter.

The blades cost appear to be a limiting factor for the increment in the rotor diameter for the large turbines scales. The results showed that the higher the power rating of the turbine, the greater its optimum power density and the lower its energy yield. Moreover, the price ratio of carbon fiber to glass fiber used in the blade cost model has a significant influence on the optimum turbine size because the lower this price ratio, the larger the optimum turbine scale. Therefore, it is expected in the next years a drop in this price ratio, which will boost the upscaling of wind turbines.

The water depth and wave climate conditions have a significant role in the component of the capital investment that has the largest contribution to the LPC in an offshore wind farm. For a site with a water depth of 40m and a Hs_50 of 6.29m, the support structure is the component of the capital investment that has the largest contribution to the LPC while in a site of 15m water depth and a Hs_50 of 4.46m the turbines have the greatest contribution.

The final production of this project was a computational model that calculates the optimum wind turbine size for two offshore wind farm cases with different characteristics. The model developed was a basic model in the sense that only one type of support structure, power transmission system or layout arrangement was selected for the model. Moreover, it was basic for the fact that not all the costs that an offshore wind farm undergoes were included. However, considering the conclusions in the paragraphs above, the model was enough to fulfill the main objective of the project, which was getting insight into the optimum size of wind turbines for offshore applications.

In retrospective, the approach proposed was sufficient to achieve the objectives set. Moreover, even though there are some cost models to be improved or complemented to attain a more realistic and flexible model, the model developed is a base and starting point to carry out future work on wind turbines upscaling for offshore applications.

7.2. Recommendations

To make the model versatile, it should be incorporated a support structure cost model that takes into account other foundations types like jacket, tripod, and floating. Besides, an electrical infrastructure cost model for HVDC transmission should be included as well. In this manner, the optimum turbine size in potential offshore wind farm sites where water levels are deeper than 40-50m and farther than 100km from the coast could be analyzed likewise.

When the increment of the consumables repairs cost was not linear to the ratio between the rated powers of the upscaled turbine and the reference turbine, the optimum turbine size changed indicating that the sensitivity of the model to a variation in this component cost was high. This was noticed especially in the Far North Sea case. Thus, it is appropriate to elaborate more on this cost model to reduce the uncertainty that it brings to the final results. One way to make a better elaboration of this cost model is by using real data of the spare part cost of different turbines scales. However, these data are hard to obtain since the turbine manufacturers and the wind farm developers do not make them available to the public.

The model has the largest sensitivity to a variation in the turbines cost. In addition, the turbine cost highly increases for large rotor diameters, and the component of the turbine that drives this cost increment is the blades. In this project, the blade cost model was developed assuming a percentage of carbon fiber used in the blade according to its length. Thus, it would be suitable to obtain actual costs of the largest blades manufactured nowadays so that these real costs could be compared to the ones given by the blade cost model. In this manner, this cost model could be corroborated and tweaked if necessary.

References

ABB. (2012). *Generators for wind power, Proven generators – reliable power .* ABB, Motors and Generators.

Ashuri et al., T. (2016). Multidisciplinary design optimization of large wind turbines— Technical, economic, and design challenges. *Energy Conversion and Management* (123), 56-70.

Ashuri, T. (2012). *Beyond Classical Upscaling: Integrated Aeroservoelastic Design and Optimization of Large Offshore Wind Turbines .* Ph.D. Thesis, Delft University of Technology, Delft.

Buljan, A., & Durakovic, A. (2016, February 17). *The Baltic – A Sea of Opportunities for Poland*. Retrieved March 15, 2017, from offshoreWIND.biz: http://www.offshorewind.biz/2016/02/17/the-baltic-a-sea-of-opportunities-for-poland/

de Vries, E. (2015, February 27). *Offshore turbine models -- the magnificent seven*. Retrieved March 25, 2017, from Wind Power Offshore: http://www.windpoweroffshore.com/article/1335243/offshore-turbine-models-magnificent-seven

de Oliveira, W. S., & Fernandes, A. J. (2012, January). Cost analysis of the material composition of the wind turbine blades for Wobben Windpower/ENERCON GmbH model E-82 . *Journal of Selected Areas in Renewable Energy (JRSE)* .

de Vries, E. (2005, May). Thinking bigger - Are there limits to turbine size? *Renewable Energy World* , 42-55.

EWEA. (2009). *Economics of wind energy.* The European Wind Energy Association.

EWEA. (2016). *The European offshore wind industry - key trends and statistics 2015.* EWEA.

Fraunhofer ISE. (2013). *Levelized cost of electricity Renewable Energy Technologies.*
GEAI. (2014). *Wind*. Retrieved July 10, 2017, from Good Energies Alliances Ireland: https://goodenergiesalliance.com/6-2-wind/

Hasager et al., C. (2011). *Wind energy resources of the South Baltic Sea.* Risø National Laboratory for Sustainable Energy, Roskilde .

inflation.eu. (2017). *Historic inflation*. Retrieved March 28, 2017, from inflation.eu: http://www.inflation.eu/inflation-rates/historic-cpi-inflation.aspx

Jamieson, P. (2011). *Innovation in Wind Turbine Design.* Chichester, West Sussex, United Kingdom: John Wiley & Sons, Ltd.

Karyotakis, A., & Bucknall, R. (2010). Planned intervention as a maintenance and repair strategy for offshore wind turbines. *Journal of Marine Engineering & Technology , 9* (1), 27-35.

Klinger et al, F. (2002). *THE FINAL FRONTIER - IS THE 10 MW TURBINE POSSIBLE?* Hochschule für Technik und Wirtschaft des Saarlandes, Forschungsgruppe Windenergie, Berlin.

L. Fingersh et al. (2006). *Wind Turbine Design Cost and Scaling Model.* NREL.

Lekou, D. (2010, September). *Scaling Limits & Costs Regarding WT Blades.* Retrieved December 15, 2016, from ResearchGate: https://www.researchgate.net/publication/263178958

Medvedev et al., I. P. (2013). Tidal oscillations in the Baltic Sea. *Oceanology , 53*, 526-538.

Moné et al., C. (2015). *2013 Cost of Wind Energy Review .* Natinal Renewable Energy Laboratory.

Nanalyze. (2016, July 5). *TPI Composites – A Wind Energy Stock*. Retrieved December 15, 2016, from nanalyze: http://www.nanalyze.com/2016/07/wind-energy-stock-tpi-composites/

OANDA. (2017). *Average Exchange rates*. Retrieved March 28, 2017, from OANDA: https://www.oanda.com/currency/average

Pettersson et al., H. (2015). *Wave climate in the Baltic Sea 2014.*

Plastics News. (2014, August 5). *Price keeping carbon fiber from mass adoption*. Retrieved December 17, 2016, from PN: http://www.plasticsnews.com/article/20140805/NEWS/140809971/price-keeping-carbon-fiber-from-mass-adoption

Power Engineering. (2011, March 1). *Direct Drive vs. Gearbox: Progress on Both Fronts*. (L. Morris, Producer) Retrieved April 24, 2017, from Power Engineering: http://www.power-eng.com/articles/print/volume-115/issue-3/features/direct-drive-vs-gearbox-progress-on-both-fronts.html

REN21. (2016). *Renewables 2016 Global Status Report .* Renewable Energy Policy Network for the 21st Century.

Rosenauer, E. (2014). *INVESTMENT COSTS OF OFFSHORE WIND TURBINES .* University of Michigan, Sustainable Systems.

Rueda, J. (2016, March 10). Electrical infrastructure of offshore wind power plants. Delft.

Sandia National Laboratories . (2003). *Cost Study for Large Wind Turbine Blades: WindPACT Blade System Design Studies.* Sandia National Laboratories , Albuquerque, New Mexico.

Schachner, J. (2004). *POWER CONNECTIONS FOR OFFSHORE WIND FARMS .* TU Delft & University of Leoben , Leoben.

Schoenmakers, D. (2008). *Optimization of the coupled grid connection of offshore wind farms.* Technical University of Eindhoven.

Shahan, Z. (2014, November 21). *History of Wind Turbines*. Retrieved May 26, 2017, from Renewable Energy World: http://www.renewableenergyworld.com/ugc/articles/2014/11/history-of-wind-turbines.html

Soomere et al., T. (2012). Wave climate in the Arkona Basin, the Baltic Sea . *Ocean Science* (8), 287-300.

Soomere, T., & Pindsoo, K. (2015). Spatial variability in the trends in extreme storm surges and weekly-scale high water levels in the eastern Baltic Sea . *Continental Shelf Research* (115), 53-64.

The Crown State. (2010). *A guide to an offshore wind farm.*

TPI Composites. (2017). *Wind Turbine and Wind Blade Fundamentals*. Retrieved December 15, 2016, from TPI Composites: http://www.tpicomposites.com/English/industries/wind-energy/wind-turbine-and-wind-blade-fundamentals/default.aspx

TU Delft. (2006, December 14). *Wind Farm Design*. Retrieved April 04, 2017, from http://mstudioblackboard.tudelft.nl/duwind/Wind%20energy%20online%20reader/Video_frames_pages/foundations_offshore.htm

Velarde, J. (2016). *Design of Monopile Foundations to Support the DTU 10 MW Offshore Wind Turbine .* DTU.

Vestas. (n.d.). Retrieved from https://www.ledsjovind.se/tolvmanstegen/Vestas%20V90-2MW.pdf

Wind-Turbines-Models.com. (2017). *AREVA M5000-135*. Retrieved March 25, 2017, from Wind-Turbines-Models.com: https://www.wind-turbine-models.com/turbines/686-areva-m5000-135

Wood, K. (2012, May 31). *Wind turbine blades: Glass vs. carbon fiber*. Retrieved December 15, 2016, from CompositesWorld: http://www.compositesworld.com/articles/wind-turbine-blades-glass-vs-carbon-fiber

Zaaijer, M. (2015). *Wind climate and energy production* . Delft, South Holland, The Netherlands.

Zaaijer, M. B. (2013). *Great expectations for offshore wind turbines - Emulation of wind farm design to anticipate their value for customers .* PhD , Delft University of Technology.

Zaaijer, M. (2015). Economic Aspects. *Introduction to Wind Energy* . Delft.

Appendix A. Cost Models

Table 25 shows the inflation rates and exchange rates used to actualize cost information. Not all currencies are visible in the cost models list because these are only used to convert data and models that are used for calibration of some of the models in the list that make part of the MZ tool.

Currency	**Annual inflation rate (%)** (inflation.eu, 2017)	**Exchange rate – Last quarter of 2016** (OANDA, 2017)
USD	2.18	0.926
GBP	1.98	1.152
DKK	1.8	0.134
SEK	1.2	0.102
NOK	2.07	0.111
EUR	1.79	1

Table 25. Applied inflation rates and Exchange rates to EUR

The following list presents the cost models used in the project final model that were not developed by the author of this work. All parameters in the equations are in basic SI-units, so e.g. W not MW, unless specified otherwise. Masses are in kg, distances, dimensions and heights are in m. The symbols are explained in the list of symbols. In addition, the reference of each cost model is indicated by a superscript, and the reference related to each superscript is presented in Table 26.

Capital Investment Costs

- $Boat\ landing^{a}\ [USD\ 2003] = 60{,}000 \cdot N_{turbines}$
- $Measuring\ tower^{a}\ [EUR\ 2003] = 2{,}050{,}000$
- $Onshore\ premises^{a}\ [EUR\ 2003] = 1{,}500{,}000$
- $Harbor\ use^{a}\ [USD\ 2002] = 0.02 \cdot P_{farm}$
- $Dune\ crossing^{a}\ [EUR\ 2003] = 1{,}200{,}000$
- $Grid\ connection^{c}\ [2008\ EUR] = 1{,}000{,}000$
- $Engineering^{a}\ [USD\ 2003] = 0.037 \cdot P_{farm}$

- $Offshore\ platform$ [a] $[SEK\ 2003] = \frac{2}{3} \cdot \left(0.4 \cdot 10^{-3} \cdot {m_{jacket}}^2 - 50 \cdot m_{jacket} - 80 \cdot 10^6\right)$, $with$: $m_{jacket} = 582 \cdot d_{water}^{0.19} \cdot \left(3 \cdot 10^{-3} \cdot P_{farm} + 0.5 \cdot 10^6\right)^{0.48}$

- $Turbines$[b]:
  - $Power\ converter\ [USD\ 2002] = 79 \cdot 10^{-3} \cdot P$
  - $Cooling\ system\ \ [USD\ 2002] = 12 \cdot 10^{-3} \cdot P$
  - $Nacelle\ cover\ [USD\ 2002] = 11.537 \cdot 10^{-3} \cdot P + 3849.7$
  - $Control\ system\ [USD\ 2002] = 55{,}000$
  - $Direct\ drive\ generator\ [USD\ 2002] = 219.33 \cdot 10^{-3} \cdot P$
  - $Brake\ system\ [USD\ 2002] = 1.9894 \cdot 10^{-3} \cdot P - 0.1141$
  - $Pitch\ Mechanism\ [USD\ 2002] = 2.28 \cdot (0.2106 \cdot D^{2.6578})$
  - $Nose\ cone\ [USD\ 2002] = (18.5 \cdot D - 520.5) \cdot 5.57$
  - $Main\ shaft\ [USD\ 2002] = 0.01 \cdot D^{2.887}$
  - $Main\ bearings\ [USD\ 2002] = \left[\left(D \cdot \frac{8}{600} - 0.033\right) \cdot 0.0092 \cdot D^{2.5}\right] \cdot 2 \cdot 17.6$
  - $Yaw\ drive\ and\ bearing\ [USD\ 2002] = 2 \cdot 0.0339 \cdot D^{2.964}$
  - $Mainframe\ [USD\ 2002] = 627.28 \cdot D^{0.85} + (1.228 \cdot D^{1.953} \cdot 0.125 \cdot 8.7)$
  - $Hub\ [USD\ 2002] = 4.25 \cdot [0.954 \cdot (blade\ mass/single\ blade) + 5680.3]$

- $Warranty$[a] $[EUR\ actual] = f_{warranty} \cdot C_{RNA} \cdot N_{turbines}$, $with$: $f_{warranty} = 0.15$

- $RNA\ onshore\ transport$[a] $[EUR\ 2001] = (5.84 \cdot 10^{-3} \cdot D + 0.4) \cdot L + 0.486 \cdot D^{2.64}$, $with$: $L = 100000m$

- $RNA\ offshore\ installation$[a] $[USD\ 2010] = 3.4 \cdot 10^3 \cdot (h_{hub} + 50) \cdot N_{turbines}$

- $Transmission\ cable\ installation$[a] $[EUR\ 2003, USD\ 2010] = 500{,}000 + 178 \cdot l$

- $Infield\ cable\ installation^{a}\ [EUR\ 2003, USD\ 2010] = 500{,}000 + 169 \cdot l$
- $Measuring\ tower\ installation\ ^{a}[EUR\ 2003] = 550{,}000$
- $Site\ assesment^{d}$:
    - $Environmental\ Survey\ [GBP] = 8 \cdot 10^{-3} \cdot P_{farm}$
    - $Sea\ bed\ surveys\ [GBP] = 18 \cdot 10^{-3} \cdot P_{farm}$
    - $Front\ end\ engineering\ and\ design\ studies\ [GBP] = 2 \cdot 10^{-3} \cdot P_{farm}$
    - $Human\ impact\ studies\ [GBP] = 100{,}000$
- $Management^{a}\ [EUR\ actual] = 0.03 \cdot C_{investment}$

O&M Costs

- $Administration^{a}\ [EUR\ 2012] = 1{,}000{,}000$
- $Grid\ charge\ energy^{a}\ [EUR\ 2009] = 3 \cdot 10^{-6} \cdot E_y$
- $Bottom\ lease^{a}\ \ [EUR\ 2009] = 60.7 \cdot 10^{-3} \cdot A_{farm}$
- $Insurance^{a}\ \ [EUR\ actual] = 0.01 \cdot C_{RNA} \cdot N_{turbines}$
- $Management^{a}\ \ [EUR\ actual] = 0.03 \cdot C_{O\&M}$

Decommissioning Costs

- $Rotor - nacelle\ assemblies\ removal^{a}\ [USD\ 2010] = 0.91 \cdot [3.4 \cdot 10^{3} \cdot (h_{hub} + 50) \cdot N_{turbines}]$
- $Offshore\ platform\ and\ measuring\ tower\ removal^{a}\ \ [USD\ 2010] = 665{,}000$
- $Transmission\ cable\ removal^{a}\ \ [USD\ 2010] = 49 \cdot l$
- $Infield\ cable\ removal^{a}\ \ [USD\ 2010] = 53 \cdot l$
- $Site\ clearance^{a}\ \ [USD\ 2010] = \ 16{,}000 \cdot N_{turbines}$

- $Rotor - nacelle\ assemblies\ disposal^{a}\ [USD\ 2010] = 150 \cdot m_{RNA} \cdot N_{turbines}$
- $Management^{a}\ [EUR\ actual] = 0.03 \cdot C_{decommissioning}$

Superscript	Reference
a	(Zaaijer M. B., 2013)
b	(Schoenmakers, 2008)
c	(L. Fingersh et al., 2006)
d	(The Crown State, 2010)

Table 26. Cost models references

The cost models for the removals of the foundations and the scour protection for the Far North Sea case and the Baltic Sea case are given by the mathematical expressions shown in Figure 44 and Figure 45 respectively. These cost models where obtained following the same procedure as for the support structure in section 3.4.

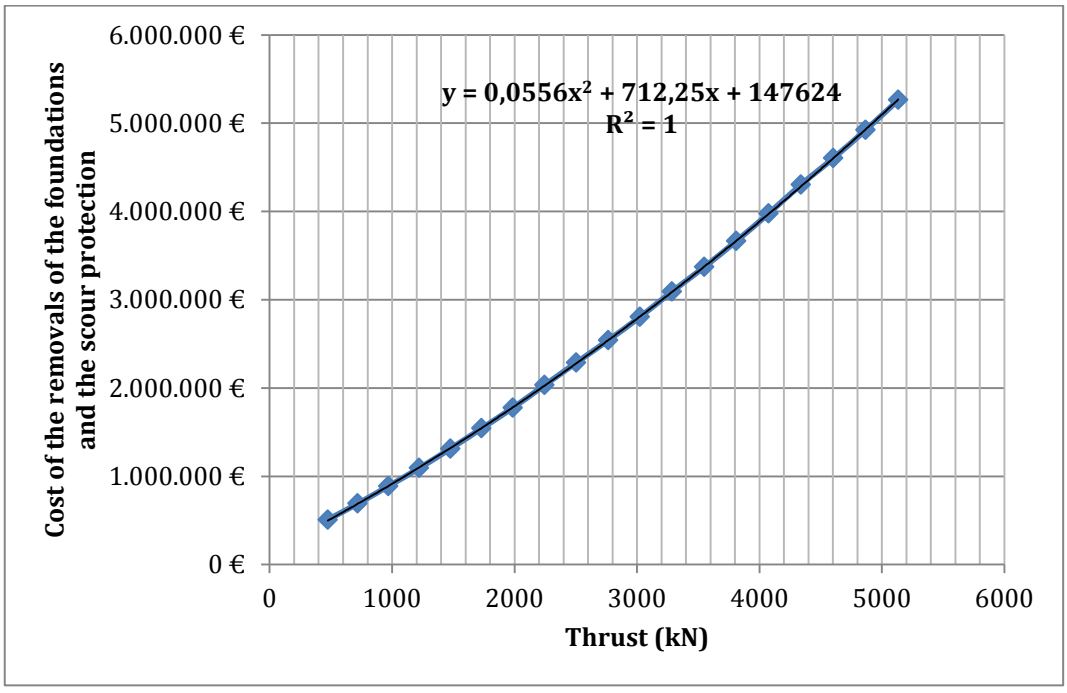

Figure 44. Cost model for the removals of the foundation and the scour protection in the Far North Sea case

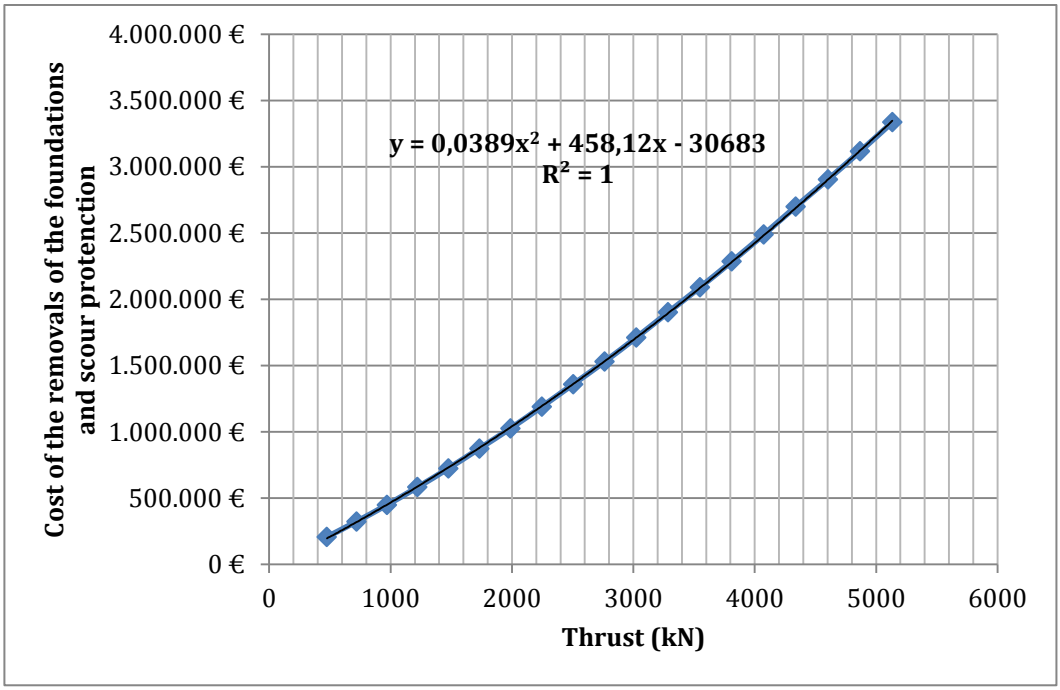

Figure 45. Cost model for the removals of the foundation and the scour protection in the Baltic Sea case

Appendix B. References for the case studies characteristics

Table 27 presents some of the characteristics of the two case studies with their respective references. The parameters used for the Far North Sea case correspond to the Horn Rev offshore wind farm. Moreover, since any information about the typical soil friction angle and the typical submerged unit weight was found for the Baltic Sea, the parameters used for the Far North Sea case are employed as well in the Baltic Sea case. In addition, the Weibull scale and shape factors for the Far North Sea case correspond to a height of 62m and for the Baltic Sea case to a 10m height.

Case study	**Far North Sea**		**Baltic Sea**	
Parameter	**Value**	**Reference**	**Value**	**Reference**
Weibull scale factor (m/s)	10.83	(Zaaijer M. B., 2013)	7.8	(Hasager et al., 2011)
Weibull shape factor (-)	2.35		2	
HAT (m)	0.8		0.2	(Medvedev et al., 2013)
LAT (m)	-0.8		-0.2	
Storm surge positive (m)	2.5		1	(Soomere & Pindsoo, 2015)
Storm surge negative (m)	-0.5		-0.5	assumed
Hs_50 year (m)	6.29		4.46	(Soomere et al., 2012)
Hs_1 year (m)	5.65		1.5	(Pettersson et al., 2015)
Depth average current_50 year (m/s)	0.8		0.6	assumed
Typical soil friction angle (°)	35		35	(Zaaijer M. B., 2013)
Typical submerged unit weight (N/m3)	10000		10000	(Zaaijer M. B., 2013)

Table 27. Case studies characteristics with their respective references

Appendix C. V80-2MW Characteristics

Table 28 shows the power and thrust curves of the V80-2MW and Table 29 presents the technical data of this turbine, which is the reference turbine used in this project.

Wind Speed (m/s)	Power (kW)	Thrust coefficient (-)
3.9999	0	0
4	66.6	0.818
5	154	0.806
6	282	0.804
7	460	0.805
8	696	0.806
9	996	0.807
10	1,341	0.793
11	1,661	0.739
12	1,866	0.709
13	1,958	0.409
14	1,988	0.314
15	1,997	0.249
16	1,999	0.202
17	2,000	0.167
18	2,000	0.140
19	2,000	0.119
20	2,000	0.102
21	2,000	0.088
22	2,000	0.077
23	2,000	0.067
24	2,000	0.060
25	2,000	0.053
25.0001	0	0

Table 28. Power and thrust curves for the V80-2MW (Zaaijer M. B., 2013)

Parameter	Value
Rotor radius (m)	40
Rotor solidity (-)	0.052
Front area nacelle (m2)	14
Height from yaw to hub (m)	2
Yaw bearing (outer) diameter (m)	2.26
Mass of RNA (kg)	98,500
Eccentricity (downwind is positive) (m)	-2
Cd rotor idling in vane (-)	0.4
Cd nacelle (-)	1.2
Maximum operational thrust (N)	475,000
Wind speed at maximum thrust (m/s)	12
Generator voltage (V)	690
Purchase price (€)	1,500,000

Table 29. V80-2MW technical data (Zaaijer M. B., 2013)

Appendix D. Generator voltage estimation

To estimate the generator voltage of the turbine, first, data of the value of this parameter for turbines currently in operation is searched. However, not much information and data is found. Therefore, an interpolation is done using the few data retrieved to calculate the generator voltage for different turbine rated powers. Table 30 shows the data retrieved. The interpolation was performed with the *interpolate.interp1d* function of scipy. The kind of interpolation selected was linear because it fitted the best with the values retrieved. It is important to mention that the generator voltage for the 20MW turbine relates to a generator with a power rating of 20MW developed by the company ABB.

Turbine Power (MW)	Generator Voltage (V)	Reference
2	690	(Zaaijer M. B., 2013)
3	1000	(Zaaijer M. B., 2013)
5	3300	(Wind-Turbines-Models.com, 2017)
6.2	6600	(de Vries, 2015)
20	15000	(ABB, 2012)

Table 30. Retrieved data of voltage generator for different turbine powers